N-I/28091--092

Evaluation of PM-3 Chemistry Data and Possible Interpretations of ^{3}H Observations

Navarro-Intera

Revision No.: 0

February 2015

UNCLASSIFIED

/s/ Joseph P. Johnston 02/26/2015

Joseph P. Johnston, N-I CO Date

Prepared for U.S. Department of Energy under Contract No. DE-AC52-09NA28091.

Approved for public release; further dissemination unlimited.

Available for sale to the public from:

U.S. Department of Commerce
National Technical Information Service
5301 Shawnee Road
Alexandria, VA 22312
Telephone: 800.553.6847
Fax: 703.605.6900
E-mail: *orders@ntis.gov*
Online Ordering: *http://www.ntis.gov/help/ordermethods.aspx*

Available electronically at *http://www.osti.gov/bridge*

Available for a processing fee to U.S. Department of Energy and its contractors, in paper, from:

U.S. Department of Energy
Office of Scientific and Technical Information
P.O. Box 62
Oak Ridge, TN 37831-0062
Phone: 865.576.8401
Fax: 865.576.5728
Email: *reports@adonis.osti.gov*

Reference herein to any specific commercial product, process, or service by trade name, trademark, manufacturer, or otherwise, does not necessarily constitute or imply its endorsement, recommendation, or favoring by the United States Government or any agency thereof or its contractors or subcontractors.

Printed on recycled paper

N-I/28091--092

Navarro-Intera

EVALUATION OF PM-3 CHEMISTRY DATA AND POSSIBLE INTERPRETATIONS OF ^{3}H OBSERVATIONS

Revision No.: 0
February 2015
Navarro-Intera, LLC
c/o U.S. DOE
P.O. Box 98952
Las Vegas, NV 89193-8952

Prepared for U.S. Department of Energy under Contract No. DE-AC52-09NA28091.

Approved for public release; further dissemination unlimited.

EVALUATION OF PM-3 CHEMISTRY DATA AND POSSIBLE INTERPRETATIONS OF ^{3}H OBSERVATIONS

Approved by: /s/ Sam Marutzky Date: 02/24/2015

Sam Marutzky, UGTA Project Manager
Navarro-Intera, LLC

TABLE OF CONTENTS

List of Figures . . . iii
List of Tables . . . vi
List of Acronyms and Abbreviations . . . vii
Acknowledgement . . . xvi

1.0 Introduction . . . 1-1

1.1 Objectives . . . 1-4
1.2 History of Field Activities at PM-3 . . . 1-4
1.3 Geologic Background . . . 1-5
1.4 Hydrogeologic Background . . . 1-7
1.5 Geochemistry Background . . . 1-11
1.6 Summary of Sampling Activities and Results at PM-3 . . . 1-14
1.7 Report Organization . . . 1-19

2.0 Chemistry Data and Evaluation . . . 2-1

2.1 Introduction . . . 2-4
2.2 Geochemistry Evaluation . . . 2-5
2.2.1 Major-Ion Data . . . 2-5
2.2.2 Stable Isotopes of Hydrogen and Oxygen . . . 2-8
2.2.3 Noble Gas Data . . . 2-12
2.2.4 DIC ^{14}C and DOC ^{14}C Data . . . 2-14
2.2.5 Other Environmental Tracer Data . . . 2-17
2.2.6 Summary of Chemistry Data . . . 2-19
2.3 Radiochemistry Evaluation . . . 2-20
2.4 Summary . . . 2-23

3.0 Possible Interpretations of ^{3}H Observations . . . 3-1

3.1 Introduction . . . 3-1
3.2 Possible Interpretations of Observed ^{3}H at PM-3 . . . 3-3
3.2.1 Possible Residual ^{3}H Contamination from the Contaminated Bailer . . . 3-4
3.2.2 Possible ^{3}H Contamination from Recompletion Activities . . . 3-4
3.2.3 Possible Infiltration of Elevated ^{3}H from Atmospheric Testing . . . 3-6
3.2.4 Analysis of Possible Vertical Transport of ^{3}H from Surface Contamination . . . 3-7
3.2.5 Analysis of Possible Lateral Transport of ^{3}H from Underground Nuclear Tests . . . 3-11
3.3 Summary . . . 3-17

4.0 Conclusions . . . 4-1

5.0 References . . . 5-1

TABLE OF CONTENTS (CONTINUED)

Appendix A - PM-3 Analytical Chemistry and Radiochemistry Results

A.1.0 Introduction A-1

A.2.0 Analytical Results A-2

A.3.0 References A-9

Appendix B - Hydrogeology and Hydraulic Properties of HSUs in the Vicinity of PM-3

B.1.0 Introduction B-1

B.2.0 Geologic Information B-2

B.3.0 Water-Level Information B-8

B.4.0 Hydraulic Properties B-10

B.4.1 PM-3 Hydraulic Testing Results B-10
B.4.2 U-20m and UE-20j Hydraulic Testing Results B-12
B.4.3 Recent Hydraulic Testing in Southwest Area 20 and the NTTR B-13
B.4.4 Summary of Hydraulic Testing Results B-16

B.5.0 Analysis of Groundwater Flow Budget in the Vicinity of PM-3 . . . . . B-18

B.6.0 Summary B-21

B.7.0 References B-22

Appendix C - Analysis of Possible Flow Path from HANDLEY to PM-3 Using Numerical Modeling

C.1.0 Introduction C-1

C.1.1 Streamtube Modeling Approach C-2
C.1.2 Streamtube Model Mathematics C-2

C.2.0 Consideration of Uncertainty C-5

C.3.0 Pahute Mesa Hydrogeologic Data C-7

C.3.1 Pahute Mesa Potentiometric Surface C-7
C.3.2 Hydraulic and Transport Parameters C-9

C.4.0 HANDLEY Source Term C-21

C.5.0 Simulation Results and Discussion C-22

C.6.0 References C-29

LIST OF FIGURES

NUMBER	TITLE	PAGE
1-1	Topographic Map of the PM-3 Area	1-2
1-2	Well Completion Diagram for PM-3	1-3
1-3	Photographs of Depth-Discrete Bailer (Upper) and Pump Jack (Lower) at PM-3	1-6
1-4	Location of PM-3 and Geologic Structural Features	1-8
1-5	Location of PM-3 and General Groundwater Flow Paths	1-9
1-6	Location of PM-3 and Local Potentiometric Surface	1-10
1-7	Groundwater Flow Paths Modeled in Rose et al. (2006)	1-13
1-8	Groundwater Flow Paths Modeled in Kwicklis et al. (2005)	1-15
1-9	^{3}H Results for the PM-3-1 (Deep) Piezometer from 1988 through 2013	1-17
1-10	^{3}H Results for the PM-3-2 (Shallow) Piezometer from 1988 to 2013	1-18
2-1	Groundwater Sampling Locations in the Vicinity of PM-3	2-2
2-2	Groundwater Sampling Location Well Groupings	2-3
2-3	Piper Diagram of Groundwater in the Vicinity of Pahute Mesa, Including PM-3-1 (Deep) and PM-3-2 (Shallow)	2-6
2-4	Sulfate and Chloride Concentrations in the Vicinity of Pahute Mesa, Including PM-3-1 (Deep) and PM-3-2 (Shallow)	2-7
2-5	δD versus $\delta^{18}O$ in the Vicinity of Pahute Mesa, Including PM-3-1 (Deep) and PM-3-2 (Shallow)	2-9
2-6	δD versus Cl in the Vicinity of Pahute Mesa, Including PM-3-1 (Deep) and PM-3-2 (Shallow)	2-10
2-7	δD and $\delta^{18}O$ Versus Groundwater Age	2-11
2-8	Helium Isotope Ratios in the Vicinity of Pahute Mesa, Including PM-3-1 (Deep) and PM-3-2 (Shallow)	2-13
2-9	Groundwater $^{234}U/^{238}U$ Activity Ratios versus Inverse Uranium Concentrations	2-18

LIST OF FIGURES (CONTINUED)

NUMBER	TITLE	PAGE
3-1	Surface Radiation Near PM-3 from 1994 Flyover	3-8
3-2	General Perspective View of Hydrostratigraphy and Major Structural Features in the Vicinity of PM-3	3-13
3-3	Straight Line Streamline Simulated Breakthrough and Observed ^3H Concentrations at PM-3-2	3-16
B-1	Map View of Major Structures and Detonations in the Vicinity of PM-3	B-3
B-2	General Perspective View of Hydrostratigraphy and Major Structural Features in the Vicinity of PM-3	B-5
B-3	Detailed Perspective View of Hydrostratigraphy and Major Structural Features in the Vicinity of PM-3	B-6
B-4	Cross Section of HSUs between HANDLEY and PM-3	B-7
B-5	Geochemical Groups in Pahute Mesa–Oasis Valley Groundwater Flow Domain	B-9
B-6	Estimated Transmissivities in the Vicinity of PM-3	B-20
C-1	Potentiometric Surface Used for Generating HANDLEY Streamtube Models	C-8
C-2	Streamlines Originating from PM-3, HANDLEY, and Pseudo-HANDLEY	C-9
C-3	Comparison of Working Point Transmissivity from the USGS Models and Streamtube Model Parameterized from HDD Data	C-18
C-4	Comparison of Working Point Transmissivity from the USGS Models and Streamtube Model Parameterized from the USGS Model Calculated as the Volumetric Average within Each HFM HSU	C-18
C-5	Comparison of Working Point Transmissivity from the USGS Models and Streamtube Model Parameterized from the USGS Model Hydraulic Conductivity Calculated as Thickness Average at All Pahute Mesa Working Points	C-19
C-6	Modified Fenelon et al. (2010) Streamline Simulated Breakthrough and Observed ^3H Concentrations at PM-3-2 (Shallow)	C-23
C-7	Modified Fenelon et al. (2010) Streamline Simulated Breakthrough and Observed ^3H Concentrations at PM-3-1 (Deep)	C-24

LIST OF FIGURES (CONTINUED)

NUMBER **TITLE** **PAGE**

C-8 Straight Line Streamline Simulated Breakthrough and Observed ^3H Concentrations at PM-3-1 (Deep) C-25

C-9 Straight Line Streamline Simulated Breakthrough and Observed ^3H Concentrations at PM-3-2 (Shallow) C-26

LIST OF TABLES

NUMBER	TITLE	PAGE
2-1	DIC $\delta^{13}C$, DIC ^{14}C, DOC $\delta^{13}C$, and DOC ^{14}C Data for Groundwater Sampling Locations on Pahute Mesa	2-15
A-1	Chemistry Data for PM-3-1 (Deep) and PM-3-2 (Shallow) from August 2013 Sampling	A-2
A-2	PM-3 Laboratory Analyses of ^{3}H	A-7
B-1	Summary of PM-3 Injection Testing Results	B-11
B-2	Comparison of N-I and USGS Interpretations of Phase II Pahute Mesa Single-Well and Multiple-Well Aquifer Tests	B-15
C-1	USGS Model Material Types Description and Permeability	C-10
C-2	Pahute Mesa Phase I HSUs Selected To Represent the Streamtube Model HGUs for the Phase I HDD Parameterization	C-11
C-3	Permeability and Porosity Data Used in the Streamtube Models	C-12
C-4	Fracture Spacing Data Summary	C-16
C-5	Streamtube Model Transmissivity at UE-20j and PM-3	C-20

LIST OF ACRONYMS AND ABBREVIATIONS

General Acronyms and Abbreviations

2-D	Two-dimensional
3-D	Three-dimensional
ac-ft/yr	Acre-feet per year
AMS	Accelerator mass spectrometer
amsl	Above mean sea level
atoms/g	Atoms per gram
bgs	Below ground surface
°C	Degrees Celsius
CS	Carbon steel
CAU	Corrective action unit
DOE	U.S. Department of Energy
DRI	Desert Research Institute
EC	Electrical conductivity
ft	Foot
ft/day	Feet per day
ft^2/day	Square feet per day
gal	Gallon
GMWL	Global meteoric water line
gpm	Gallons per minute
HDD	Hydrologic data document
HFM	Hydrostratigraphic framework model
HGU	Hydrogeologic unit
HRMP	Hydrology and Radionuclide Migration Program
HSU	Hydrostratigraphic unit
in.	Inch
km	Kilometer
kt	Kiloton
L	Liter
LANL	Los Alamos National Laboratory
LLNL	Lawrence Livermore National Laboratory

LIST OF ACRONYMS AND ABBREVIATIONS

LMWL	Local meteoric water line
L/µg	Liters per microgram
m	Meter
m^2	Square meter
m^2/yr	Square meters per year
m^3/yr	Cubic meters per year
m/day	Meters per day
MDC	Minimum detectable concentration
mg/L	Milligrams per liter
mi	Mile
min	Minute
mm/yr	Millimeters per year
M&O	Management and operating
Mt	Megaton
MWAT	Multiple-well aquifer test
m/yr	Meters per year
NA	Not available
NAD	North American Datum
ND	Not determined
N-I	Navarro-Intera, LLC
NNSS	Nevada National Security Site
NR	Not recorded
NSPC	Nevada State Plane Coordinates
NSTec	National Security Technologies, LLC
NTTR	Nevada Test and Training Range
pCi/L	Picocuries per liter
pCi/mL	Picocuries per milliliter
PM-3	Pahute Mesa #3
pmc	Percent modern carbon
R_c	Cavity radius
REECo	Reynolds Electrical & Engineering Co., Inc.
RREMP	Routine Radiological Environmental Monitoring Program

LIST OF ACRONYMS AND ABBREVIATIONS

SDWA	*Safe Drinking Water Act*
SS	Stainless steel
SWAT	Single-well aquifer test
TD	Total depth
TU	Tritium unit
UGTA	Underground Test Area
USGS	U.S. Geological Survey
UTM	Universal Transverse Mercator
µCi/mL	Microcuries per milliliter
µg/L	Micrograms per liter
µmhos/cm	Micromhos per centimeter
µR/hr	Microroentgens per hour
%meq/L	Percent milliequivalents per liter
‰	Per mil

Stratigraphic, Geologic, Hydrostratigraphic, and Hydrogeologic Unit Abbreviations and Symbols

A20SM	Area 20 caldera structural margin
AA	Alluvial aquifer
ATCCU	Ammonia Tanks caldera confining unit
ATICU	Ammonia Tanks intrusive confining unit
ATMLFA	Ammonia Tanks mafic lava-flow aquifer
ATWTA	Ammonia Tanks welded-tuff aquifer
BA	Benham aquifer
BFCU	Bullfrog confining unit
BMCSM	Black Mountain Caldera structural margin
BMICU	Black Mountain intrusive confining unit
BRA	Belted Range aquifer
BWCU	Buttonhook Wash confining unit
BWWTA	Buttonhook Wash welded-tuff aquifer
CA	Carbonate aquifer

LIST OF ACRONYMS AND ABBREVIATIONS

CCICU	Claim Canyon intrusive confining unit
CFCM	Crater Flat composite unit
CFCU	Crater Flat confining unit
CHCU	Calico Hills confining unit
CHICU	Calico Hills intrusive confining unit
CHLFA1	Calico Hills lava-flow aquifer 1
CHLFA2	Calico Hills lava-flow aquifer 2
CHLFA3	Calico Hills lava-flow aquifer 3
CHLFA4	Calico Hills lava-flow aquifer 4
CHLFA5	Calico Hills lava-flow aquifer 5
CHVTA	Calico Hills vitric-tuff aquifer
CHZCM	Calico Hills zeolitic composite unit
CPA	Comb Peak aquifer
DVA	Detached volcanics aquifer
DVCM	Detached volcanics composite unit
FCA	Fortymile Canyon aquifer
FCCM	Fluorspar Canyon composite unit
FCCU	Fluorspar Canyon confining unit
FCLLFA	Fortymile Canyon lower lava-flow aquifer
FCLMLFA	Fortymile Canyon lower mafic lava-flow aquifer
FCULFA1	Fortymile Canyon upper lava-flow aquifer 1
FCULFA2	Fortymile Canyon upper lava-flow aquifer 2
FCULFA3	Fortymile Canyon upper lava-flow aquifer 3
FCULFA4	Fortymile Canyon upper lava-flow aquifer 4
FCULFA5	Fortymile Canyon upper lava-flow aquifer 5
FCULFA6	Fortymile Canyon upper lava-flow aquifer 6
FCULFA7	Fortymile Canyon upper lava-flow aquifer 7
FCUMLFA	Fortymile Canyon upper mafic lava-flow aquifer
FCWTA	Fortymile Canyon welded-tuff aquifer
FCWTA1	Fortymile Canyon welded-tuff aquifer 1
IA	Inlet aquifer
ICU	Intrusive confining unit

LIST OF ACRONYMS AND ABBREVIATIONS

KA	Kearsarge aquifer
LCA	Lower carbonate aquifer
LCA3	Lower carbonate aquifer-thrust plate
LCCU	Lower carbonate confining unit
LCCU1	Lower carbonate confining unit-thrust plate
LFA	Lava-flow aquifer
LPCU	Lower Paintbrush confining unit
LVTA2	Lower vitric-tuff aquifer
MGCU	Mesozoic granite confining unit
MPCU	Middle Paintbrush confining unit
NTMMSZ	Northern Timber Mountain Moat structural zone
PBPCU	Post-Benham Paintbrush confining unit
PBRCM	Pre-Belted Range composite unit
PCM	Paintbrush composite unit
PFLA	Paintbrush lava-flow aquifer
PLTA	Paintbrush lava-flow aquifer
PVTA	Paintbrush vitric-tuff aquifer
RMICU	Rainier Mesa intrusive confining unit
RMWTA	Rainier Mesa welded-tuff aquifer
RVICU	Redrock Valley intrusive confining unit
SCCC	Silent Canyon caldera complex
SCCCSM	Silent Canyon caldera complex structural margin
SCICU	Silent Canyon intrusive confining unit
SCVCU	Subcaldera volcanic confining unit
SMLFA	Shoshone Mountain lava-flow aquifer
SPA	Scrugham Peak aquifer
SWA	Stockade Wash aquifer
SWA20SM	Southwest Area 20 structural margin
Tbgb	Grouse Canyon tuff, bedded
Tbgp	Crystal poor Grouse Canyon tuff
TCA	Tiva Canyon aquifer
Tcbs	Bullfrog tuff, Stockade Wash lobe

LIST OF ACRONYMS AND ABBREVIATIONS

Tcg	Latite of Grimy Gulch
TCU	Tuff confining unit
TCVA	Thirsty Canyon volcanic aquifer
Tfbr	Rhyolite of Chukar Canyon
THCM	Tannenbaum Hill composite unit
THCU	Tannenbaum Hill confining unit
THLFA	Tannenbaum Hill lava-flow aquifer
Thr	Mafic-rich Calico Hills formation
TMA	Timber Mountain aquifer
Tmab	Bedded Ammonia Tanks tuff
Tmap	Mafic-poor Ammonia Tanks tuff
TMCC	Timber Mountain caldera complex
TMCCSM	Timber Mountain caldera complex structural margin
TMCM	Timber Mountain composite unit
TMCM2	Timber Mountain composite unit 2
TMD	Timber Mountain dome
TMLVTA	Timber Mountain lower vitric-tuff aquifer
Tmrf	Rhyolite of Fluorspar Canyon
Tmrp	Mafic-poor Rainier Mesa tuff
Tmrr	Mafic-rich Rainier Mesa tuff
Tmt	Basalts of Tierra
TMUWTA	Timber Mountain upper welded-tuff aquifer
TMWTA	Timber Mountain welded-tuff aquifer
Tpc	Tiva Canyon tuff
Tpcm	Pahute Mesa lobe of Tiva Canyon tuff
Tpcx	Tiva Canyon, landslide or breccia
Tpcy	Tuff of Pinyon Pass
Tpd	Rhyolite of Delirium Canyon
Tptm	Pahute Mesa lobe of Topopah Spring tuff
Tptx	Topopah Spring, landslide or breccia
Tqh	Middle rhyolite of Quartz Mountain
TSA	Topopah Spring aquifer

LIST OF ACRONYMS AND ABBREVIATIONS

Ttcl	Lower comendite of Ribbon Cliff
Ttcm	Middle comendite of Ribbon Cliff
Ttp	Pahute Mesa tuff
Ttt	Trail Ridge tuff
UCCU	Upper clastic confining unit
UPCU	Upper Paintbrush confining unit
WSCSZ	Western Silent Canyon structural zone
WTA	Welded-tuff aquifer
WWA	Windy Wash aquifer
YMCFCM	Yucca Mountain Crater Flat composite unit
YVCM	Younger volcanic composite unit

Elements and Compounds

Ac	Actinium
Ag	Silver
Al	Aluminum
Am	Americium
Ar	Argon
As	Arsenic
Ba	Barium
Be	Beryllium
Bi	Bismuth
Br	Bromide
C	Carbon
Ca	Calcium
Cd	Cadmium
Ce	Cerium
Cl	Chlorine
Co	Cobalt
CO_3	Carbonate
Cr	Chromium

LIST OF ACRONYMS AND ABBREVIATIONS

Cs	Cesium
DIC	Dissolved inorganic carbon
DOC	Dissolved organic carbon
Eu	Europium
F	Fluorine
Fe	Iron
H	Hydrogen
^3H	Tritium
HCO_3	Bicarbonate
He	Helium
Hg	Mercury
I	Iodine
K	Potassium
Kr	Krypton
Li	Lithium
LiBr	Lithium bromide
Mg	Magnesium
Mn	Manganese
Na	Sodium
Nb	Niobium
Ne	Neon
O	Oxygen
Pb	Lead
Pm	Promethium
Pu	Plutonium
Ru	Ruthenium
Sb	Antimony
Se	Selenium
SiO_2	Silicon dioxide
SO_4	Sulfate
Sr	Strontium
Tc	Technetium

LIST OF ACRONYMS AND ABBREVIATIONS

Th	Thorium
Tl	Thallium
U	Uranium
Xe	Xenon
Y	Yttrium
δD	Delta deuterium
$\delta^{13}C$	Delta carbon-13
$\delta^{18}O$	Delta oxygen-18
$\delta^{34}S$	Delta sulfur-34

ACKNOWLEDGEMENT

This document is the result of the contributions of several individuals from the Underground Test Area (UGTA) Activity participant organizations. These individuals have contributed to either the technical content of the document, the editorial and graphical display of the technical information, or the technical and quality review of the document. In addition, the management of the activities and staff supporting the document are acknowledged.

Technical contributions to the document were provided by Robert Andrews, Irene Farnham and Pete Martian (Navarro-Intera, LLC [N-I]); Ron Hershey (Desert Research Institute [DRI]); Ed Kwicklis (Los Alamos National Laboratory [LANL]); and Ate Visser and Mavrik Zavarin (Lawrence Livermore National Laboratory [LLNL]).

Technical reviews of the draft of this document significantly improved the quality and content of this report. These reviews were performed by Mavrik Zavarin (LLNL), Joe Fenelon (U.S. Geological Survey [USGS]), Sig Drellack (National Security Technologies, LLC [NSTec]), Ed Kwicklis (LANL), and Chuck Russell (DRI).

The editorial and graphical display of information in this document was greatly aided by Ellen Cook, Afief Fadil, and Christy Morris (N-I). Quality reviews of the document were performed by Janet Richardson, Susan Krenzien, and Joe Johnston (N-I).

Management of the staff and activities supporting this document include the Pahute Mesa Corrective Action Unit (CAU) Lead, Greg Ruskauff (N-I), and UGTA Project Manager Sam Marutzky (N-I). This work was sponsored by the UGTA management team at the U.S. Department of Energy, National Nuclear Security Administration Nevada Field Office, notably UGTA Activity Lead Bill Wilborn.

1.0 INTRODUCTION

Well Pahute Mesa #3 (PM-3) was constructed in 1988 and recompleted in 1992 for the U.S. Department of Energy's (DOE) Hydrology and Radionuclide Migration Program (HRMP) (DOE/NV, 1996). The well is located at northing 4,121,281 meters (m) and easting 539,012 m (North American Datum [NAD] 1983 Universal Transverse Mercator [UTM] Zone 11) in the Thirsty Canyon area of Nye County, Nevada, on the Nevada Test and Training Range (NTTR). It is approximately 3.2 kilometers (km) (2 miles [mi]) west of operable Area 20 of the Nevada National Security Site (NNSS) and is at an elevation of 1,774.9 m (5,823 feet [ft]) above mean sea level (amsl). Figure 1-1 shows the location of PM-3 relative to existing wells, boreholes, NNSS and NTTR boundaries, and underground nuclear tests.

Well development and sampling activities were conducted at PM-3 between July 30 and August 27, 2013, in order to evaluate the geochemistry and radiochemistry of the groundwater at this location and compare the results to previous sampling using depth-discrete bailers. The upper interval accessed the Upper Paintbrush confining unit (UPCU) (upper piezometer PM-3-2). The lower interval accessed the Tiva Canyon aquifer (TCA) and the upper portion of the Lower Paintbrush confining unit (LPCU) (lower piezometer PM-3-1) (Figure 1-2). Well development objectives included removing residual fluids from the two piezometers that accessed the completion intervals by pumping the well using a pump jack in order to improve the hydraulic connection to the formation and to restore the natural groundwater chemistry within the completion intervals. Groundwater sampling activities consisted of non-depth-discrete bailer samples for low-level tritium (^3H) before pump installation and groundwater characterization sampling of the completion intervals for hydrogeologic, geochemical, and radiochemistry data after purging and stable water quality was achieved. Throughout the remainder of the report, the PM-3 deep completion zone will be referred to as PM-3-1 (deep), and the PM-3 shallow completion zone will be referred to as PM-3-2 (shallow).

This report summarizes the analyses of the groundwater results from sampling of PM-3-1 (deep) and PM-3-2 (shallow), with a particular focus of evaluating the groundwater geochemistry data in comparison to the geochemistry observed in other wells in the Thirsty Canyon area as well as to

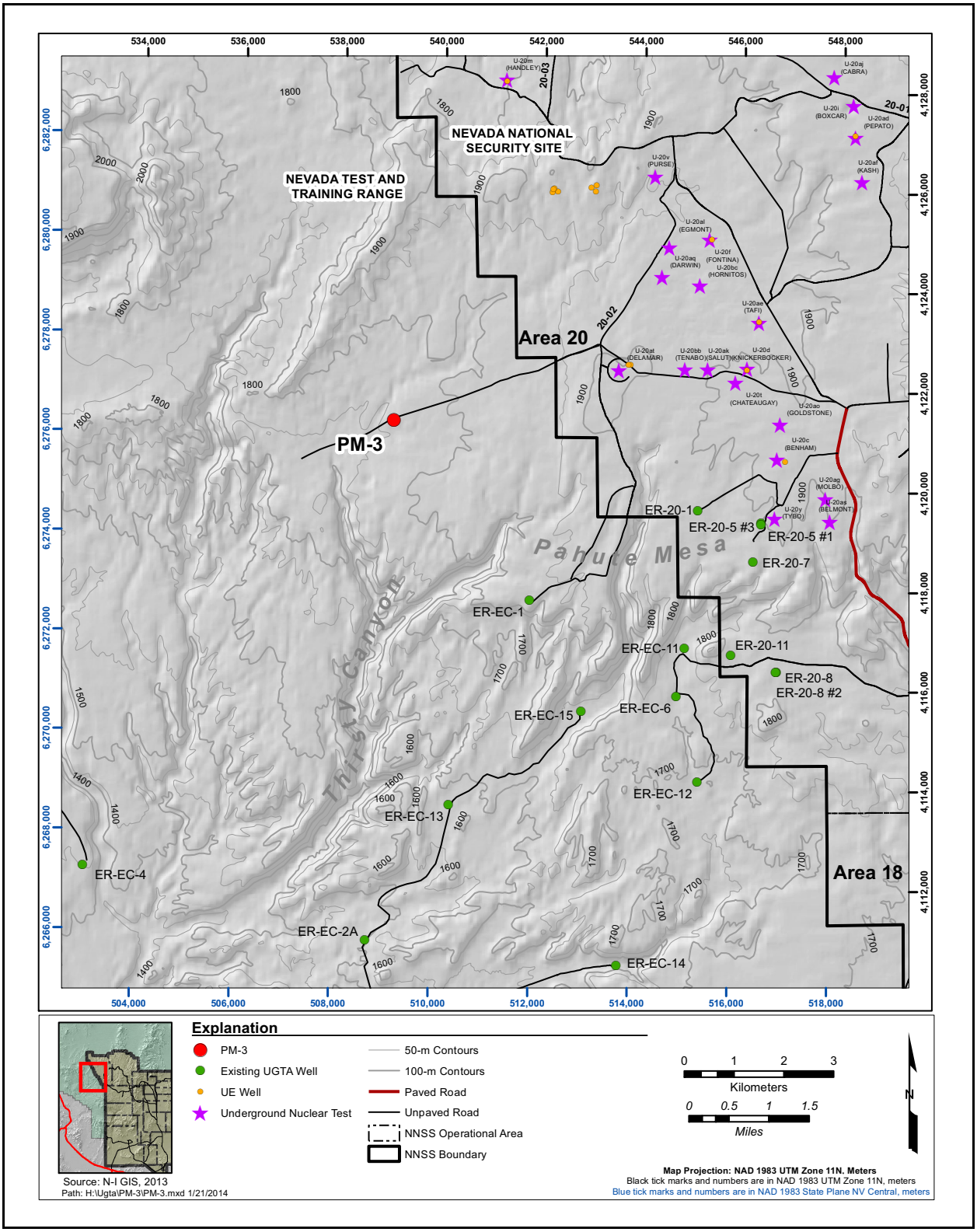

Figure 1-1
Topographic Map of the PM-3 Area
Source: N-I, 2014b

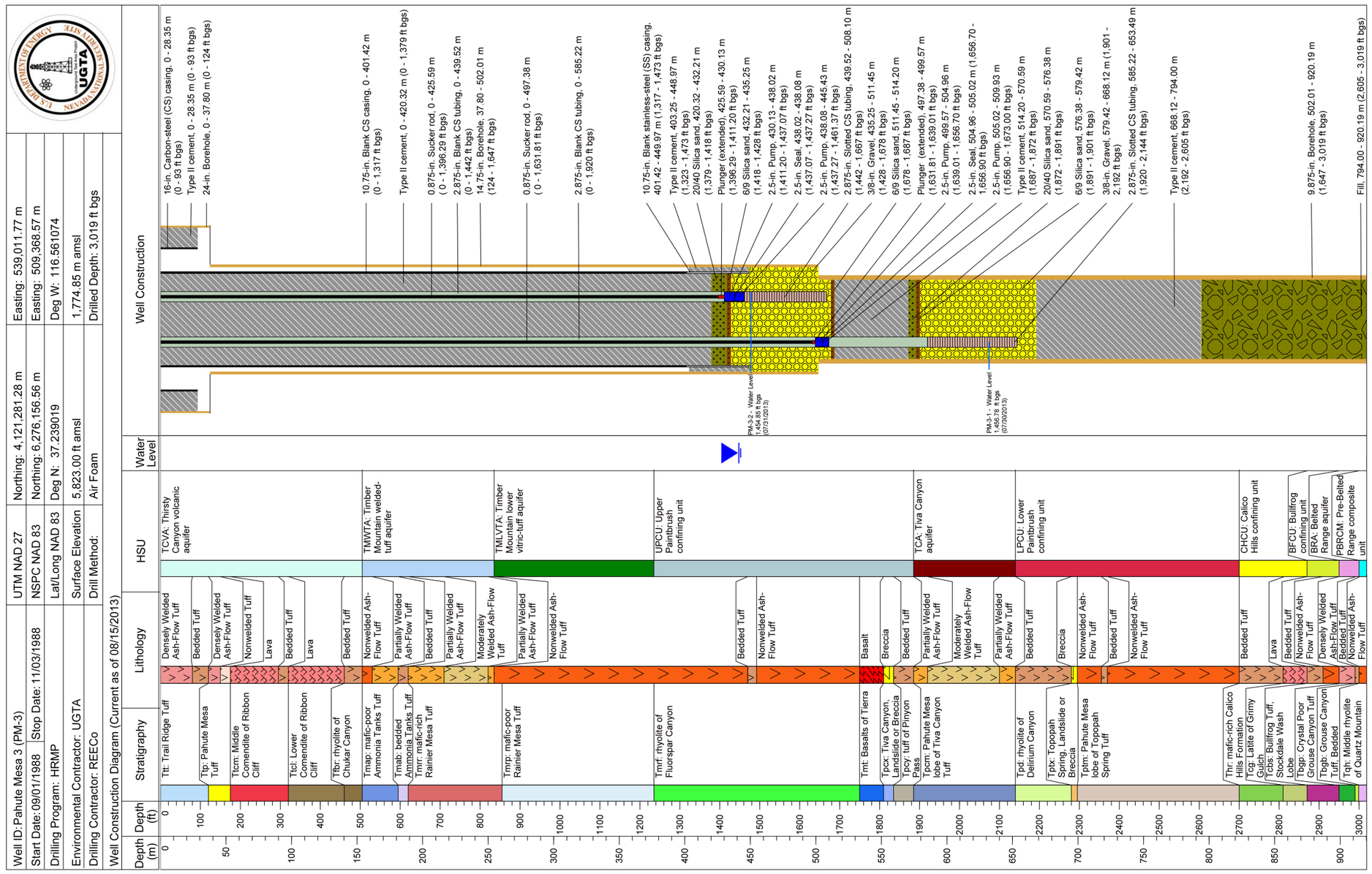

Figure 1-2
Well Completion Diagram for PM-3
Source: N-I, 2014b

evaluate the potential source of ^3H observed in these piezometers from previous sampling activities, which employed depth-discrete bailers or a Bennett submersible piston pump.

1.1 Objectives

The primary purpose for well development and purging was to collect groundwater samples from the PM-3-1 (deep) and PM-3-2 (shallow) piezometers to characterize the groundwater chemistry from an area located west and southwest of areas of historic underground nuclear tests on the NNSS. An important objective of this evaluation was to confirm the presence of ^3H measured in sampled groundwater from depth-discrete bailed water samples collected by Routine Radiological Environmental Monitoring Program (RREMP) in 2010 and 2011 and by the Underground Test Area (UGTA) Project (now UGTA Activity) in 2011. The results of the RREMP sampling and the 2011 bailer sampling are summarized in the *Data Report for Well Pahute Mesa #3 (PM-3) Groundwater Sampling* (N-I, 2011). The results of the well development and sampling using the pump jack are summarized in the *Well Pahute Mesa #3 (PM-3) Well Development and Sampling Data Report* (N-I, 2014b) and in Appendix A.

The objective of this report is to compare the analyzed chemistry data to other geochemical data in the Thirsty Canyon area, and to evaluate the possible sources of the ^3H observed in the sampled groundwater from both PM-3-1 (deep) and PM-3-2 (shallow).

1.2 History of Field Activities at PM-3

Drilling and construction of PM-3 occurred from September to November 1988. The borehole was drilled to a total depth (TD) of 3,019 ft below ground surface (bgs) and was completed to a depth of 1,473 ft bgs with 10.75-in. carbon-steel (CS) and stainless-steel (SS) casing (DOE/NV, 1991). The borehole was left open from 1,473 ft to the TD of 3,019 ft bgs.

The well was recompleted between January and March of 1992 with the installation of a deep piezometer, PM-3-1 (deep), and a shallow piezometer, PM-3-2 (shallow) (DOE/NV, 1996). The well recompletion design was based on the results of hydraulic testing conducted in 1988, which identified two transmissive intervals of interest.

The deep piezometer (PM-3-1 [deep]) was installed to a depth of 2,144 ft bgs and consists of 2.875-in. CS slotted tubing from 1,919 to 2,144 ft bgs with gravel and sand placed in the borehole

annulus from 1,872 to 2,192 ft bgs. The shallow piezometer (PM-3-2 [shallow]) was installed to a depth of 1,667 ft bgs and consists of 2.875-in. CS slotted tubing from 1,442 to 1,667 ft bgs with gravel and sand placed in the borehole annulus from 1,379 to 1,687 ft bgs. The screened interval of PM-3-1 (deep) spans the TCA, which is a welded-tuff aquifer (WTA); and the screened interval of PM-3-2 (shallow) spans the UPCU, which is a tuff confining unit (TCU). The well completion diagram for the recompleted configuration is illustrated in Figure 1-2.

During recompletion activities, approximately 105,000 gallons (gal) of water believed to be derived from U-20 WW with a lithium bromide (LiBr) tracer was introduced in the well. However, circulation to the surface was never achieved, and the fluids used during recompletion remained in the hole. Because of the small size of the piezometers, it was not feasible to install an electric submersible pump to remove the completion fluids. The piezometers were partially developed using a 1.9-inch (in.) swabbing assembly in each piezometer. During well development, approximately 20,200 gal of water was swabbed from the piezometers (DOE/NV, 1996). Further development was not performed. Additional details on recompletion activities are discussed in the *PM-3 Well Recompletion Summary for the Groundwater Characterization Project (GCP)* (DOE/NV, 1992) and the *Recompletion Report and Summary of Well History for Well PM-3* (DOE/NV, 1996).

After drilling and well recompletion activities, PM-3 has been sampled by a number of different sampling techniques. Most sampling has used a depth-discrete bailer sampler. However, Desert Research Institute (DRI) used a low-flow Bennett pump for sampling in 2000. Most recently, a pump jack was used to ensure the gravel pack around the PM-3-1 (deep) and PM-3-2 (shallow) piezometers was adequately purged before sampling. Photographs of both the depth-discrete bailer and the pump-jack sampling activities are presented in Figure 1-3.

1.3 Geologic Background

PM-3 is located between the Silent Canyon caldera complex (SCCC) to the east–northeast, the Timber Mountain caldera complex (TMCC) to the south, the Black Mountain caldera to the northwest, and Thirsty Canyon to the southwest. The well is located in the vicinity of the north–northeast trending Thirsty Canyon lineament located over 1 km west of PM-3. This lineament forms the western boundaries of the TMCC and SCCC and is characterized by a zone of en echelon faults that are 2 to 3 km wide (BN, 2002). PM-3 is located less than 2 km west of the Purse Fault, which generally strikes north–south in the area, and about 1 km north of the Northern Timber

Figure 1-3
Photographs of Depth-Discrete Bailer (Upper) and Pump Jack (Lower) at PM-3

Mountain Moat structural zone (NTMMSZ), which trends northwest–southeast in the area. The location of PM-3 to these volcanic and structural features is illustrated in Figure 1-4.

The hydrostratigraphic units (HSUs) intersected by PM-3 are, from the surface, the Thirsty Canyon volcanic aquifer (TCVA), Timber Mountain welded-tuff aquifer (TMWTA), Timber Mountain lower vitric tuff Aquifer (TMLVTA), Upper Paintbrush confining unit (UPCU), Tiva Canyon aquifer (TCA), Lower Paintbrush confining unit (LPCU), the Calico Hills zeolitic composite unit (CHZCM), Bullfrog confining unit (BFCU), Belted Range aquifer (BRA), and Pre-Belted Range composite unit (PBRCM). The water table at PM-3 is in the UPCU. The UPCU generally consists of zeolitic bedded and nonwelded tuffs that occurs above the welded and zeolitic nonwelded and bedded Tiva Canyon tuff (Tpc). The TCA is a WTA composed of welded ash-flow tuffs. The PM-3-2 (shallow) piezometer is open to the UPCU, while the PM-3-1 (deep) piezometer is open to the TCA and a small amount of the LPCU, as illustrated in the well completion diagram (Figure 1-2).

1.4 Hydrogeologic Background

PM-3 is located in the Black Mountain tributary flow system of the Oasis Valley flow system within the alluvial/volcanic aquifers of the NNSS area (Fenelon et al., 2010). The locations of the regional groundwater flow directions in the flow system near PM-3 are illustrated in Figure 1-5. The potentiometric surface of the volcanic aquifers in the vicinity of PM-3 is depicted in Figure 1-6.

Water levels in PM-3 have been monitored by the U.S. Geological Survey (USGS) from 1992 to present and indicate a 4-ft rising trend from 1992 to present. These water-level measurements are interpreted to represent steady-state conditions in the volcanic aquifers open to the well. The rising water-level trend is a response to wetter-than-normal climatic conditions. The water-level trend in PM-3-1 (deep) is nearly identical to the trend in PM-3-2 (shallow). Water levels in PM-3-1 (deep) are about 2 ft lower than in PM-3-2 (shallow), indicating an apparent downward vertical gradient in the vicinity of the well (Fenelon et al., 2010).

Shortly after drilling of PM-3 was completed, an electric submersible pump was installed. A constant-rate test was conducted in September 1988 at a pumping rate of 639.7 liters per minute (169 gallons per minute [gpm]) for a period of 31 hours. The drawdown recorded after 31 hours was 23.7 m (78 ft). In addition to the constant-rate test, six injection tests and flow logging were conducted in October 1988. The results of the constant-rate test, injection tests, and flow logging

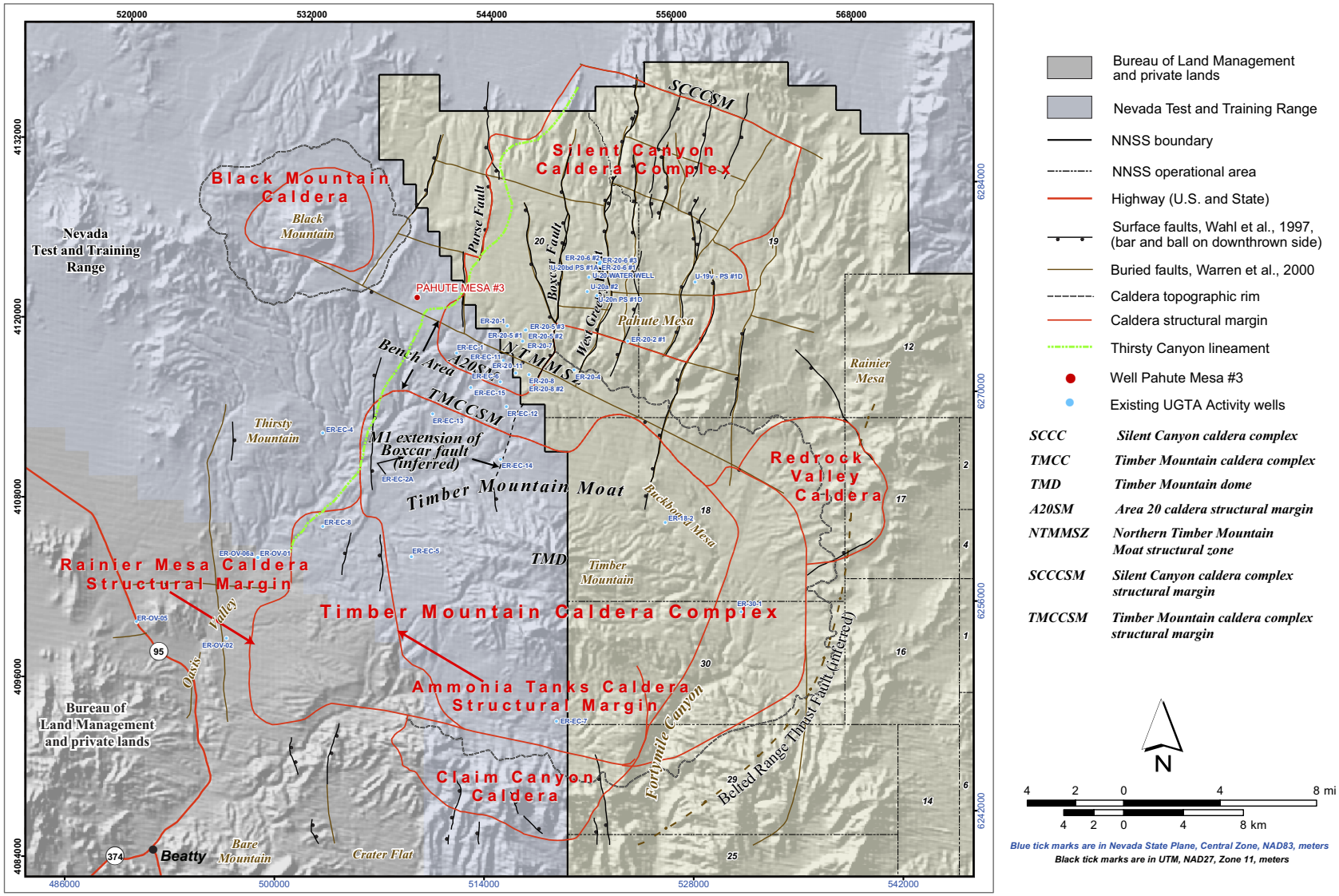

Figure 1-4
Location of PM-3 and Geologic Structural Features
Source: Modified from NNSA/NSO, 2009

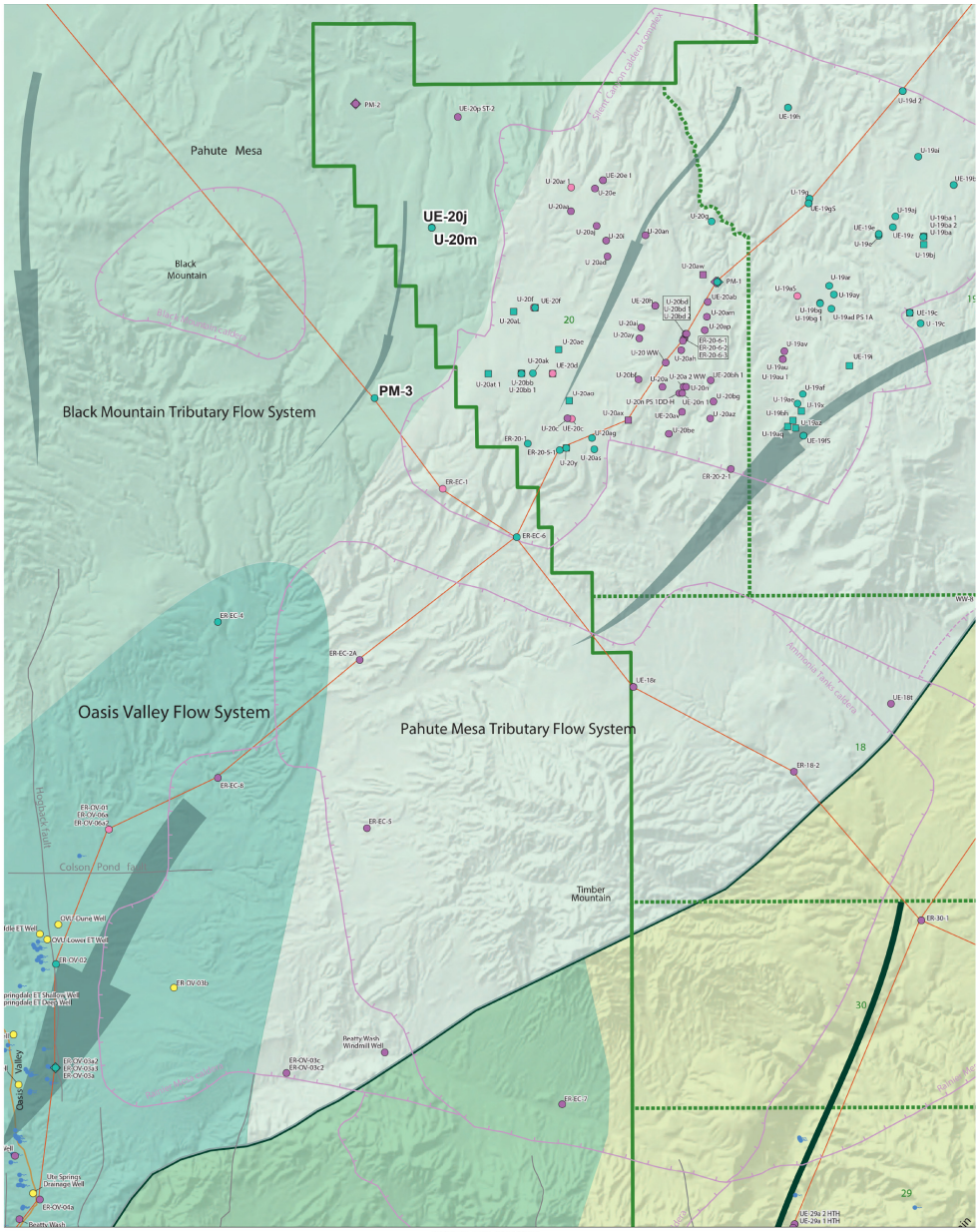

EXPLANATION

Regional groundwater flow—Arrow indicates regional flow direction. Arrow width indicates relative flow volume. Arrow and flow-system outline color identifies downgradient flow system. Shading color delineates tributary flow system or flow system labeled on map. The mapped locations of the boundaries of the tributary flow systems and flow systems could be in error by several miles

Local groundwater system—Defined by permeable alluvial and volcanic rock of limited extent. Downward leakage is source of localized or diffuse flow to underlying flow system

19 **Boundary of Nevada Test Site**—Dashed line indicates boundaries of internal operational areas at Nevada Test Site. Number identifies operational area

B B′ **Line of hydrogeologic section**—Sections shown on plate 2

Army 1 WW **Borehole on section with name**—Gray circle and bold name identify borehole on section only

Spring

Major geologic structure or feature important to flow in regional alluvial-volcanic flow system—Locationshown on map is below l and surface at about the depth of saturation. Line dashed where uncertain, inferred, or approximately located

Caldera structural margin

Normal fault

Strike-slip fault

Hydraulic head measurement location—Shows name of borehole used to develop potentiometric contours in the regional alluvial-volcanic aquifer

J-12 WW Borehole name

Well open to alluvial aquifer

Well open to volcanic aquifer

Well open to volcanic composite unit

Well open to alluvial aquifer and volcanic aquifer

Well open to alluvial aquifer and alluvial confining unit

Well open to volcanic aquifer and local or regional carbonate aquifer

Well open to volcanic aquifer and the volcanic composite unit

Hydraulic head anomalously high. Symbol color on map indicates rock type at opening

Hydraulic head anomalously low. Symbol color on map indicates rock type at opening

Figure 1-5
Location of PM-3 and General Groundwater Flow Paths
Source: Modified from Fenelon et al., 2010

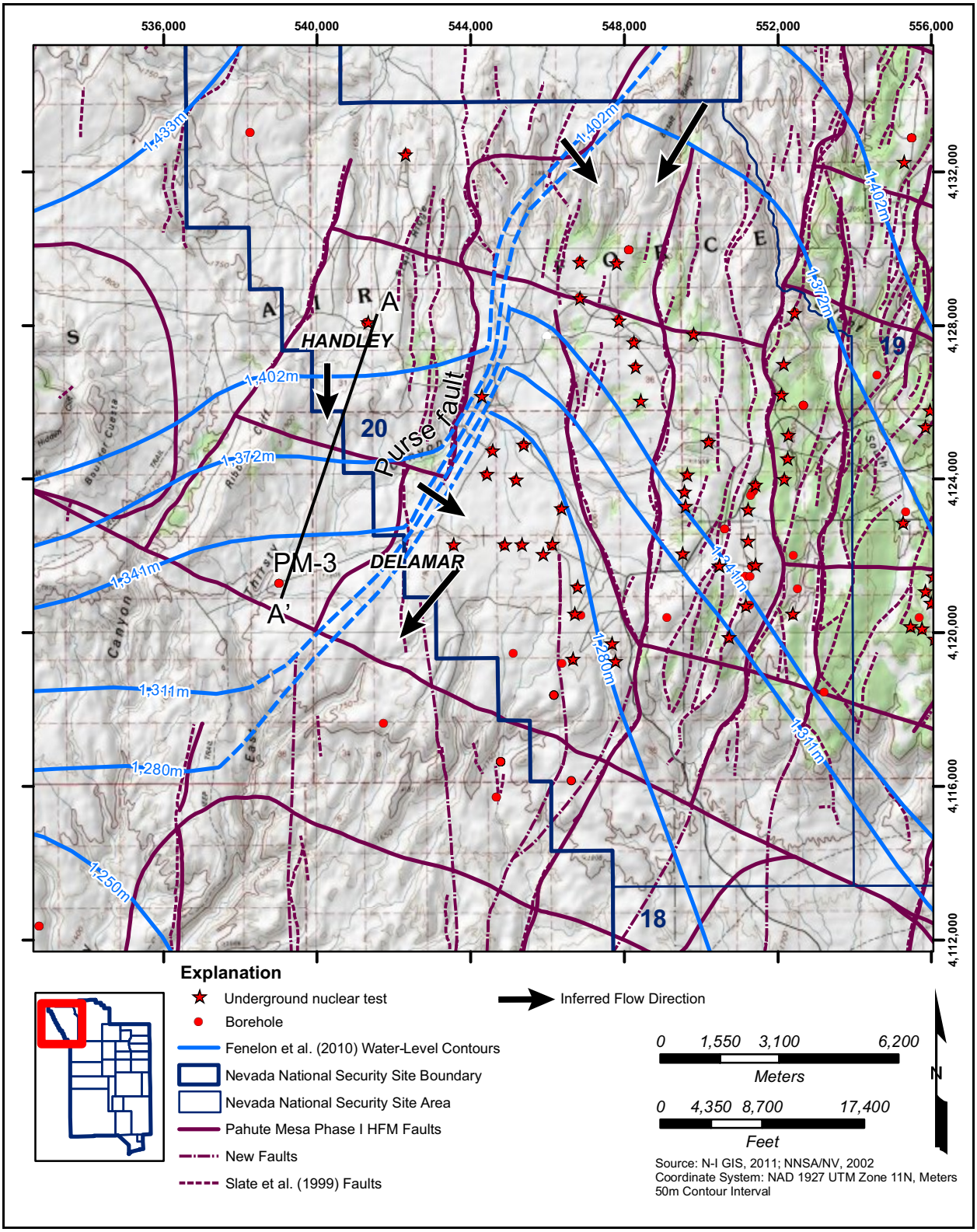

Figure 1-6
Location of PM-3 and Local Potentiometric Surface
Source: N-I, 2011

identified two transmissive zones (DOE/NV, 1996). The first transmissive interval is located within the rhyolite of Fluorspar Canyon (Tmrf) between 1,473 to 1,667 ft bgs, where a thermal anomaly was noted and fractures were identified within the borehole. The second transmissive interval is located within the Tiva Canyon tuff (Tpc) between 1,934 to 2,134 ft bgs, where again fractures were identified within the borehole (Kilroy and Savard, 1996). Details of the hydraulic testing operations are discussed in the *Hydrology Radionuclide Migration Program, Final Draft Well Completion Report Well PM-3* (DOE/NV, 1991).

Additional analysis of the hydraulic testing performed in the PM-3 borehole is presented in Appendix B.

1.5 Geochemistry Background

Previous geochemistry studies in the vicinity of PM-3 identified potential groundwater flow paths in the Pahute Mesa–Oasis Valley flow system (Thomas et al., 2002; Kwicklis et al., 2005; Rose et al., 2006) where PM-3 resides. The key conclusions of these studies as they relate to groundwater flow in the Thirsty Canyon area around PM-3 are summarized in this subsection.

Thomas et al. (2002) identified five different flow paths that included Pahute Mesa groundwater. These flow paths were (1) Pahute Mesa groundwater flowing to Oasis Valley, (2) groundwater north of Oasis Valley mixing with Pahute Mesa groundwater flowing to Oasis Valley, (3) groundwater north of Oasis Valley flowing to northwest Oasis Valley, (4) Pahute Mesa groundwater flowing south of Timber Mountain through Beatty Wash area to Oasis Valley, and (5) Pahute Mesa groundwater flowing down Fortymile Canyon. This study included boreholes and wells on Pahute Mesa and wells and springs in the Oasis Valley area; UGTA Activity wells between Pahute Mesa and Oasis Valley (ER wells) had not been drilled at that time. Geochemical water-rock reactions models did not specifically include PM-3 as an end-member groundwater; rather, an “average” Pahute Mesa groundwater was used. Thomas et al. (2002) flow-paths 1 and 2 would have included some component of groundwater in the vicinity of PM-3, but only as it contributed to the “average” Pahute Mesa groundwater. Groundwater travel times from Pahute Mesa to Oasis Valley using dissolved organic carbon (DOC) carbon-14 (^{14}C) and water-rock reaction model-corrected dissolved inorganic carbon (DIC) ^{14}C ranged from 1,700 to 6,800 years.

Rose et al. (2006) updated the work of Thomas et al. (2002) by including new geochemical and isotopic data from eight new wells (ER-EC-1 to ER-EC-8) drilled between western Pahute Mesa and the Oasis Valley area. They identified two chemically and isotopically distinct groundwater masses roughly separated by the hydraulic discontinuity near the Purse Fault in western Pahute Mesa. Groundwater east of the discontinuity has low chlorine (Cl) and sulfate (SO_4) concentrations, with an average delta deuterium (δD) value near -113 per mil (‰); while groundwater west of the discontinuity has higher Cl and SO_4 concentrations, and δD value near -116 ‰. PM-3 penetrates the chemically distinct groundwater west of the discontinuity. Groundwater downgradient from these two chemically different groundwater masses has intermediate chemical and isotopic compositions, suggesting mixing of the two water masses.

Rose et al. (2006) modeled a sixth groundwater flow path (Figure 1-7) from central Pahute Mesa ± upper Thirsty Canyon = Crater Flat groundwater. The other five flow paths were similar to those in Thomas et al. (2002) except that the two chemically and isotopically distinct groundwaters were treated as two different end members for water-rock reaction modeling (upper Thirsty Canyon and central Pahute Mesa). PM-3 was grouped into the upper Thirsty Canyon end member. Geochemical water-rock reactions models did not specifically use PM-3 as a representative end-member groundwater in these flow paths.

Water-rock reaction modeling and mixing of conservative tracers for flow-path 1(A) indicated that the more chemically dilute groundwater lower in Thirsty Canyon (represented by ER-EC-2A, ER-EC-6, and ER-EC-8) could be derived by mixing central Pahute Mesa groundwater (represented by U-20 WW) with upper Thirsty Canyon groundwater (ER-EC-1) and local recharge. Upper Thirsty Canyon groundwater made up between 5 and 22 percent of the mixture. Water-rock reaction corrected DIC ^{14}C travel times for the mixture to lower Thirsty Canyon were less than 1,000 years, the younger limit of ^{14}C dating.

Geochemical mixing models of flow-path 1 down to Oasis Valley (ER-OV-1) consisted of 29 to 51 percent of upper Thirsty Canyon groundwater or 1,750 to 3,100 acre-feet per year (ac-ft/yr). The groundwater travel time from central Pahute Mesa to Oasis Valley ranged from less than 1,000 years to 4,000 years using corrected DIC ^{14}C and DOC ^{14}C groundwater ages. Groundwater flow velocities along a straight line from Pahute Mesa (U-20 WW) to Oasis Valley (Goss Springs) ranged from 8 to less than 37 meters per year (m/yr).

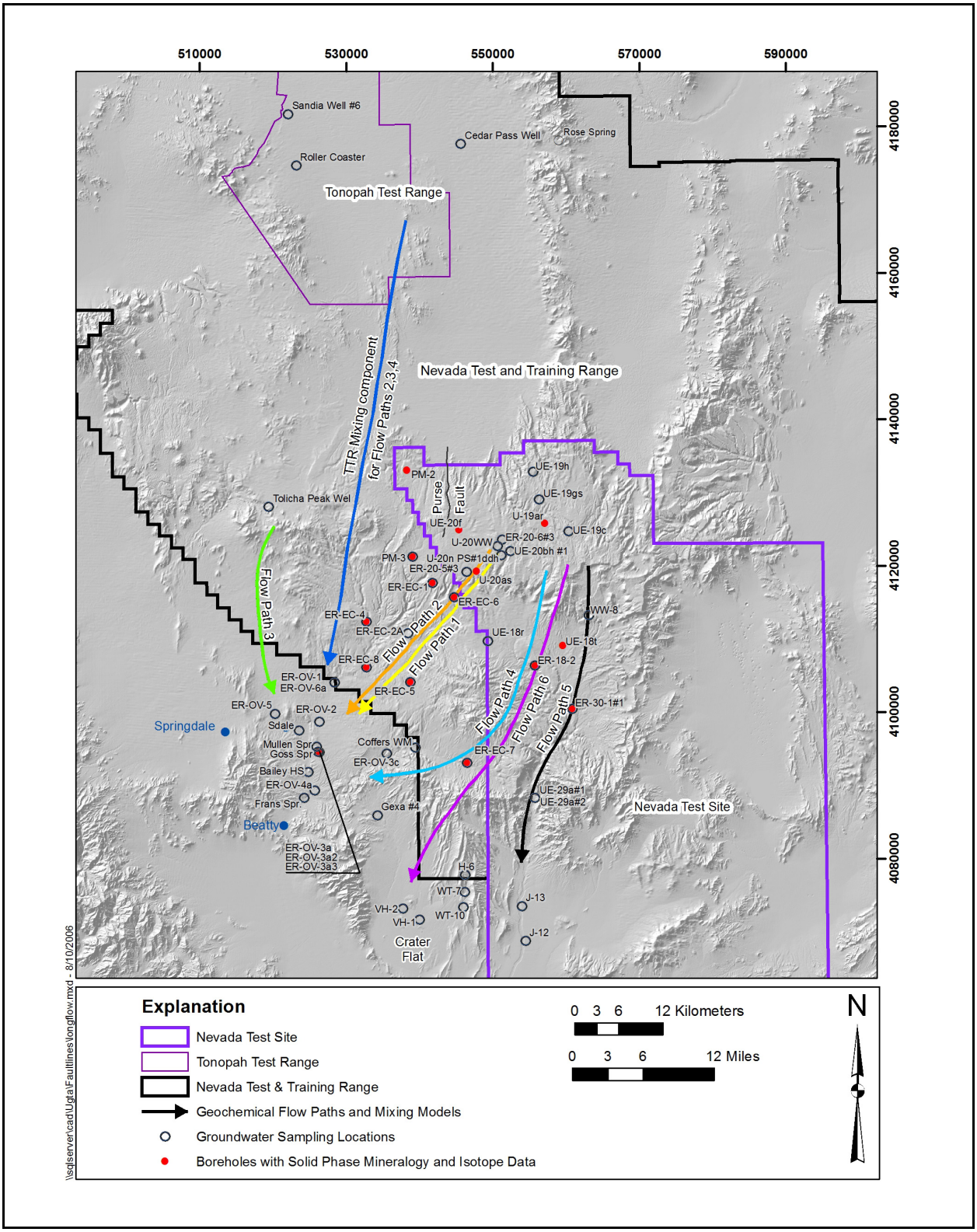

Figure 1-7
Groundwater Flow Paths Modeled in Rose et al. (2006)

Geochemical mixing models of flow-path 2 were successful to lower Thirsty Canyon (upper Oasis Valley) at Well ER-OV-1 but unsuccessful further into central Oasis Valley (ER-OV-3a). Flow-path 2 was similar to flow-path 1 but also included a component of groundwater north of Oasis Valley from the area of the Tonopah Test Range (Gold Flat and Cactus Flat). Successful models to lower Thirsty Canyon (upper Oasis Valley) consisted of 10 to 40 percent upper Thirsty Canyon groundwater with travel times for the mixture from less than 1,000 years to 2,300 years.

Kwicklis et al. (2005) also conducted an analysis of groundwater flow using chemical and isotopic tracers from Pahute Mesa to Oasis Valley (Figure 1-8) similar to Rose et al. (2006) and Thomas et al. (2002). In their analysis, Kwicklis et al. (2005) reexamined flow-paths 1 and 2 of Rose et al. (2006), but used slightly different wells to represent the various end-member groundwater chemistries.

Water-rock reaction modeling resulted in 29 to 47 percent of groundwater from upper Thirsty Canyon (represented by the water chemistry at ER-EC-1) making up the groundwater in central Oasis Valley (ER-OV-3a). In the reanalysis of flow-path 2, again using several different wells to represent the end-member groundwater chemistries, the water of upper Thirsty Canyon (more saline and isotopically lighter) had a greater contribution to the groundwater of lower Thirsty Canyon at ER-OV-,1 ranging from 55 to 93 percent. The water chemistry at PM-3 was not used as an end member in water-rock reaction modeling.

1.6 Summary of Sampling Activities and Results at PM-3

One of the principal purposes of the drilling of PM-3 was to provide a location to sample groundwater in the area west of the identified hydrologic discontinuity to the west of the Purse fault. The history of the sampling activities performed at PM-3 is summarized below with a particular focus on the sampling conducted to evaluate the presence of ^3H.

PM-3 was sampled during drilling, well development, and hydraulic testing in 1988 and resampled in 1989. The samples were collected at the surface by pumping, air lift, and depth-discrete bailers. The ^3H concentrations from these samples were less than the minimum detectable concentration (MDC) of 16 picocuries per liter (pCi/L). The well was not sampled during recompletion activities performed in 1992 due to the drilling water still present in the well and the formations surrounding the well.

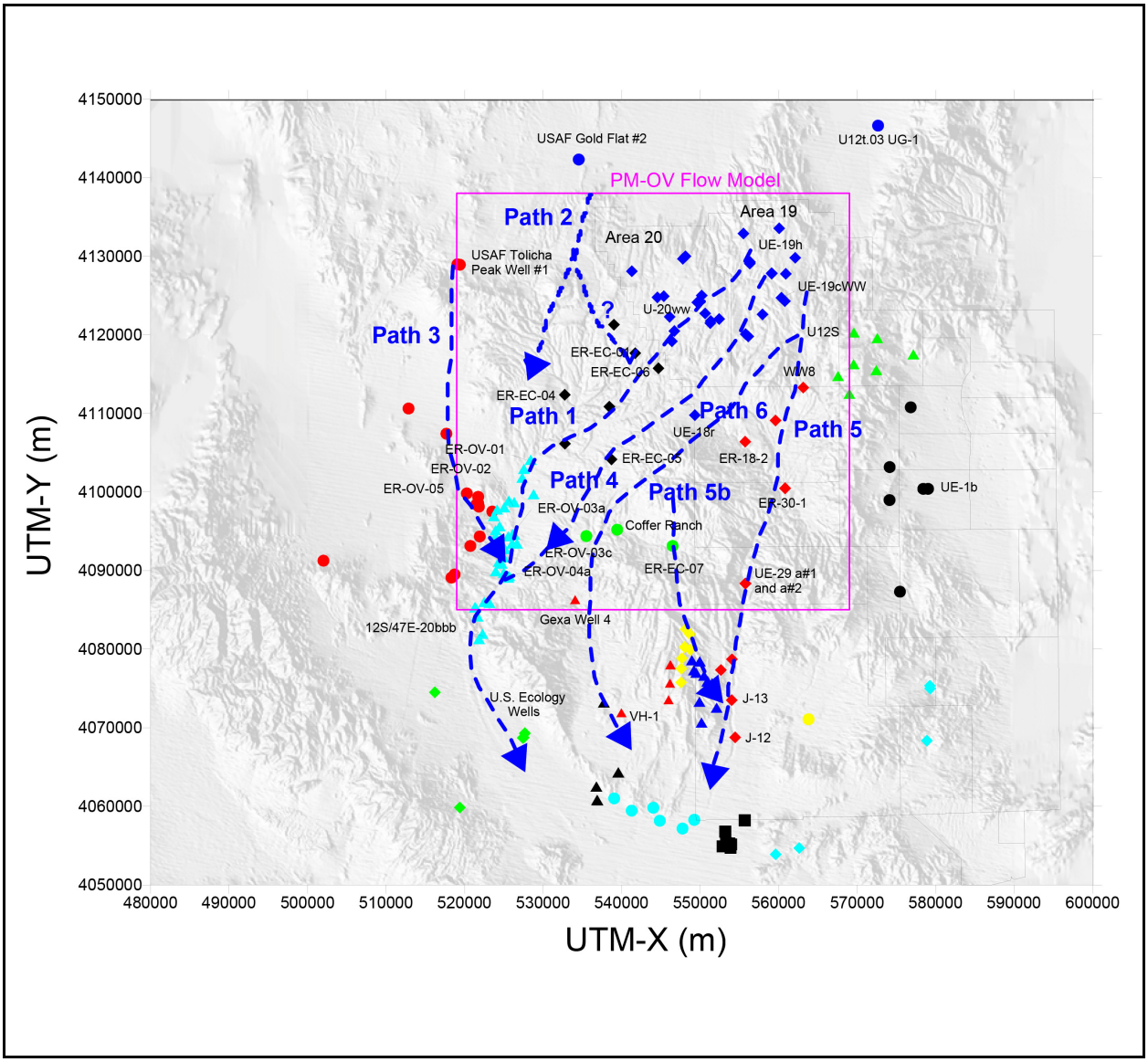

Figure 1-8
Groundwater Flow Paths Modeled in Kwicklis et al. (2005)

In December 1999, depth-discrete bailer samples from PM-3-2 (shallow) and PM-3-1 (deep) were collected, and the ^{3}H field-screening analysis reported elevated levels of ^{3}H of 246,847 pCi/L and 4,663 pCi/L, respectively. An evaluation of the 1999 sample collection activity determined the elevated ^{3}H levels were attributed to a ^{3}H-contaminated bailer used in sample collection from PM-3-2 (shallow) (Wycoff, 2000).

In January 2000, groundwater samples from PM-3-2 (shallow) were collected. The ^{3}H results of the samples were below the MDC of 280 pCi/L. In September 2000, ^{3}H samples were collected from PM-3-2 (shallow) and PM-3-1 (deep) using a wireline-deployed depth-discrete bailer. In October

2000, an additional ^3H sample was collected from PM-3-2 (shallow) using a Bennett pump. Analysis of the samples collected in September 2000 indicated no ^3H above the MDCs of 6.48 and 6.45 pCi/L. Analysis of the sample collected in October 2000 indicated low levels of ^3H at 12.1 pCi/L. These data were flagged as highly uncertain and likely overestimated ^3H concentrations.

Depth-discrete bailer sampling has been conducted annually by the RREMP beginning in November 2000. The samples collected by RREMP have been analyzed for ^3H and additional parameters. Samples collected by RREMP between November 2000 and April 2009 did not indicate ^3H above the sample MDCs, which ranged from 9 to 29 pCi/L.

In May 2010, RREMP collected a ^3H sample from PM-3-2 (shallow) that yielded a result of 48.3 pCi/L (above the 25.5-pCi/L MDC). In June 2010, a ^3H sample was collected from PM-3-1 (deep) that yielded a result below the MDC of 27.8 pCi/L. In July 2011, the RREMP returned to PM-3 and collected ^3H samples from PM-3-2 (shallow) and PM-3-1 (deep) that yielded results of 58.0 pCi/L and 63.2 pCi/L from PM-3-2 (shallow), and 33.8 pCi/L and 19.5 pCi/L from PM-3-1 (deep). In March 2012, analysis of samples yielded ^3H results of 64.6 and 73.4 pCi/L from PM-3-2 (shallow) and 39 and 52.9 pCi/L from PM-3-1 (deep). Analytical results for these samples are presented in Appendix A.

In July 2013, UGTA returned to PM-3 and conducted well development and sampling from both PM-3-2 (shallow) and PM-3-1 (deep). The deep and shallow piezometers were configured with a pump jack and pumped at 3 to 4 gpm until the water quality was observed to stabilize. Once the water quality had stabilized (after about 24,200 gal on August 11, and 28,800 gal on August 12 from PM-3-1 [deep]; and about 31,800 gal on August 22, and about 36,000 gal on August 23 from PM-3-2 [shallow]), water samples were taken and analyzed for the full characterization suite of geochemical and radiochemical parameters. The laboratory and field results for these samples are presented in Appendix A and discussed in Section 2.3.

Complete details on the groundwater sampling conducted in 2010 using depth-discrete bailers are presented in the *Data Report for Well Pahute Mesa #3 (PM-3) Groundwater Sampling* (N-I, 2011). Complete details on the well development and groundwater sampling conducted in 2013 using both depth-discrete bailers and the pump jack are presented in the *Well Pahute Mesa #3 (PM-3) Well Development and Sampling Data Report* (N-I, 2014b). Figures 1-9 and 1-10 compile the

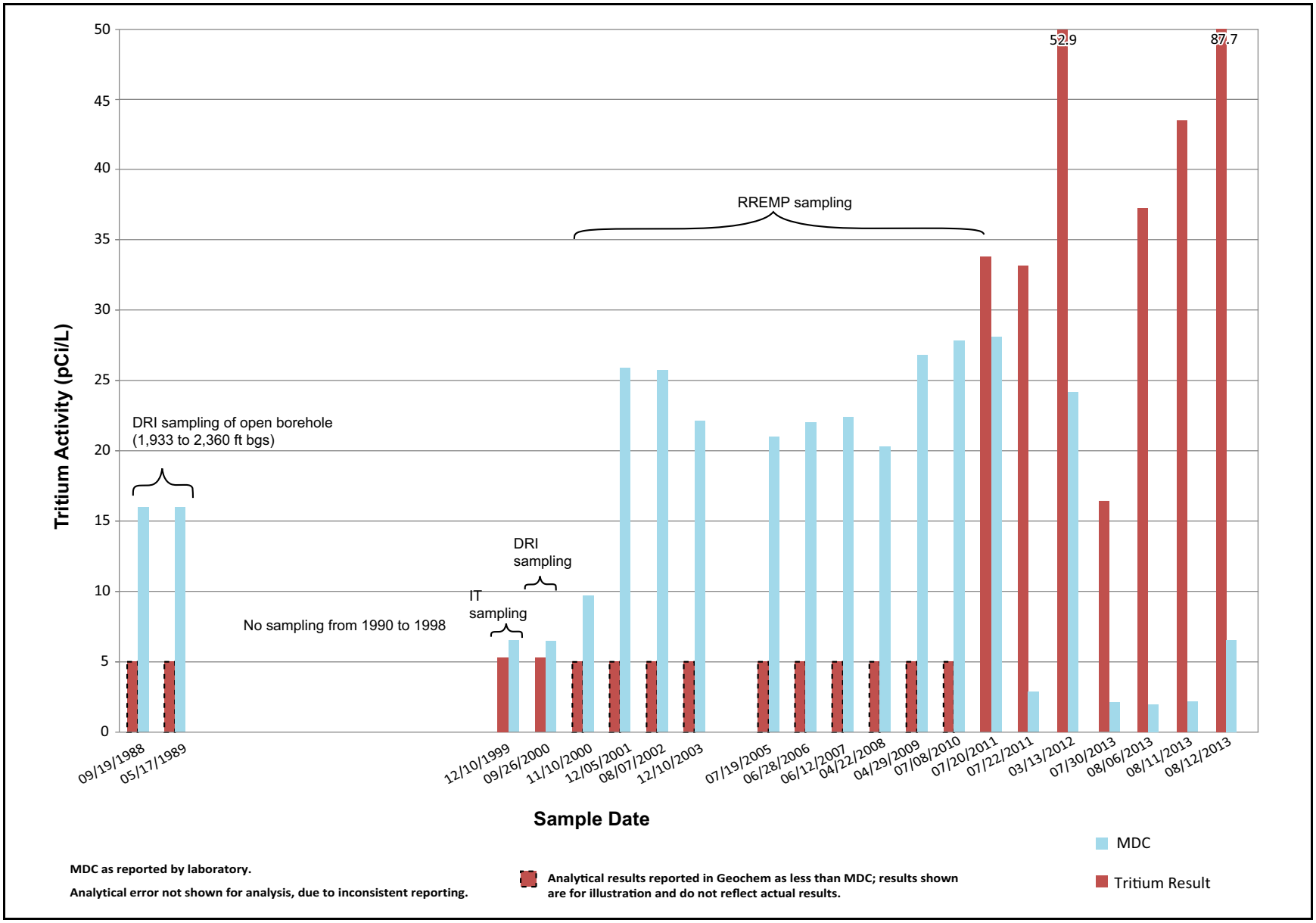

Figure 1-9
^3H Results for the PM-3-1 (Deep) Piezometer from 1988 through 2013
Source: Modified from N-I (2011, Figure 11)

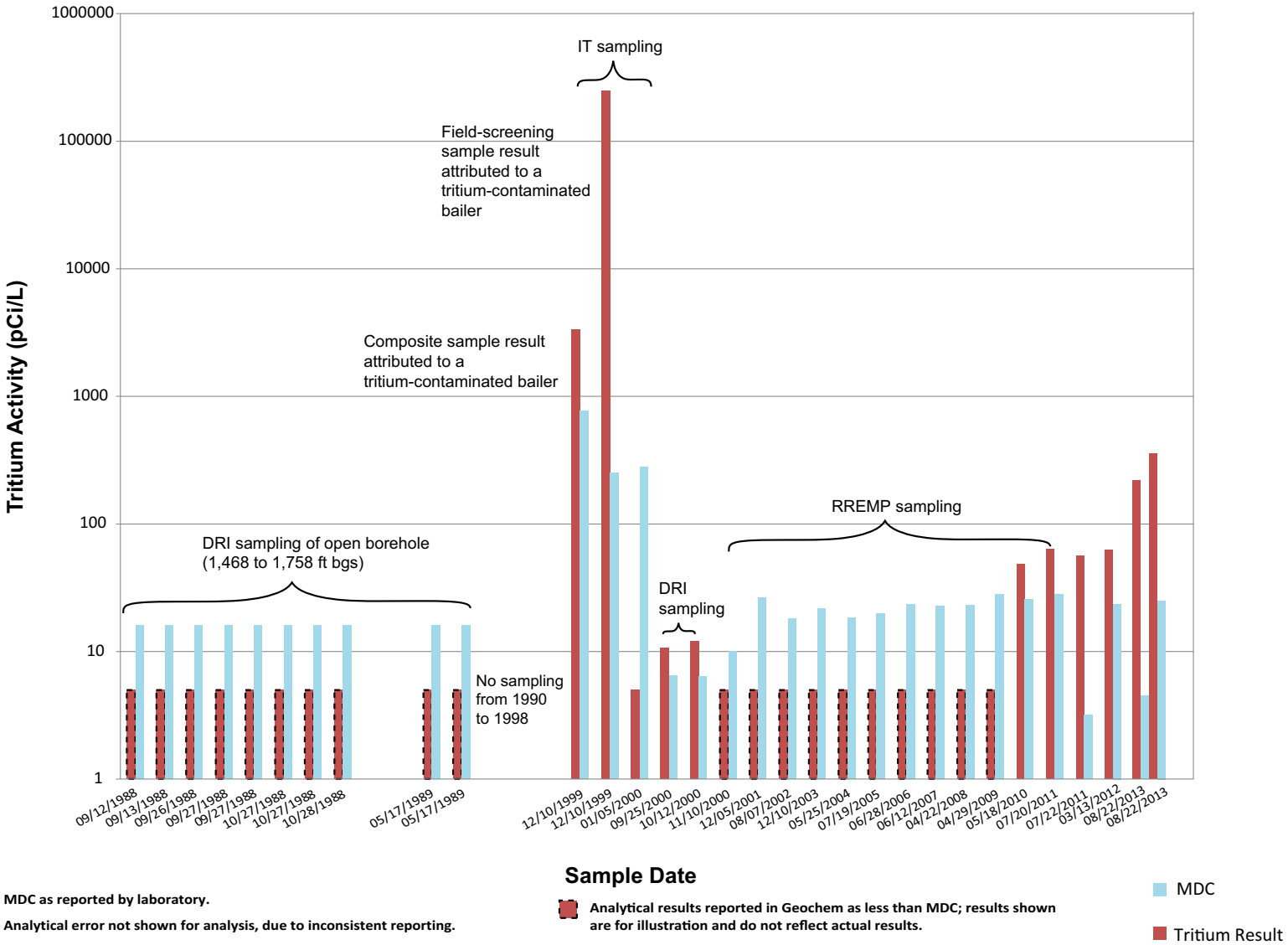

Figure 1-10
^3H Results for the PM-3-2 (Shallow) Piezometer from 1988 to 2013
Source: Modified from N-I (2011, Figure 10)

observed ^3H data from the various sampling campaigns including the most recent sampling conducted in August 2013.

1.7 Report Organization

This report is organized into the following sections:

- Section 1.0 in an introduction that summarizes the objectives of the evaluation, the history of activities at PM-3, and the geology and hydrogeology in the vicinity of PM-3.
- Section 2.0 summarizes the results and evaluation of the geochemical data from the groundwater samples collected in August 2013. This evaluation includes comparisons to earlier data collected at PM-3 and in nearby wells within the Thirsty Canyon flow domain. The geochemical data include major ions, environmental isotopes, dissolved noble gases, trace elements, and radioisotope data.
- Section 3.0 provides possible interpretations of the ^3H data from the groundwater samples collected in August 2013 and previous bailing activities. The interpretations evaluated include (1) possible ^3H contamination from recompletion activities; (2) possible ^3H contamination from surface contamination; (3) possible infiltration and vertical percolation of elevated ^3H from atmospheric testing; and (4) possible lateral ^3H transport from upgradient underground nuclear test sources on Pahute Mesa, most notably the HANDLEY detonation.
- Section 4.0 summarizes the results and interpretations, and discusses potential future activities that may be performed to confirm the source of the observed ^3H at PM-3.
- Section 5.0 provides the references used in the document.
- Appendix A presents the results of the geochemical data and radiochemical data collected at PM-3. The geochemical data are compared to other geochemical data used in the *Geochemical Data Analysis and Interpretation of the Pahute Mesa - Oasis Valley Groundwater Flow System, Nye County, Nevada, August 2002* (Rose et al., 2006).
- Appendix B presents additional analyses of the hydraulic test response from hydraulic testing performed in PM-3 and related hydrogeologic information.
- Appendix C presents the results of groundwater flow and ^3H transport modeling along possible groundwater flow tubes between HANDLEY and PM-3 to evaluate the possibility that residual ^3H contamination resulting from underground nuclear testing could have migrated south–southwest toward PM-3.

2.0 CHEMISTRY DATA AND EVALUATION

Samples from PM-3-1 (deep) and PM-3-2 (shallow) were collected in August 2013 to investigate the source of the ^3H previously detected in these piezometers (N-I, 2011 and 2014b). Because of questions related to the representativeness of the earlier samples collected using depth-discrete bailers and concerns that the gravel-packed intervals open to PM-3-2 (shallow) and PM-3-1 (deep) were not adequately purged before these sampling activities, the piezometers accessing both open intervals were configured with a pump jack in August 2013, and the intervals were pumped to develop the intervals and achieve stable water quality. Stable water quality was achieved after pumping 24,200 gal from PM-3-1 (deep) and 31,800 gal from PM-3-2 (shallow). Samples were then collected, and a large suite of parameters was analyzed by a commercial laboratory and also by laboratories at DRI, USGS, and Lawrence Livermore National Laboratory (LLNL) that provide specialized capabilities to support this investigation (see Table A-1).

The source of the ^3H observed at PM-3 is unknown. Several possibilities have been hypothesized. One possibility is lateral groundwater transport from underground nuclear tests such as HANDLEY, the closest underground nuclear test upgradient of PM-3 on the same side of the hydraulic discontinuity, or PURSE along the Purse fault upgradient of PM-3 (Figures 1-6, 2-1, and 2-2). Another possibility is infiltration of surface contamination from the nearby Plowshare tests at PALANQUIN or CABRIOLET and subsequent vertical percolation and transport to the water table. In this hypothesis, either melting snow or runoff from summer thunderstorms could transport radionuclides from surface contamination downward through the unsaturated zone along the upper East Thirsty Canyon drainage channel near PM-3 to the water table.

A limiting factor to test these hypotheses is the lack of groundwater sampling locations upgradient of PM-3 on the west side of the hydraulic discontinuity. Currently, there are only two wells upgradient from PM-3: UE-20j WW and PM-2 (Figure 2-1). Only one water sample was collected from UE-20j WW (also called UE-20j Instrument Hole) in 1964 before it was destroyed by the HANDLEY detonation (March 26, 1970). The constituents analyzed were limited to major-ion chemistry, a few trace elements, temperature, pH, and electrical conductivity (EC). PM-2, which is near the SCHOONER surface test crater, has only bailed groundwater samples from four different depths with

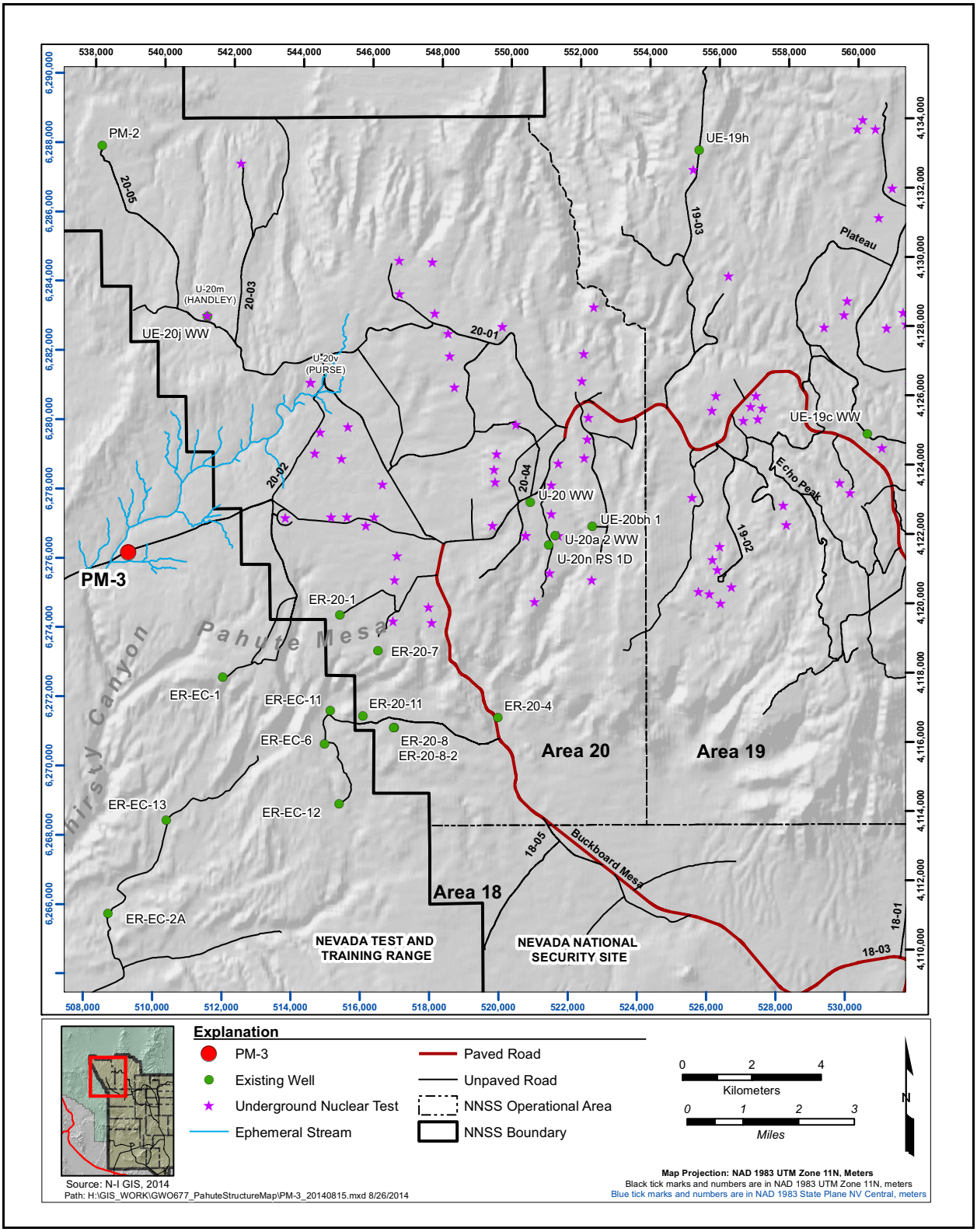

Figure 2-1
Groundwater Sampling Locations in the Vicinity of PM-3

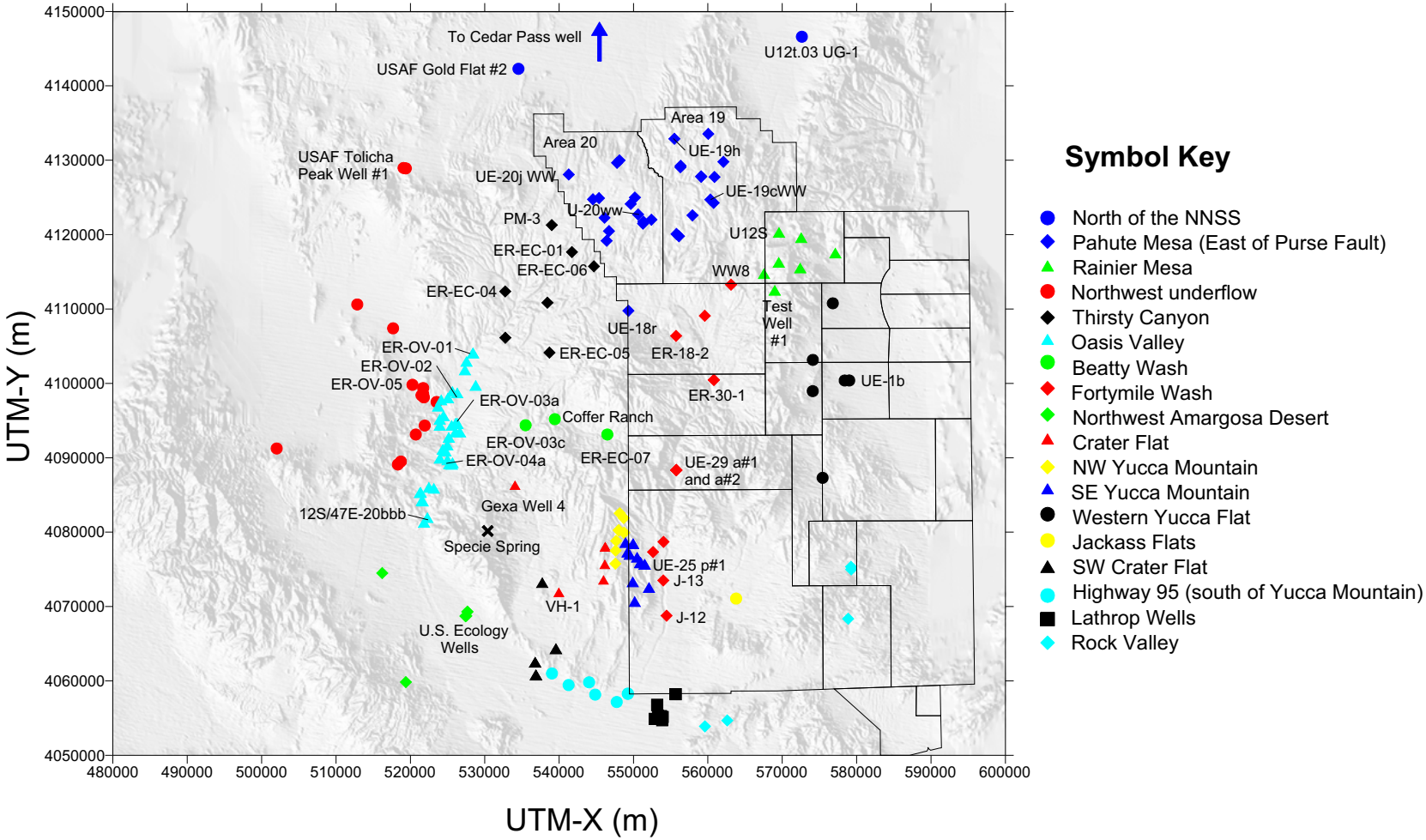

Figure 2-2
Groundwater Sampling Location Well Groupings
Source: Modified from Kwicklis et al. (2005, Figure 3)

more groundwater chemistry and isotopic analyses; however, groundwater in the vicinity of PM-2 is impacted by the SCHOONER test, and the bailed groundwater sample is not considered to be representative of natural unimpacted groundwater in this area of Pahute Mesa (Russell and Locke, 1997; Zavarin et al., 2008). This section presents an evaluation of PM-3 groundwater chemistry data collected over the past 25 years with a goal of evaluating potential distinguishing characteristics that may be used to infer the likely source of groundwater sampled in the piezometers at PM-3.

2.1 Introduction

As described in Section 1.0, PM-3 drilling, development, and hydraulic testing were accomplished between 1988 and 1989. LiBr was added to the drilling fluid as a tracer (approximately 20 milligrams per liter [mg/L]) to help identify whether drilling fluids were adequately removed from the aquifer during development and purging. Samples were collected by pumping, air lift, and depth-discrete bailers. Only samples collected during hydraulic testing (i.e., pumped samples) between October 27 and 28, 1988, are considered representative of the native groundwater; however, bromide (Br) concentrations in these samples ranged from 0.55 to 0.65 mg/L. These concentrations are well above naturally occurring background concentrations in Pahute Mesa groundwater (less than 0.01 to 0.1 mg/L), indicating that some residual drilling fluid was present in the samples.

Groundwater samples collected during recompletion activities are not considered representative of aquifer conditions because drilling fluid and recompletion water remained in the formations surrounding the well (DOE/NV, 1996). This is indicated by the high Br concentration (7.5 mg/L) in a groundwater sample collected in March 1992. With the exception of a single sample from PM-3-2 (shallow) on October 12, 2000, collected using a low-flow Bennett pump and the recent (August 2013) samples collected from both piezometers collected using the pump jack, only bailed samples are available after well recompletion (i.e., installation of PM-3-1 and PM-3-2 piezometer strings). Bailing removes very small amounts of groundwater and typically does not produce samples representative of groundwater in the surrounding formations. Samples collected before 2013 were not analyzed for Br; therefore, it is unknown to what extent they may represent native groundwater.

The detailed results of sampling activities at PM-3 are summarized in Section 1.6. The analysis of the most recent sampling conducted in 2013 is presented in Appendix A.

2.2 Geochemistry Evaluation

Groundwater samples were collected in 2013 from PM-3-1 (deep) and PM-3-2 (shallow) after significant purging had stabilized the chemistry. During sampling, the Br concentrations ranged from 0.50 to 0.68 mg/L, similar to the values observed after pumping in 1988, again indicating the presence of a small amount of residual drilling fluid and/or recompletion water. These samples were analyzed for a large suite of geochemical parameters including major ions, stable isotopes, noble gases, and other environmental tracers (see Table A-1). An evaluation of these data is presented in the following subsections. The evaluation includes the newly collected samples from PM-3-1 (deep) and PM-3-2 (shallow). Some historical data are reported, but these data are limited to samples thought to be representative of formation water and not impacted by drilling fluids. Other samples collected in the vicinity of PM-3 are also examined for comparison purposes. Sampling locations included in this evaluation were selected to represent the geochemical and isotopic variability within the Pahute Mesa area (Figures 2-1 and 2-2).

2.2.1 Major-Ion Data

Major ions in groundwater typically consist of calcium (Ca^{2+}), potassium (K^+), magnesium (Mg^{2+}), sodium (Na^+), chloride (Cl^-), sulfate (SO_4^{2-}), bicarbonate (HCO_3^-), and carbonate (CO_3^{2-}). The concentrations of major ions in groundwater can provide insight on the sources and flow directions of groundwater because major-ion concentrations reflect the minerals encountered as water moves through an aquifer. The relative concentrations of major ions observed at PM-3-1 (deep), PM-3-2 (shallow), and other Pahute Mesa wells are presented in the Piper diagram in Figure 2-3. This figure is analogous to the same figure in Rose et al. (2006, Figure 4-4) with the addition of the recent PM-3 data and other recent results from Phase II corrective action investigations for the Pahute Mesa corrective action unit (CAU). The relative concentrations of cations and anions are presented in the left and right triangles, respectively, and are projected onto the central diamond to present the combined major-ion chemistry. A Piper diagram is used to classify various groundwater chemistry types, or facies, and illustrate the relationships that may exist between water samples. The major-ion chemistry results from sampling of PM-3-1 (deep) and PM-3-2 (shallow) are consistent with the results observed at PM-3 before recompletion activities.

Pahute Mesa groundwaters vary from the Na+K-HCO_3/SO_4/Cl type (relatively equal concentrations of the three anions are present) observed at PM-3, UE-20j WW, and ER-EC-1 to the Na+K-HCO_3

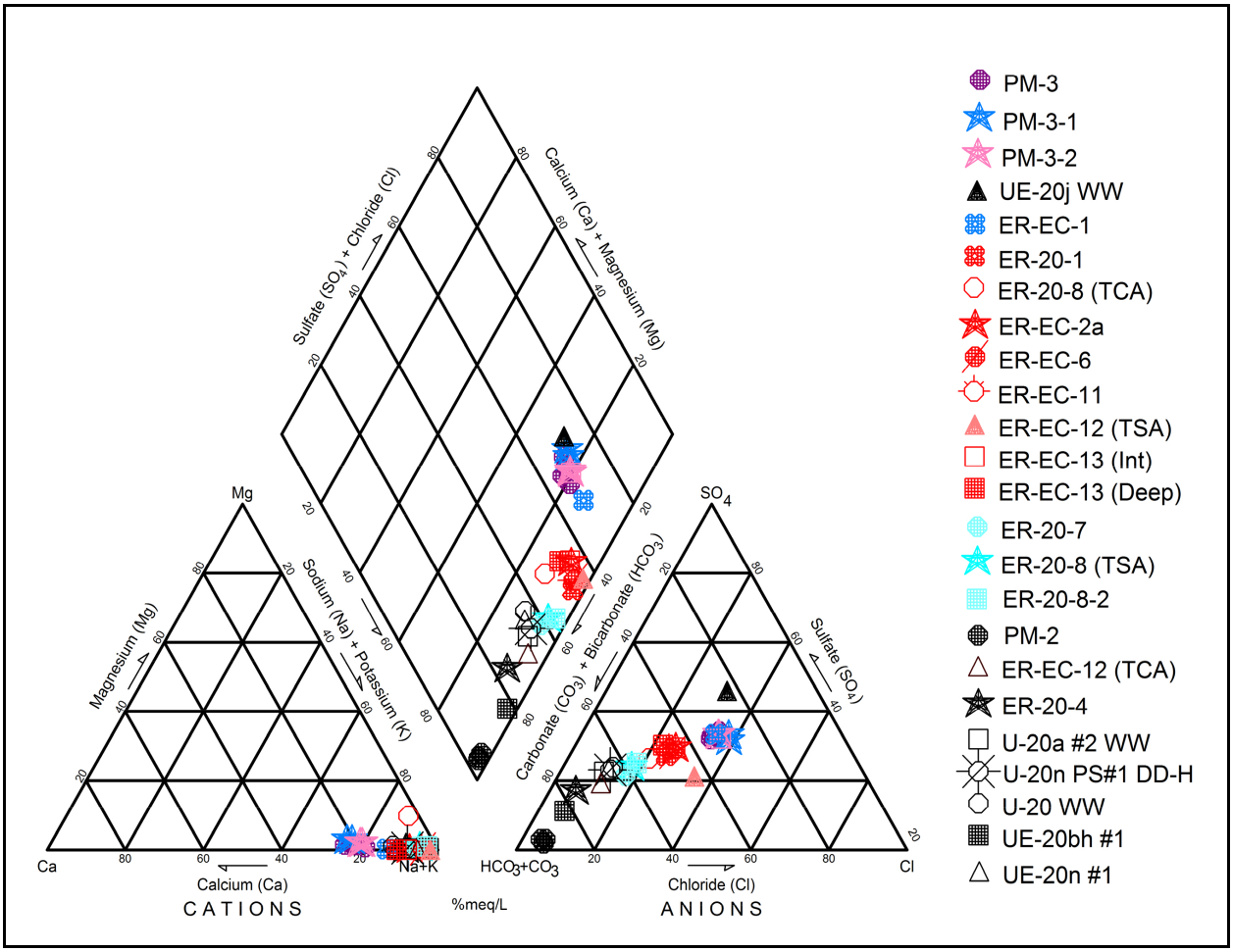

Figure 2-3
Piper Diagram of Groundwater in the Vicinity of Pahute Mesa, Including PM-3-1 (Deep) and PM-3-2 (Shallow)

type (greater than 50 percent HCO_3^- as the dominant anion) observed at PM-2 and other wells in Pahute Mesa (Figure 2-3). Other groundwater samples (e.g., ER-20-1, ER-20-8, ER-EC-6) lie intermediate between the two end-members. These groundwater types are characteristic of waters that have dissolved volcanic rhyolitic lava, ash-fall and ash-flow tuffs, and associated volcanic alluvium.

These results are consistent with the interpretations of Rose et al. (2006); PM-3 has a unique major-ion chemistry relative to groundwater east of the hydraulic discontinuity (i.e., Purse Fault). PM-3 has elevated Cl and SO_4 concentrations relative to other groundwater in Pahute Mesa and further downgradient in the Thirsty Canyon area. The Cl and SO_4 concentrations at PM-3-2 (shallow) and PM-3-1 (deep) are slightly more dilute than those observed at UE-20j WW and lie approximately along a mixing line between UE-20j WW and U-20 WW, the latter well used as the source for makeup water during the recompletion activities at PM-3 in 1992 (Figure 2-4). This figure is based on

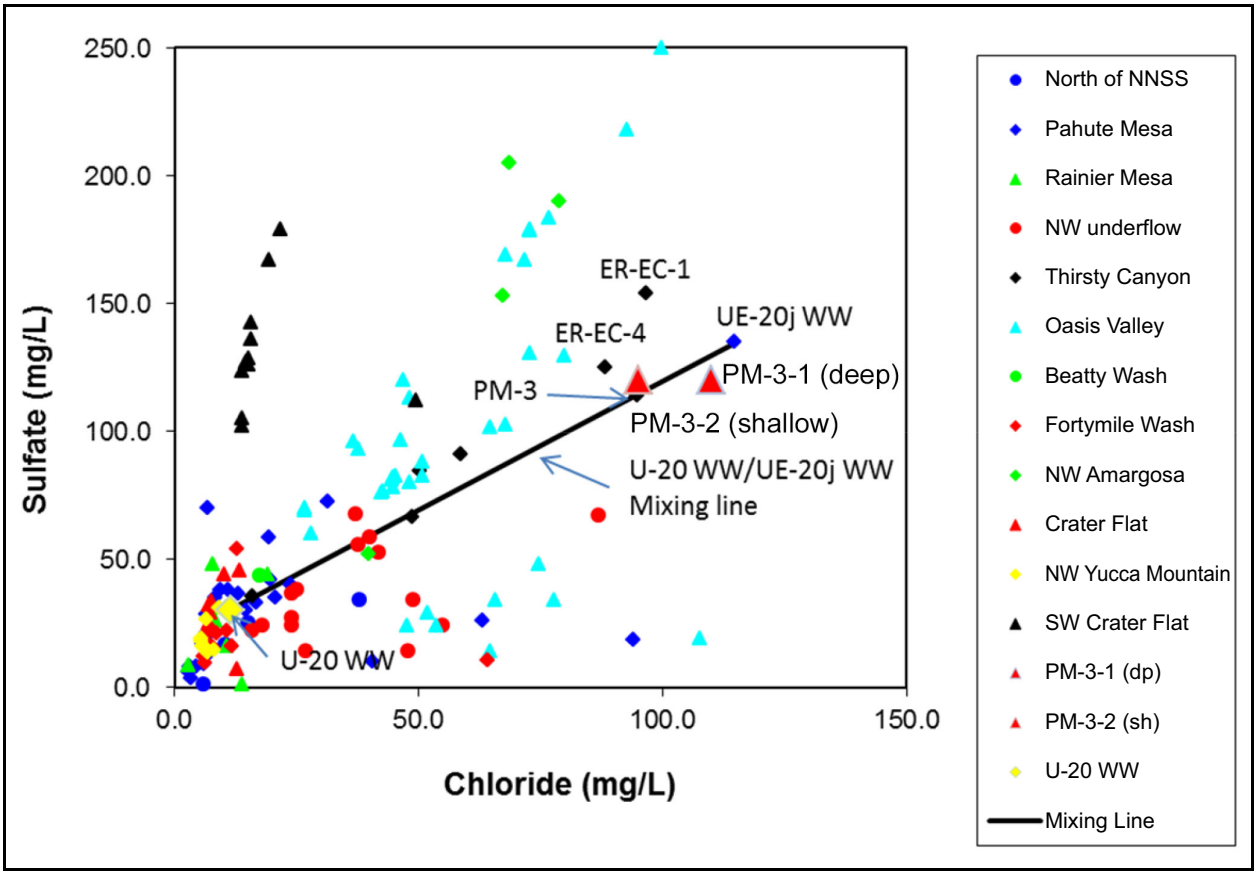

Figure 2-4
Sulfate and Chloride Concentrations in the Vicinity of Pahute Mesa, Including PM-3-1 (Deep) and PM-3-2 (Shallow)
Source: Modified from Kwicklis et al. (2005) with PM-3 data from Table A-1.

the data presented in Kwicklis et al. (2005, Figure 4) with some data from Yucca Flat, Rock Valley, Lathrop Wells and Nye County wells near Highway 95 removed for clarity. Using a simple mixing ratio of the two end-member waters, UE-20j WW and U-20 WW, it is possible to estimate that less than 10 percent of the groundwater sampled from PM-3 is derived from residual water derived from U-20 WW that was lost during the recompletion activities, with the remainder being consistent with lateral groundwater flow down the flow path from UE-20j WW as identified in Kwicklis et al. (2005) and illustrated in Figure 1-8. Because local recharge derived from surface runoff along Thirsty Canyon would be expected to be similar to the dilute Cl and SO_4 groundwater from Fortymile Canyon (which is similar to U-20 WW), it is not possible to use the major-ion chemistry data to rule out the possibility of some small amount of local recharge being present in the groundwater at PM-3.

2.2.2 Stable Isotopes of Hydrogen and Oxygen

The stable isotopes of hydrogen ($^{2}H/^{1}H$ or $\delta D/^{1}H$) and oxygen ($^{18}O/^{16}O$) are intrinsic to the water molecule and therefore behave conservatively in most groundwater systems. In the water cycle, these isotopes are fractionated (partitioned) between the liquid and vapor phases during evaporation and condensation processes. Once precipitation has infiltrated to the water table, the stable-isotope values are unaffected by water-rock interaction at temperatures below approximately 100 degrees Celsius (°C) (Criss, 1999). These isotopes are therefore used along with Cl as conservative tracers for evaluating groundwater origin and flow paths. Hydrogen and oxygen isotopes are conventionally reported as delta (δ) values representing permil (‰) variations in the isotope ratio of the sample relative to a reference standard.

Plots of δD versus $\delta^{18}O$ are presented in Figure 2-5. The three data points for Wells ER-EC-1 and ER-EC-6 represent averages of the multiple samples collected for each of the three sampling events. For reference, the global meteoric water line (GMWL) defined by Craig (1961) and the local meteoric water line (LMWL) defined by Ingraham et al. (1990) are included as are the average isotopic compositions of winter precipitation and the average isotopic composition of total annual precipitation as presented in Rose et al. (2006, Figure 4-2). The meteoric water lines represent the observed correlations in $\delta^{18}O$-δD values of precipitation samples from around the world and from the NNSS, respectively. The GMWL is defined by the equation $\delta D = 8\delta^{18}O + 10$ (Craig, 1961), while the LMWL is defined by the equation $\delta D = 6.87\delta^{18}O - 6.5$ (Ingraham et al., 1990). Most samples plot well below the present-day global or local meteoric water lines, suggesting that the groundwater is unrelated to present precipitation (Merlivat and Jouzel, 1979); however, it is possible that local recharge water has been fractionated due to evaporation which could affect the isotopic ratios.

As shown by Rose et al. (2006) and Kwicklis et al. (2005), the isotopic signature of most groundwater in Pahute Mesa is isotopically light, particularly the groundwater west of the hydraulic discontinuity (-116 ‰ δD). The uncertainty associated with this measurement is generally ±2 ‰. The isotopic signature of the average of summer and winter precipitation on Pahute Mesa is isotopically heavier than groundwater (Figure 2-5); however, there is a wide variability in the isotopic signature of groundwater recharge depending on whether the recharge occurred during the summer or winter months, complicating the interpretation.

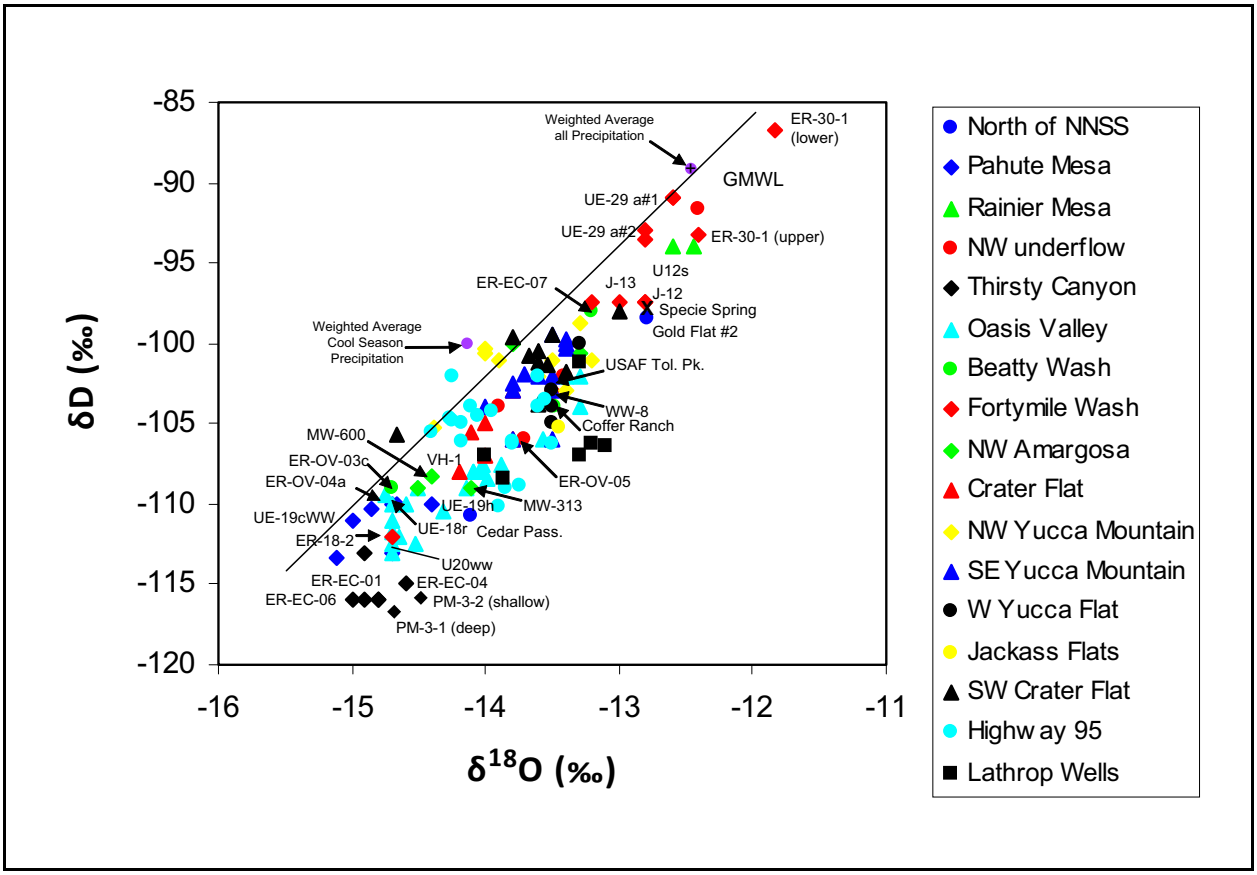

Figure 2-5
δD versus δ¹⁸O in the Vicinity of Pahute Mesa, Including PM-3-1 (Deep) and PM-3-2 (Shallow)
Source: Modified from Kwicklis et al. (2005, Figure 5) and Rose et al. (2006, Figure 4-2) with PM-3 data from Table A-1.

Figure 2-6 shows a plot of δD versus Cl for PM-3-1, PM-3-2, U-20 WW, and other groundwater samples from and near the Pahute Mesa–Oasis Valley flow system. As noted by Thomas et al. (2002), Kwicklis et al. (2005), and Rose et al. (2006), almost all of the groundwater within and near the Pahute Mesa–Oasis Valley area plots within or near the edge of a triangular area on a plot of δD versus Cl. The vertices of the triangle are described by an isotopically light (very negative), concentrated groundwater in the lower right (Thirsty Canyon end member); an isotopically light dilute groundwater in the lower left (Pahute Mesa end member); and an isotopically heavy (less negative), dilute groundwater in the upper left (Fortymile Wash/recent recharge end member). The Fortymile Wash end member is comparatively young (modern to a few thousand years, as shown in Fig. 3) and is a near-perfect analog for what modern recharge beneath Thirsty Canyon might look like chemically and isotopically. Because the PM-3-1 (deep) and PM-3-2 (shallow) samples plot on the lower edge of the triangle (which can also be thought of as a mixing line between U-20 WW and

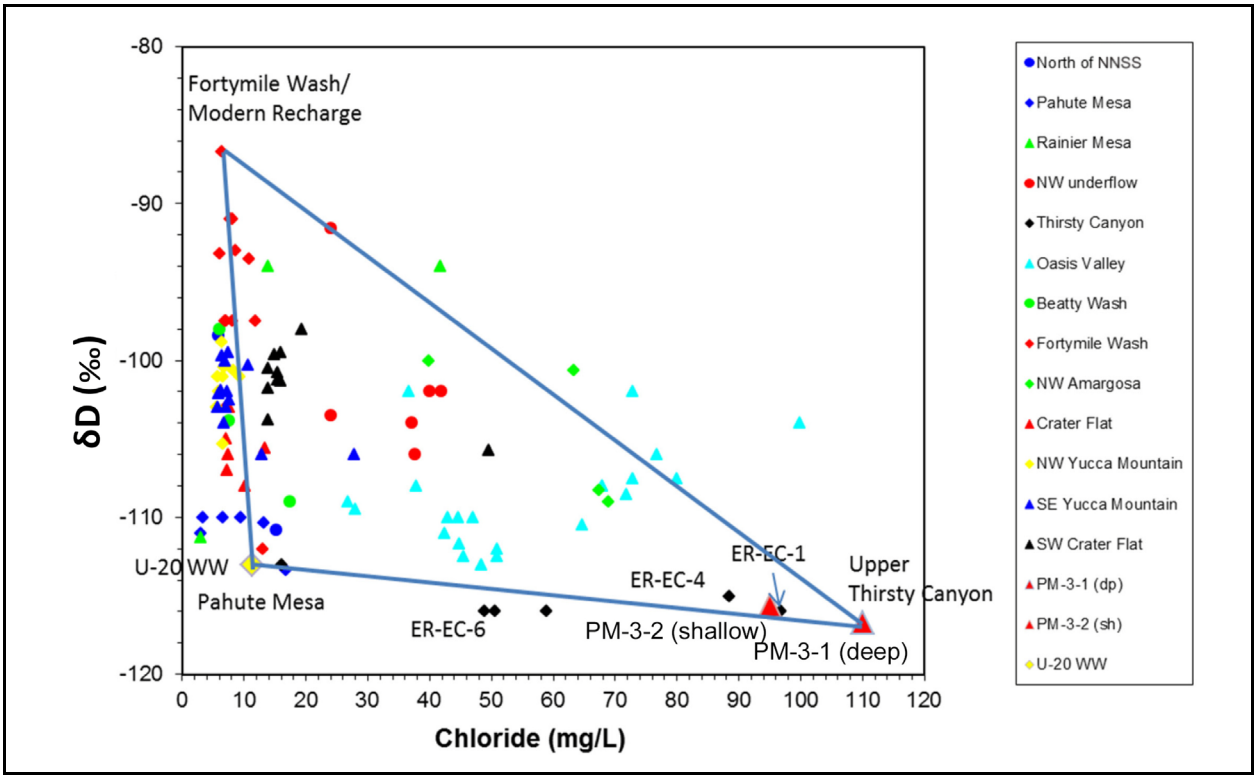

Figure 2-6
δD versus Cl in the Vicinity of Pahute Mesa, Including PM-3-1 (Deep) and PM-3-2 (Shallow)
Source: Modified from Kwicklis et al. (2005, Figure 6) and Rose et al. (2006, Figure 4-7) with PM-3 data from Table A-1.

PM-3-1), there is no evidence of significant modern recharge in these samples or in other Thirsty Canyon wells.

Additional insights into the evolution and sources of groundwater can be discerned by evaluating the trends in groundwater stable isotopes with the groundwater age for different groups of wells. Such plots are presented in Figure 2-7 using the ages from Appendix D of SNJV (2009). These plots illustrate that for the bulk of the groundwater domains in the area, the stable-isotope composition become progressively lighter with age. In Oasis Valley, the stable-isotope compositions are inherited from upgradient groundwaters in Thirsty Canyon and Pahute Mesa, and the groundwater ^{14}C ages have been "reset" through groundwater interaction with shallow soil gas and non-marine carbonates under "open system" conditions (White and Chuma, 1987).

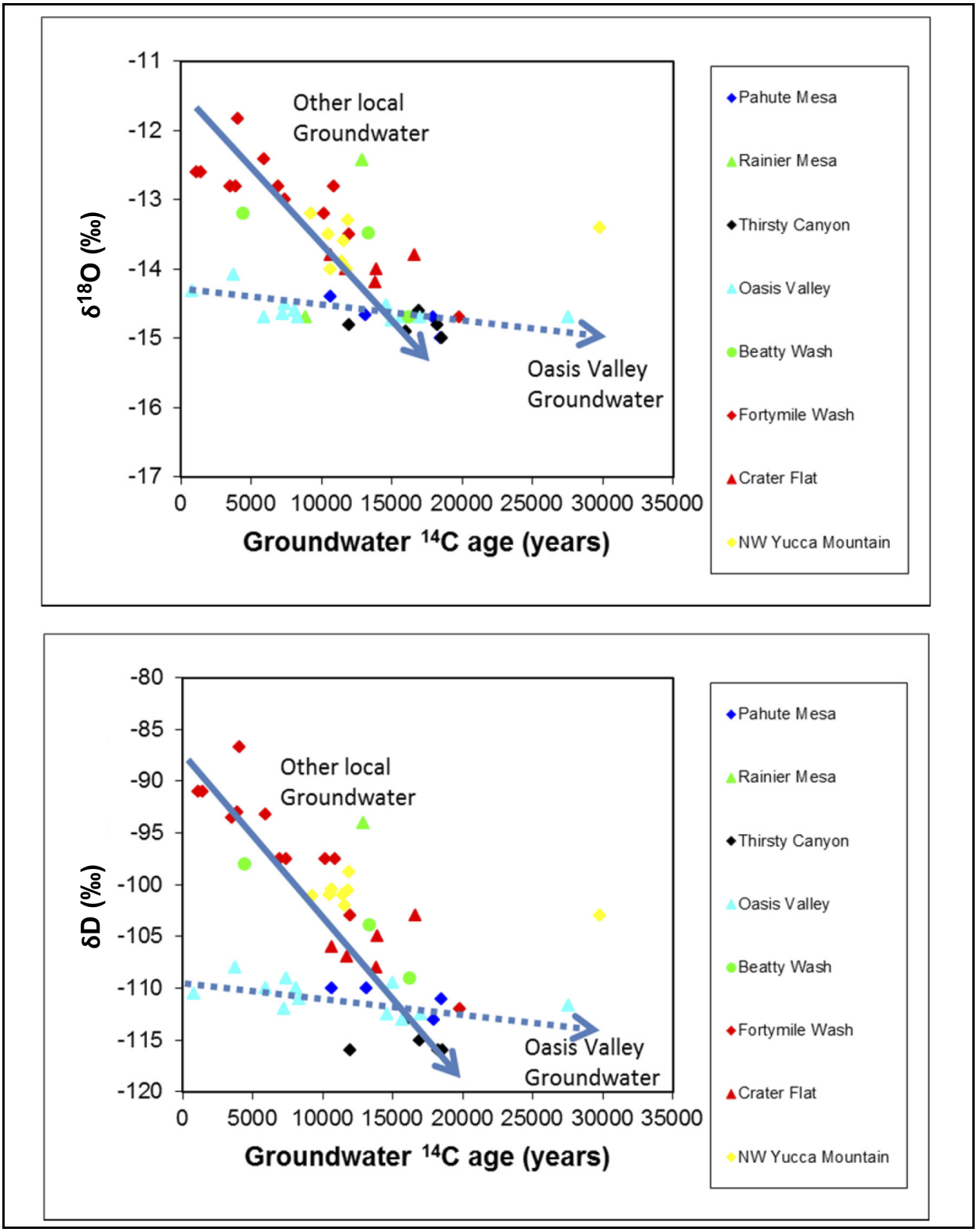

Figure 2-7
δD and δ¹⁸O Versus Groundwater Age

Source: δD and $\delta^{18}O$ data are from N-I (2014a); groundwater ^{14}C ages are from SNJV (2009, Appendix D).

2.2.3 Noble Gas Data

The combination of ^3H and noble gas data can be used to reveal the potential sources, pathways and residence times of groundwater samples. The accumulation of tritiogenic helium (^3He) in groundwater from ^3H decay is a marker for the residence time since the last contact with a gas phase. In principle, the sum of ^3H and dissolved ^3He equals the initial ^3H concentration. Analysis of other noble gases and the helium isotope ratio is required to distinguish ^3He from atmospheric and terrigenic sources. Accumulation of radiogenic ^4He from the decay of naturally occurring uranium and thorium provides a constraint on the time-scale of groundwater flow on the thousand to million year time-scale. The presence of both ^3H and radiogenic helium is evidence for mixing of modern and pre-modern (pre-1950) water sources.

Helium data from recent UGTA samples are plotted together with PM-3-2 and PM-3-1 analyses in Figure 2-8. The plot compares the helium isotope ratio of equilibrium+terrigenic+tritiogenic helium normalized to atmospheric (i.e., R/Ra where R is the $^3He/^4He$ ratio of the water sample relative to the $^3He/^4He$ ratio of air) against one over the terrigenic+equilibrium helium. Air equilibrated water plots at 1,1. Addition of tritiogenic ^3He, for example by the decay of ^3H, increases the isotope ratio but does not change the ^4He concentration, so it moves samples vertically upward. Addition of radiogenic helium (isotope ratio 1.5 percent of atmospheric) moves samples toward the 0,0. Addition of terrigenic helium with a mantle helium component (mantle isotope ratio is 8 to 10) moves samples to the left, typically along a straight trend line. The intercept of the terrigenic He isotope trend line with the vertical axis represents the isotope ratio of the terrigenic helium.

Analyses of groundwater samples from several recent Pahute Mesa wells, including PM-3, contain radiogenic helium. Radiogenic helium is produced as a result of alpha decay of elements contained in the subsurface. This helium is predominantly the result of uranium decay.

Based on an estimated accumulation rate of ^4He, a radiogenic ^4He age can be calculated. ER-EC-13 and ER-EC-15 samples contain terrigenic helium with a helium isotope ratio of about 0.9 times atmospheric. In natural systems, this indicates a mix of radiogenic helium with mantle-derived helium. However, at the NNSS, the source of ^3He and ^4He might also be anthropogenic (alpha decay produces ^4He; ^3H decay produces ^3He). The ^4He ages for this groundwater range from about 5,000 years for ER-EC-13 (deep) to about 30,000 years for the ER-EC-15 intermediate zone.

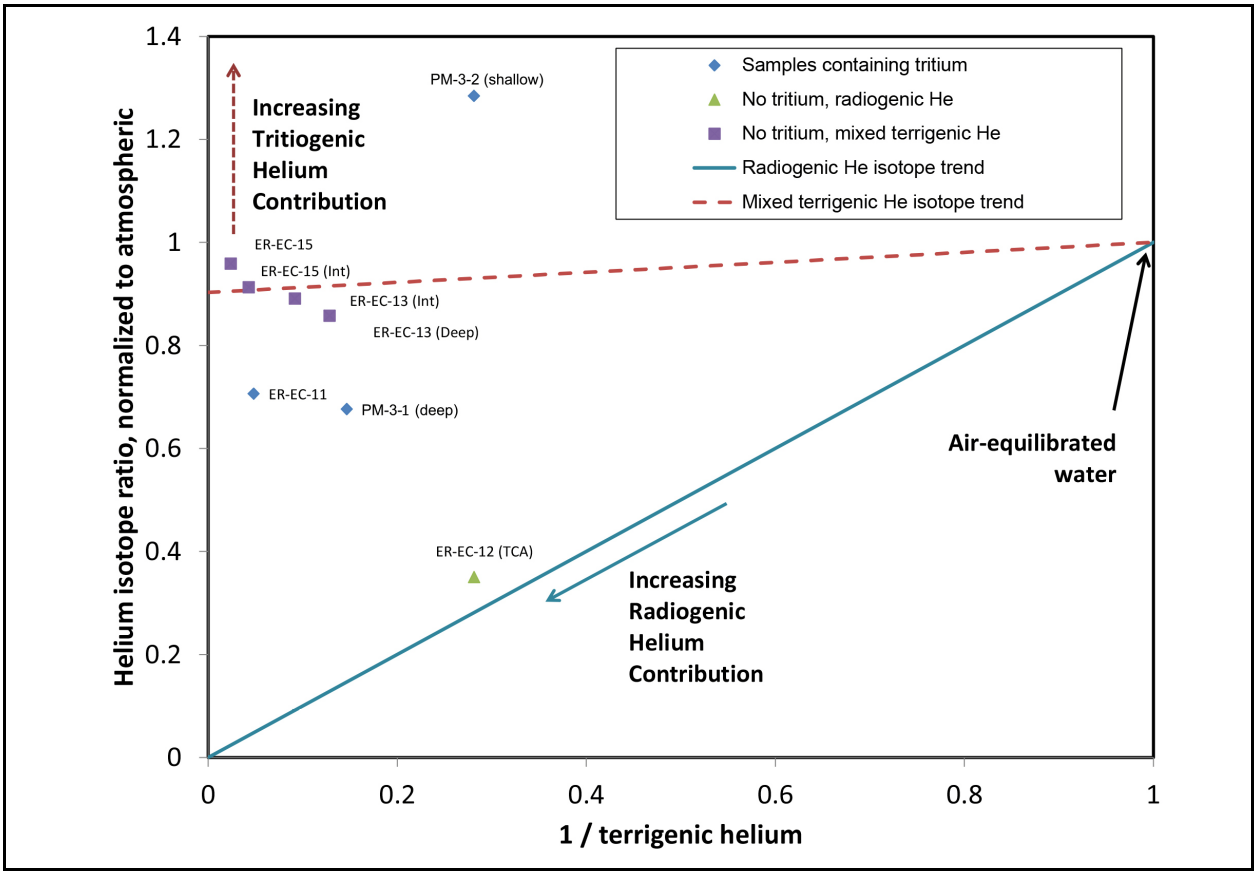

Figure 2-8
Helium Isotope Ratios in the Vicinity of Pahute Mesa, Including PM-3-1 (Deep) and PM-3-2 (Shallow)

Samples from PM-3-1 (deep) and PM-3-2 (shallow) contain ^3H in the range of 37 to 88 and 225 to 355 pCi/L, respectively. Their ^4He age is 4,000 and 2,000 years, respectively, which is younger than the ER-EC-13 and ER-EC-15 samples and consistent with shallow groundwater from ER-EC-12. The helium isotope ratios are elevated above the radiogenic trend line, and PM-3-2 (shallow) is also elevated above the mixed terrigenic helium isotope trend line. However, the contribution of tritiogenic ^3He depends on the terrigenic helium isotope ratio. When ^3He activities are well above natural abundances, the relationship between ^3He and ^3H can be used to calculate a groundwater age relative to the emplacement of ^3H in the groundwater. In this case, assuming a radiogenic helium isotope ratio, the contribution of tritiogenic ^3He appears to be relatively small, the equivalent of 237±13 pCi/L ($4.9 \times 10^6 \pm 2.6 \times 10^5$ atoms per gram [atoms/g]) and 238±11 pCi/L ($4.9 \times 10^6 \pm 2.2 \times 10^5$ atoms/g) for PM-3-1 (deep) and PM-3-2 (shallow), respectively. If it is assumed that ^3H at the activities presently observed at PM-3 has existed for approximately 40 years (the approximate time since detonation of the HANDLEY test), a tritiogenic ^3He concentration of 1.6×10^7 and

6.3×10^7 atoms/g would be expected. Both these values exceed the total ^3He in both PM-3-1 (deep) and PM-3-2 (shallow) samples. Thus it is possible that the ^3H may have been present in groundwater for a substantially shorter period of time, or that tritiogenic helium has escaped to the unsaturated zone. Due to the low concentrations of both the ^3H and tritiogenic ^3He it is not possible to distinguish between these different hypotheses. Nevertheless, a 40-year-old ^3H-He age for PM-3 waters is not supported by these data. The presence of both terrigenic helium and ^3H indicates that these samples contain a mixture of pre-modern groundwater and modern ^3H, the latter source being the result of anthropogenic nuclear testing.

2.2.4 DIC ^{14}C and DOC ^{14}C Data

DIC ^{14}C and DOC ^{14}C data for PM-3-1 (deep) and PM-3-2 (shallow) from samples collected in August 2013 are shown in Tables 2-1 and A-1. The DIC ^{14}C values are biased high by approximately 10 percent modern carbon (pmc) because a higher background concentration existed in the hot extraction line and accelerator mass spectrometer (AMS) instrumentation used for high activity ^{14}C measurements that were used for the analysis. As a result, the reported results have an estimated positive bias of 5 to 10 pmc.

DIC $\delta^{13}C$ data for PM-3-2 and PM-3-1 (deep) are listed in Table 2-1. Samples from September through October 15, 1988, were collected during drilling and well development and are not representative of the *in situ* groundwater. A sample collected from PM-3-2 (shallow) by pumping on October 12, 2000, indicates that the DIC $\delta^{13}C$ is consistent with previous DIC $\delta^{13}C$ data from PM-3 (Table 2-1). DIC $\delta^{13}C$ results for the samples collected in August 2013 from PM-3-1 (deep) and PM-3-2 (shallow) are isotopically heavier than previous samples by more than 3 ‰. DIC $\delta^{13}C$ is not thought to be impacted by underground testing.

Although there are no historical DIC ^{14}C data for PM-3, PM-3-1 (deep), and PM-3-2 (shallow), DIC ^{14}C values are available from other boreholes and wells on Pahute Mesa for comparison (Table 2-1). The DIC ^{14}C results for August 2013 from PM-3-1 (deep) and PM-3-2 (shallow) are higher than in other groundwater samples from Pahute Mesa and are consistent with above-background ^3H activities, suggesting impact from underground testing. DOC ^{14}C values for groundwater on Pahute Mesa are higher than DIC ^{14}C values. DOC ^{14}C is thought to be less reactive with surrounding rocks than DIC ^{14}C (e.g., Wassenaar et al., 1991), and therefore better for estimating groundwater ages (by radioactive decay of ^{14}C) than DIC ^{14}C. Estimating groundwater ages with DIC ^{14}C requires

Table 2-1
DIC $\delta^{13}C$, DIC ^{14}C, DOC $\delta^{13}C$, and DOC ^{14}C Data
for Groundwater Sampling Locations on Pahute Mesa
(Page 1 of 2)

Name	Date	DIC $\delta^{13}C$	DIC ^{14}C	DOC $\delta^{13}C$	DOC ^{14}C
		(‰)	(pmc)	(‰)	(pmc)
PM-3 (1,647 ft)[a]	09/13/1988	-8.3	--	--	--
PM-3 (3,019 ft)[b]	09/19/1988	-5.2	--	--	--
	09/26/1988	-5.8	--	--	--
	09/27/1988	-5.0, -5.0	--	--	--
	10/05/1988	-9.1, -11.8	--	--	--
	10/27/1988	-6.8, -6.3	--	--	--
	10/28/1988	-6.7	--	--	--
PM-3-2	10/12/2000	-6.8	--	--	--
	08/22/2013	-2.83, -3.39	82.9[c]	-27.4	51.5
PM-3-1	08/11/2013	-3.57, -3.44	68.4[c]	-26.6	55.9
ER-20-4	09/20/2011	-8.6	--	-21.5	77.7
	09/21/2011	1.8	18.6	--	--
ER-EC-1	02/01/2000	-4.0, -4.3	5.9	--	--
	06/03/2003	-3.1, -3.4, -3.8	7.2	-22.7	86.7
	04/02/2009	-4.6	--	-23.6	48.8
	04/03/2009	-2.9	15.2[c] J+, 8.8[c] J+	--	--
ER-EC-2A	07/27/2000	-1.5, -2.7	7.7	--	--
	07/08/2003	-2.0, -2.2, -2.4	7.7	-27.4	57.5
ER-EC-6	02/10/2000	-3.4, -4.4	5.4	--	--
	06/10/2003	-2.7, -3.1, -3.4	6.6	--	31.8
	04/09/2009	-2.6	16.3[c] J+, 9.5[c] J+	--	--
	04/11/2009	-4.3	--	-22.8	58.5
ER-EC-12 (TCA)	11/27/2011	-2.4[d] J+, -2.5[d] J+	18.4[c] J+	--	--
	11/28/2011	-6.9	--	-25.6	82.92
ER-EC-12 (TSA)	03/26/2012	-15.2	--	-27.4	43.21
	03/26/2012	-9.8[d] J+, -9.9[d] J+	118[c,e] J+, 120[c,e] J+	--	--
ER-EC-13 (Int)	07/12/2012	-0.45, -0.41, -4.6	11.7[c] J+	-25.2	47.05
ER-EC-13 (Deep)	03/29/2013	-1.3[d] J+	43.0[c] J+, 39.8[c] J+	--	--
UE-19h	08/12/1992	-3.3	9.4	--	--
	12/11/1999	-1.4[f], -2.3[f]	10.8	-28.5	43
UE-19c WW	08/13/1992	-5.3	8.1, 11.4	--	--

Table 2-1
DIC $\delta^{13}C$, DIC ^{14}C, DOC $\delta^{13}C$, and DOC ^{14}C Data
for Groundwater Sampling Locations on Pahute Mesa
(Page 2 of 2)

Name	Date	DIC $\delta^{13}C$	DIC ^{14}C	DOC $\delta^{13}C$	DOC ^{14}C
		(‰)	(pmc)	(‰)	(pmc)
U-20 WW	11/05/1997	-6.2, -7.2	8.6	--	-26.1
UE-20bh #1	06/20/1993	-9.2	21.0	--	--
	12/08/1999	-9.7, -10.5	22.4	-27.5	--

Source: N-I, 2014a and b

[a] PM-3 (1,647 ft) represents PM-3 when drilled to a 1,647 ft TD.
[b] PM-3 (3,019 ft) represents PM-3 when drilled to a 3,019 ft TD (drilling from 1,647 ft to 3,019 ft began on 09/14/1988).
[c] Result is biased high because of a hot extraction line and AMS instrumentation used for high-activity ^{14}C measurements were used for the analysis. It is assumed that the bias is on the order of 10 pmc based on the ER-EC-1 and ER-EC-6 analyses; however, the impact of the bias on other samples is indeterminate.
[d] Samples were analyzed outside of a 60-day hold time, and the results are biased high.
[e] Sample was collected from a poor groundwater production zone and is likely impacted by drilling fluids.
[f] Filtered result reported.

TSA = Topopah Spring aquifer

-- = Not available
J+ = Estimated, biased high

corrections for water/rock reactions and other physical processes such as matrix diffusion. DIC ^{14}C values from wells impacted by underground testing cannot be used to date groundwater using standard groundwater dating techniques. It is unknown whether underground testing impacts DOC ^{14}C values.

DIC $\delta^{13}C$ values from other boreholes and wells on Pahute Mesa have a wide range from -15.2 to +1.8 ‰ (Table 2-1). DIC $\delta^{13}C$ values from PM-3, PM-3-1 (deep), and PM-3-2 (shallow) also have a wide range (-11.8 to -2.83 ‰) but fall within the range observed for groundwater on Pahute Mesa. The isotopically heavier DIC $\delta^{13}C$ values from PM-3-1 (deep) and PM-3-2 (shallow) collected in August 2013 suggest that the DIC $\delta^{13}C$ values in PM-3 have changed over time, which may be the result of the purging of the gravel-packed intervals open to the slotted piezometers in the more recent samples. Because DIC $\delta^{13}C$ is thought not to be impacted by underground testing, the change in DIC $\delta^{13}C$ in PM-3-1 (deep) and PM-3-2 (shallow) could indicate a different source of water than the water developed when PM-3 was drilled in 1988.

Because of the wide range in DIC $\delta^{13}C$, DIC ^{14}C, and DOC ^{14}C data in PM-3 and other Pahute Mesa groundwater, carbon isotope data cannot discern the source of elevated ^{3}H observed in water samples taken from the PM-3 piezometers. The isotopically heavier DIC $\delta^{13}C$ values from the August 2013 samples could indicate a different source of water than when PM-3 was originally drilled in 1988. The DIC ^{14}C results for August 2013 from PM-3-1 and PM-3-2 are much higher than seen in other groundwater samples from Pahute Mesa and are consistent with increasing ^{3}H activities, suggesting transport of radionuclides from nuclear testing. However, the DIC ^{14}C cannot be used to assess the viability of the different transport pathway hypotheses, as both the lateral and vertical transport hypotheses could result in higher DIC ^{14}C values in groundwater.

DOC ^{14}C, which may not be impacted by nuclear testing, in Pahute Mesa groundwater is generally much higher than DIC ^{14}C, indicating that groundwater velocities are much faster than estimated with DIC ^{14}C. The DOC ^{14}C values above 50 pmc for both piezometers indicate average groundwater ages of less than 5,000 years from the time of recharge until reaching PM-3. As previously discussed, with noble gas data and groundwater ages, DOC ^{14}C ages represent average ages where one or more sources of groundwater—some very old, some very young—mix together to produce the average age measured at a well. Therefore, a young source of groundwater (i.e., surface water recharge along the drainages) could be present in the PM-3 piezometers.

2.2.5 Other Environmental Tracer Data

Samples for strontium ($^{87}Sr/^{86}Sr$), uranium ($^{234}U/^{238}U$ activity ratio), chloride ($^{36}Cl/Cl$), and sulfur ($\delta^{34}S$) were collected in August 2013, and the results are shown in Table A-1. Although there are no historical data for these isotopes for PM-3, PM-3-1 (deep), and PM-3-2 (shallow), values are available from other boreholes and wells on Pahute Mesa for comparison. Variations in $^{87}Sr/^{86}Sr$ can be used to evaluate the extent of water-rock reactions and groundwater mixing along flow paths provided there are strongly contrasting strontium isotopic signatures. There is a lack of systematic variation in $^{87}Sr/^{86}Sr$ values in Pahute Mesa groundwater in the general vicinity of PM-3, so strontium isotopic ratios are not helpful in delineating groundwater flow directions and flow paths in the volcanic rock aquifers of Pahute Mesa. A similar conclusion was reached by Rose et al. (2006).

Uranium concentrations and $^{234}U/^{238}U$ activity ratios vary within groundwater in Pahute Mesa in the vicinity of PM-3. PM-2, upgradient of PM-3 on the west side of the hydraulic discontinuity, has a low uranium concentration (0.24 µg/L) and a low $^{234}U/^{238}U$ activity ratio (2.43) relative to groundwater at

PM-3 (see Table A-1) and in Pahute Mesa (Figure 2-9). In the general direction of groundwater flow, uranium concentrations and $^{234}U/^{238}U$ activity ratios increase at PM-3, suggesting dissolution of volcanic rocks containing uranium with higher $^{234}U/^{238}U$ activity ratios (Figure 2-9). Other groundwater in Pahute Mesa has even higher uranium concentrations, with higher $^{234}U/^{238}U$ activity ratios indicating the presence of rocks with uranium with higher activity ratios in Pahute Mesa aquifers.

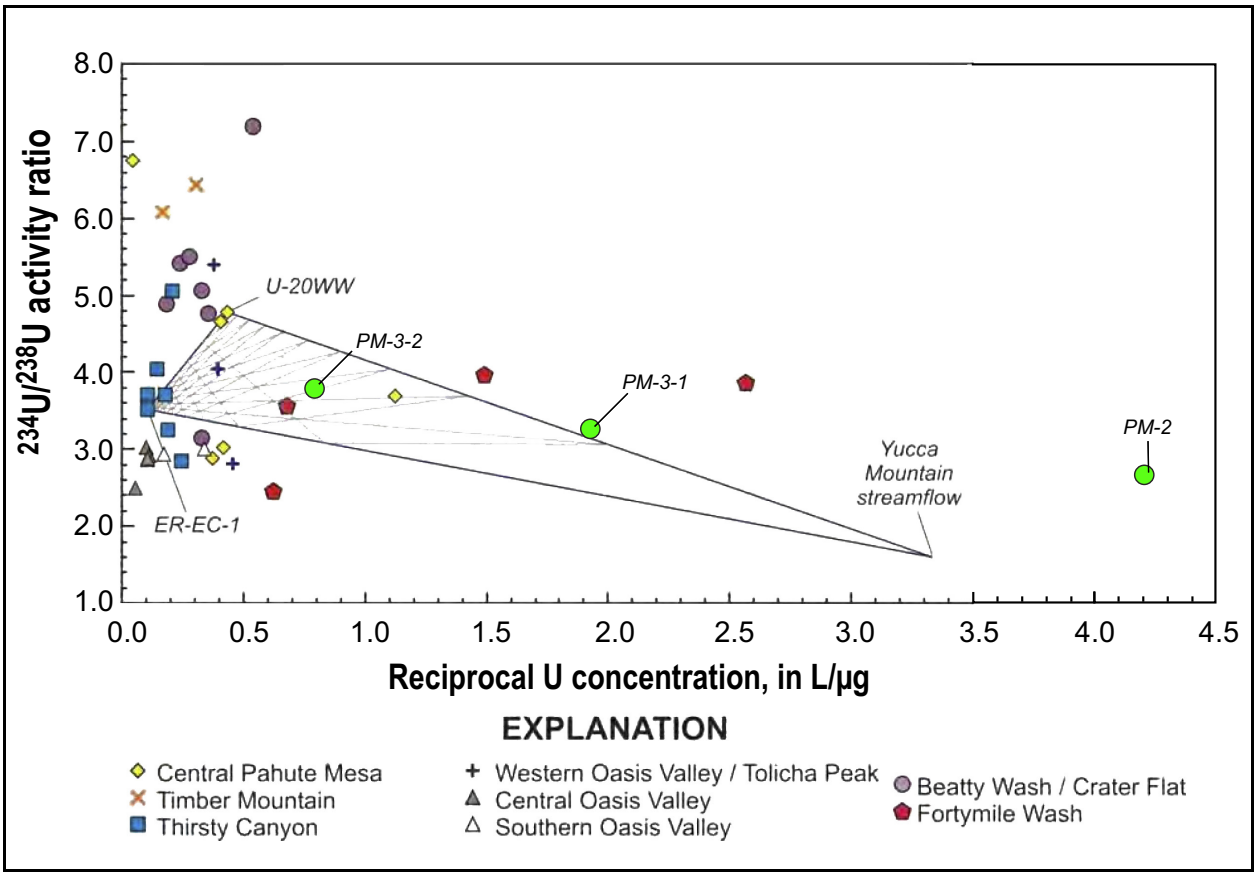

Figure 2-9
Groundwater $^{234}U/^{238}U$ Activity Ratios versus Inverse Uranium Concentrations
Source: Modified from Rose et al. (2006, Figure 4-12) with data from Table A-1.

$^{36}Cl/Cl$ in precipitation in southern Nevada ranges from 4.0E-15 to 5.0E-15 (SNJV, 2006). Ratios above this range possibly suggest elevated ^{36}Cl from anthropogenic nuclear reactions or groundwater recharge under different climatic conditions. The $^{36}Cl/Cl$ in PM-3-1 (deep) and PM-3-2 (shallow) reported in Table A-1 are close to values found in other wells on Pahute Mesa and only slightly above the range of precipitation. However, these ratios at PM-3 are reflective of higher Cl concentrations in the PM-3 groundwater and corresponding higher ^{36}Cl concentrations. It is

therefore uncertain whether these $^{36}Cl/Cl$ values are related to underground nuclear testing or surface radionuclide contamination. As noted in Appendix C, the ^{36}Cl values are similar to the ratio of ^{36}Cl concentrations in the exchange volume of a nuclear detonation, which may imply the ^{36}Cl source is an underground nuclear detonation.

Few $\delta^{34}S$ data currently exist for groundwater in the vicinity of PM-3 and Pahute Mesa. Of the available data, $\delta^{34}S$ isotopic signatures range narrowly from 17.7 to 20.0 ‰. Recent $\delta^{34}S$ data from PM-3-1 (deep) and PM-3-2 (shallow) fall at the end of this range (see Table A-1).

2.2.6 Summary of Chemistry Data

Groundwater at PM-3 has unique major-ion chemistry relative to groundwater east of the hydraulic discontinuity. The similarity of major-ion chemistry from the two upgradient wells where data are available supports the general groundwater flow path from the vicinity of the HANDLEY test to PM-3. However, the greater activity of ^{3}H in PM-3-2 (shallow) piezometer does not present a consistent interpretation that might either prove or disprove the rapid infiltration of surface contamination along drainages hypothesis.

The similarity of stable isotopic data (δD and $\delta^{18}O$) and the uncertainty in the interpretation of these data with respect to the timing of recharge events in the vicinity of PM-3, the stable-isotope data cannot be used to evaluate the potential that groundwater at PM-3 is the result of groundwater transport from HANDLEY cannot be evaluated.

Noble gas data indicate that groundwater at PM-3 is a mixture of modern ^{3}H and older groundwater. The ^{3}H found in PM-3-1 (deep) and PM-3-2 (shallow), based upon ^{3}H-^{3}He dating, was deposited in groundwater relatively recently. Also, because ^{3}He activities were very low in nearby wells, the ^{3}H in the PM-3 piezometers is too young to be from the HANDLEY test. Alternatively then, these data suggest that the source of ^{3}H might be from rapid infiltration of surface water. However, very low ^{3}He activities in these groundwater samples might also be because of ^{3}He exchange with noble gases in the vadose zone, which adds uncertainty to these interpretations.

The DIC ^{14}C values in PM-3-1 (deep) and PM-3-2 (shallow) from August 2013 are higher than in other groundwater samples from Pahute Mesa and are consistent with above-background ^{3}H activities, suggesting the higher DIC ^{14}C is from underground testing. Isotopically heavier DIC $\delta^{13}C$

values from August 2013 could indicate a different source of water in PM-3 now than when PM-3 was drilled in 1988, but the origin of a different source cannot be identified. Despite these differences, DIC isotopic values cannot confirm or refute transport of radionuclides by groundwater from the HANDLEY test or from rapid infiltration of surface contamination along ephemeral drainages.

The DOC ^{14}C values above 50 pmc for both PM-3 piezometers indicate average groundwater ages of less than 5,000 years from the time of recharge until reaching PM-3. DOC ^{14}C ages are average ages of one or more sources of groundwater that could be a mixture of very old with very young waters that produce the average age measured at a well. Therefore, a young source of groundwater could be present in the PM-3 piezometers (e.g., from rapid infiltration of winter melting precipitation or surface runoff from summer thunderstorms).

Because of a lack of variation in both $^{87}Sr/^{86}Sr$ and $\delta^{34}S$ ratios in Pahute Mesa groundwater, these isotopic tracers cannot be used to test the different hypothesis for the source of elevated ^{3}H in PM-3 piezometers. The increase in both uranium concentration and $^{234}U/^{238}U$ activity ratio suggest a possible flow path between PM-2 and PM-3, which then suggests than groundwater from HANDLEY could flow toward PM-3. However, these increases could also be explained by rapid infiltration of winter melting precipitation or surface runoff from summer thunderstorms dissolving uranium-rich rocks as water moves through the vadose zone to PM-3. $^{36}Cl/Cl$ values in PM-3 piezometers are similar to other nearby wells and are close to natural background levels, so they cannot be attributed directly to underground nuclear testing.

2.3 Radiochemistry Evaluation

Groundwater samples collected during the various sampling campaigns conducted from 1988 to 2013 were analyzed for a range of radionuclide constituents. The MDC ranged depending on the radionuclide and the analytical method. The radionuclides analyzed for and the MDC range (rounded to 1 pCi/L except when less than 1 pCi/L) are as follows:

- ^{228}Ac (26 to 64 pCi/L MDC)
- ^{26}Al (7 to 11 pCi/L MDC)
- ^{241}Am (7 to 250 pCi/L MDC)
- ^{7}Be (54 to 67 pCi/L MDC)
- ^{212}Bi (104 to 180 pCi/L MDC)
- ^{214}Bi (11 to 30 pCi/L MDC)

- ^{14}C (1×10^{-4} to 460 pCi/L MDC)
- ^{144}Ce (25 to 48 pCi/L MDC)
- ^{36}Cl (1×10^{-8} pCi/L MDC)
- ^{58}Co (7 to 9 pCi/L MDC)
- ^{60}Co (6 to 14 pCi/L MDC)
- ^{134}Cs (6 to 12 pCi/L MDC)
- ^{137}Cs (5 to 10 pCi/L MDC)
- ^{152}Eu (27 to 78 pCi/L MDC)
- ^{154}Eu (31 to 66 pCi/L MDC)
- ^{155}Eu (12 to 32 pCi/L MDC)
- ^{3}H (2 to 340 pCi/L MDC)
- ^{129}I (1×10^{-7} pCi/L MDC)
- ^{40}K (123 to 238 pCi/L MDC)
- ^{94}Nb (7 to 9 pCi/L MDC)
- ^{212}Pb (6 to 19 pCi/L MDC)
- ^{214}Pb (21 to 23 pCi/L MDC)
- ^{144}Pm (6 to 14 pCi/L MDC)
- ^{146}Pm (7 to 13 pCi/L MDC)
- ^{238}Pu (0.01 to 0.05 pCi/L MDC)
- $^{239/240}Pu$ (0.006 to 0.05 pCi/L MDC)
- ^{106}Ru (53 to 97 pCi/L MDC)
- ^{125}Sb (13 to 27 pCi/L MDC)
- ^{90}Sr (0.3 to 0.6 pCi/L MDC)
- ^{99}Tc (6 to 13 pCi/L MDC)
- ^{227}Th (34 to 57 pCi/L MDC)
- ^{234}Th (80 to 270 pCi/L MDC)
- ^{208}Tl (8 to 13 pCi/L MDC)
- ^{235}U (23 to 56 pCi/L MDC)
- ^{238}U (0.03 µg/L MDC)
- ^{88}Y (7 to 16 pCi/L MDC)
- Gross alpha activity (0.5 to 5 pCi/L MDC)
- Gross beta activity (0.9 to 5 pCi/L MDC)

Although MDCs are sufficiently low to detect natural levels of some radionuclides (^{14}C, ^{36}Cl, ^{129}I, and ^{238}U), most radionuclides are below their associated MDC. The range of measured values for gross alpha is 1.2 to 6 pCi/L for PM-3-2 (shallow), and 1.2 to 10.7 pCi/L for PM-3-1 (deep). The range of measured gross beta is from 10.8 to 22.2 pCi/L for PM-3-2 (shallow), and from 1.4 to 15.5 for PM-3-1 (deep). Other values reported above the MDC (^{214}Bi, ^{214}Pb, ^{238}Pu, and $^{239/240}Pu$) are only slightly above the MDC (generally within the measurement error) and are therefore considered nondetects. This will be verified through future analyses.

Tritium has been analyzed in all samples collected from the PM-3-1 (deep) and PM-3-2 (shallow) piezometers from 1999 to the most recent sampling conducted using the pump jack in 2013. All ^{3}H results from groundwater samples that are greater than the MDC are tabulated in Table A-2.

Tritium activities for the August 2013 samples were 225, 249, and 355 pCi/L for PM-3-2 (shallow); and 43.7, 37.0, and 87.8 pCi/L for PM-3-1 (deep). Additional radionuclide data are presented in Table A-2. The fact that different samples (i.e., field and duplicate samples) and different laboratories (i.e., commercial laboratories and LLNL) yield comparable ^{3}H results in comparison to the MDC and laboratory error provides additional confidence that the observed values are reasonable and representative of the sampled groundwater at this location. Based on the ^{3}H-^{3}He analyses, it appears that the ^{3}H was deposited in the groundwater relatively recently; however, it is also possible that ^{3}He ingrowth was masked by the exchange of noble gases with the vadose zone.

The ^{14}C activity is well above the activities typically observed in clean wells from this area. The activities in PM-3-1 (deep) and PM-3-2 (shallow) represent isotope ratios of 68.4 and 82.9 pmc. These results are noted as being affected by a hot extraction line and bio-AMS instrumentation with an estimated positive bias of 5 to 10 pmc based on a comparisons with other samples. This positive bias suggests that ^{14}C activity may be only slightly lower than the reported concentrations of 0.12 and 0.15 pCi/L for PM-3-1 (deep) and PM-3-2 (shallow), respectively. Two sources of the high ^{14}C are possible: contamination migrating from a nearby underground nuclear test, or migration of modern recharge with a modern ^{14}C signature. Because the activities are slightly below modern ^{14}C activities, it is not possible to discount modern recharge as a potential source.

The ^{36}Cl activity is relatively consistent with natural background levels observed in the area. The $^{36}Cl/Cl$ isotope ratios (5.6×10^{-13} and 6.6×10^{-13}) for PM-3-1 (deep) and PM-3-2 (shallow), respectively, are similar to nearby ER-EC-1 (5.5×10^{-13}) and ER-EC-6 (5.6×10^{-13}) sampled in 2009. PM-3-2 (shallow) has a slightly elevated $^{36}Cl/Cl$ ratio; however, it is too close to natural background levels to attribute an anthropogenic signal. The elevated Cl concentration of the groundwater at PM-3 imply that the ^{36}Cl concentration is higher than other wells in the area. The similarity of the ratio of the observed ^{36}Cl concentration at PM-3-2 (shallow) relative to the ^{36}Cl that may be expected in the cavity of an underground nuclear test such as HANDLEY (see Appendix C) implies this may be an anthropogenic ^{36}Cl signal. However, this is not conclusive based on the low levels observed at this well.

The ^{129}I concentration at this site is extremely low (1.6×10^{-5} and 8.8×10^{-5} pCi/L for PM-3-1 and PM-3-2, respectively). These activities represent $^{129}I/^{127}I$ ratios of 3.5×10^{-9} and 2.0×10^{-8} for PM-3-1 and PM-3-2, respectively. However, the activities are higher than typically observed in clean wells from this area. For example, $^{129}I/^{127}I$ ratios from ER-EC-12 (upper), ER-EC-13 (upper and lower), and ER-EC-15 are 6.3×10^{-10}, 4.2×10^{-11}, 5.4×10^{-11}, and 3.3×10^{-10}, respectively. This suggests that a trace anthropogenic ^{129}I signal is present at PM-3. However, the activities are quite low.

2.4 Summary

This section summarizes the interpretation of the geochemical and radiochemical data collected from the PM-3 piezometers and compares these results to observations made in other Pahute Mesa wells along the likely groundwater travel path from recharge in or north of Pahute Mesa, and discharge in Oasis Valley. The recent data presented in Appendix A are consistent with trends and interpretations made in previous geochemistry syntheses documented in Thomas et al. (2002), Kwicklis et al. (2005) and Rose et al. (2006). The recent data generally support the concept that groundwater at PM-3 is derived from similar groundwater north of PM-3 such as UE-20j WW and similar groundwater observed in other wells in the Thirsty Canyon area.

While the major-ion and stable-isotope chemistry observations support the conclusion that the bulk of groundwater at PM-3 has a similar origin as other locations west of the Purse fault in the Thirsty Canyon area, it is not possible to determine whether there is a small amount of local recharge that may be present in the sampled groundwater at PM-3. This is simply because small amounts of local vertical recharge containing high values of ^{3}H when mixed with groundwater that has moved laterally from upgradient areas of recharge would not significantly affect the bulk observed geochemistry. The evaluation of different sources of ^{3}H is discussed in Section 3.0.

3.0 POSSIBLE INTERPRETATIONS OF ^3H OBSERVATIONS

Section 2.3 and Appendix A present the ^3H data above the minimum detection level obtained from sampling at PM-3-1 (deep) and PM-3-2 (shallow). Different interpretations have been provided for the observed ^3H concentrations at this location. This section summarizes the different possible interpretations with a particular focus on the possibility that the observed concentrations may be the result of groundwater flow and transport from ^3H sources that resulted from underground nuclear testing on the NNSS. Note that in this document, the ^3H concentrations are presented in units of pCi/L rather than using the standard measure of tritium units (TU).

3.1 Introduction

Tritium has been observed at low levels (i.e., values up to several hundred pCi/L) in samples collected from both the PM-3-1 (deep) and PM-3-2 (shallow) piezometers in recent sampling events (see Table A-2). As discussed in Section 2.3 and in greater detail in N-I (2011), a contaminated bailer was inadvertently used in sampling of PM-3-1 (deep) in December 1999, which resulted in significant uncertainty in the interpretation of ^3H analyses from samples collected in the years subsequent to that event. This uncertainty was the result of the inability to determine the degree of contamination that may have been introduced into the piezometer by the use of the contaminated bailer. The uncertainty was exacerbated by three facts:

1. The low levels of ^3H measured in laboratory analyses of bailed samples collected in 2000, 2004, 2010, and 2011 were close to the minimum detection limits possible in the laboratory when considering the error in the measurement technique (i.e., the reported value was less than or approximately equal to the sum of the minimum detection limit and the laboratory identified error [to two standard deviations] in the measurement).

2. Laboratory analyses of bailed samples collected in 2001, 2002, 2003, 2005, 2006, 2007, 2008, and 2009 indicated ^3H levels below the minimum detection limit.

3. All laboratory ^3H analyses of PM-3 water samples between 1999 and 2011 were based on samples collected with a depth-discrete bailer or a low-flow Bennett pump (in October 2000) rather than allowing the well to be purged before sampling.

Based on these facts, there was significant uncertainty as to whether (1) the ^3H results were real or simply due to unquantifiable laboratory measurement uncertainty at the low levels of detection or (2) the samples were not representative of groundwater in the HSUs the two piezometers penetrate because of the low volume of water extracted and the fact that the piezometers were never sufficiently purged to provide a representative sample of the formation water.

The first uncertainty was addressed in the laboratory ^3H results from the depth-discrete bailer samples collected on July 22, 2011. The results for both PM-3-1 (deep) and PM-3-2 (shallow) (between 18.64 and 56.65 pCi/L) were more than a factor of 10 greater than the reported minimum detection limits (between 2.54 and 3.16 pCi/L) and more than a factor of three greater than the reported error (between 5.87 and 17.01 pCi/L) (see Table A-2). However, these results were not believed to be representative because depth-discrete bailer samples may not be representative of formation groundwater.

To address the uncertainty that samples collected by bailing may not be representative of groundwater from the formation, a pump jack was used to collect samples from PM-3-1 (deep) and PM-3-2 (shallow) in 2013. Both zones were pumped at about 3.5 gpm until the piezometers had at least three well-bore volumes removed and water-quality parameters had stabilized. Samples were collected after pumping 31,800 and 36,000 gal from PM-3-2 (shallow), and after pumping 24,200 and 28,800 gal from PM-3-1 (deep). The two different pumping volumes represent the difference of continued pumping overnight from each zone and samples taken in the prior afternoon and the next morning. For both intervals, both a field and field duplicate sample were provided to the commercial laboratory for ^3H analyses, and an additional sample was provided to LLNL for an interlaboratory comparison. These results indicated the presence of ^3H ranging in concentrations from 37.04 to 43.67 pCi/L in PM-3-1 (deep) and from 224.68 to 355.2 pCi/L in PM-3-2 (shallow). These results are at levels well above the minimum detection limits and reported laboratory error. These results are approximately a factor of 100 below the *Safe Drinking Water Act* (SDWA) maximum permissible contaminant level of 20,000 pCi/L (USC, 2012).

To identify the possible source of the ^3H, LLNL also analyzed the ^3He and ^4He to determine whether the source of the ^3H was the result of anthropogenic sources. Their results, summarized in Section 2.0, also support the assertion that the ^3H observed in the sampled groundwater from PM-3 is likely the result of anthropogenic ^3H, which decays to ^3He. In addition, the observed concentrations of

^{14}C, ^{36}Cl and ^{129}I presented in Table A-1 are also indicative of test-derived radionuclide concentrations because the concentrations of these mobile, long-lived radionuclides have approximately the same relative concentration to the initial cavity concentration as ^{3}H, considering that ^{3}H has undergone decay since the time of the testing (1965 for PALANQUIN, 1968 for CABRIOLET, and 1970 for HANDLEY).

3.2 Possible Interpretations of Observed ^{3}H at PM-3

The results of the 2013 sampling performed using the pump jack confirm that the observed ^{3}H results are (1) likely representative of formation water and (2) appear to be of an anthropogenic origin; however, there remains uncertainty on this conclusion. Based on the amount of water purged from the piezometers and the stable water-quality parameters, the samples are the best that can be obtained at this time. Multiple hypotheses can be proffered for the source of the ^{3}H:

- Residual ^{3}H contamination from the contaminated bailer
- ^{3}H-contaminated water used in recompletion of PM-3
- ^{3}H transported from local recharge of elevated ^{3}H during atmospheric testing
- ^{3}H transport vertically from leaching contaminated surface soils and percolating to the depth of PM-3
- ^{3}H transported laterally from upgradient underground nuclear test sources on the NNSS

These hypotheses are discussed in this section. The first three hypotheses can be ruled out by reasonable mixing arguments but are included here for completeness. The latter two hypotheses related to either vertical transport of test-derived contamination from shallow Plowshare tests or lateral transport of test-derived contamination from deep underground nuclear tests have different types of support, and at present neither can be confirmed or refuted with the available information.

Information that generally supports the vertical transport hypothesis includes (1) higher ^{3}H and other mobile radionuclide concentrations in PM-3-2 (shallow) than PM-3-1 (deep); (2) an apparent vertical hydraulic gradient between PM-3-2 (shallow) to PM-3-1 (deep), indicating the possibility of downward vertical flow; and (3) He concentrations suggesting less than a 50-year travel time.

Information that generally supports the lateral transport hypothesis includes (1) a significant horizontal hydraulic gradient along the postulated groundwater flow path between HANDLEY and PM-3; (2) a similar groundwater geochemistry at HANDLEY and PM-3; (3) the presence of a continuous fractured HSU (i.e., the BRA) that is penetrated by the HANDLEY chimney and PM-3; and (4) observed concentrations of mobile radionuclides (i.e., ^{3}H, ^{14}C, ^{36}Cl, and ^{129}I) at PM-3-2 (shallow) and PM-3-1 (deep) that have similar ratios to the HANDLEY cavity concentration when considering the effects of ^{3}H decay.

3.2.1 Possible Residual ^{3}H Contamination from the Contaminated Bailer

Tritium introduced by a contaminated bailer has been identified as the source of anomalous elevated ^{3}H values in PM-3 samples collected in 1999 (Wycoff, 2000). It has been hypothesized that residual contamination from this contaminated bailer could still be present in the groundwater that has been recently sampled from pumping the isolated intervals. The process that is invoked in this hypothesis is that ^{3}H introduced by the contaminated bailer could mix in the piezometer and gravel pack, and that the natural flow of groundwater through the gravel pack could displace the ^{3}H into the formation. When the well is pumped, the formation water flows back to the gravel pack, where it mixes as it is pumped to the surface. This hypothesis is extremely unlikely to have resulted in the observed ^{3}H concentrations because (1) the volume of contaminated water in the bailer would be very low (1 to 2 liters [L]), even though the concentration may have been very high; (2) the contamination was confined to the interior of the bailer; and (3) the volume of water withdrawn by the pump jack was significant. For example, assuming the contaminated bailer volume was 2 L with a ^{3}H concentration of 250,000 pCi/L (as observed in the sample taken on December 10, 1999), the total ^{3}H activity would be about 500,000 pCi. Assuming the water withdrawn by the pump jack from PM-3-2 (shallow) was about 100,000 L at an average ^{3}H concentration of 250 pCi/L, the total ^{3}H activity pumped would be about 25,000,000 pCi. Therefore, the ^{3}H removed by the pump jack is about 100 times greater than the ^{3}H potentially resident in the borehole or formation from the contaminated bailer. As a result, it is not possible that the observed ^{3}H concentration from sampling in 2013 is due to residual contamination from the contaminated bailer introduced to the well in 1999.

3.2.2 Possible ^{3}H Contamination from Recompletion Activities

As summarized in N-I (2011), during the recompletion activities in 1992, about 105,000 gal of water with LiBr tracer was lost in the PM-3 borehole. The ^{3}H concentration of this water was not measured

at the time of the recompletion activities, but given the source of water was U-20 WW, it is likely the water used had a ^3H concentration in the range of 110, 28, and 120 pCi/L as reported from analysis of U-20 WW samples collected on March 11, 1991; April 11, 1991; and July 12, 1993, respectively (N-I, 2014a). During recompletion activities in 1992, the well was "cleaned out" before installation of the piezometers. After the well was "cleaned out," 20,200 gal of drilling fluid was removed from the well by swabbing. The two piezometers were then installed. Because of the small diameter of the piezometers, normal well-development techniques could not be employed, so no additional well development was conducted at that time (N-I, 2011).

During pumping with the pump jack, Br concentrations were analyzed daily to determine the presence of any previously traced drilling or recompletion water. The results of these analyses indicated a slow decline in Br concentrations as the piezometers were pumped, with stable values of about 0.7 mg/L in PM-3-1 (deep) (after an initial value of 10.6 mg/L) and steady decline from about 1.2 to about 0.8 mg/L over the first 30,000 gal of water purged from PM-3-2 (shallow) (N-I, 2014b). However, these concentrations are well above naturally occurring Br background concentrations for Pahute Mesa, which range from less than 0.01 to 0.1 mg/L. It was assumed that the observed Br values were sufficiently low, along with other stable water-quality parameters (including temperature, pH, EC, turbidity, and dissolved oxygen), that the sampled groundwater adequately represented ambient formation water from the two open intervals. While this assumption seems reasonable, it also noted that the total water withdrawn from the two piezometers since the recompletion activities of about 81,300 gal (20,200 gal removed in 1992, plus 29,300 gal removed in 2013 from PM-3-1 [deep]; plus 31,800 gal removed in 2013 from PM-3-2 [shallow]) is less than the 105,000 gal of water lost during the recompletion activities. As a result, there is some possibility that the sampled waters are not representative of ambient formation water. In addition, the fraction of the water lost during recompletion activities in 1992 that could have been lost to the deeper BRA, which is assumed to be very permeable, is indeterminate.

Assuming the remaining low levels of detectable Br is the result of recompletion activities and assuming the recompletion water was spiked to a Br concentration of between 10.6 mg/L (derived from the maximum value observed in PM-3-1 [deep]) and 7.5 mg/L (derived from the measured concentration during the recompletion activities in 1992 [N-I, 2014a]), simple mixing implies that there may be as much as 5 to 8 percent of the water being the result of the recompletion water from U-20 WW. If the initial ^3H concentration in the recompletion water in 1992 was 120 pCi/L

(which has now decayed to about 50 pCi/L) and this represents as much as 5 to 8 percent of the total sample, the ^3H concentration at PM-3 that results from U-20 WW recompletion water would be about 3 to 4 pCi/L, well below the observed concentrations in PM-3-1 (deep) and PM-3-2 (shallow). As a result, even though there may be some residual recompletion water present in the mixed groundwater sampled from the PM-3 piezometers (which is also noted in the major-ion and stable-isotope geochemistry data discussed in Section 2.0), this residual water does not significantly affect the observed ^3H concentrations.

3.2.3 Possible Infiltration of Elevated ^3H from Atmospheric Testing

Atmospheric testing of nuclear weapons in the 1950s and 1960s significantly elevated the ^3H concentration in precipitation. Estimates of the concentrations of ^3H in rain and snow melt in the early 1960s were several thousand picocuries per liter, and it is possible it may have been much higher in the vicinity of the NNSS. Elevated atmospheric ^3H concentrations would result in elevated concentrations in precipitation, and therefore elevated concentrations in water than infiltrates below the root zone and eventually percolates to the water table. The amount of precipitation and the resulting infiltration and percolation rates in the vicinity of PM-3 are unknown. Average infiltration and percolation fluxes in the regional groundwater flow model range from 1 to 10 millimeters per year (mm/yr) in the area (Belcher et al., 2004). Assuming a low effective porosity of 10 percent for the vitric tuffs and a saturation of about 10 percent, this would imply interstitial vertical velocities in the order of 100 to 1,000 mm/yr, or total transport distances of 5 to 50 m in the 50 years since the peak atmospheric ^3H concentrations in the early 1960s. As a result, it is unlikely that the observed concentrations in PM-3-2 (shallow) of several hundred picocuries per liter are the result of the recharge of elevated ^3H levels from atmospheric testing.

Another simple analysis also can be used to refute the possibility that the elevated ^3H at PM-3 is due to atmospheric testing. Assuming the atmospheric ^3H concentration was 10,000 pCi/L in the 1960s, the current concentration would have decayed to about 600 pCi/L. The observed ^3H concentration on the order of 200 to 300 pCi/L at PM-3-2 (shallow) would them imply that one-third to one-half of the sampled groundwater would be modern, which is counter to the stable-isotope compositions presented in Section 2.2.2. As a result, the possible vertical transport of ^3H derived from atmospheric testing can be ruled out as a source of the observed ^3H at PM-3.

3.2.4 Analysis of Possible Vertical Transport of ^3H from Surface Contamination

A possible source of the observed low levels of ^3H in samples from PM-3-2 (shallow) and PM-3-1 (deep) is from downward percolation of tritiated water that was recharged from the nearby ephemeral stream in the Thirsty Canyon drainage system. The evidence that supports this possible hypothesis include (1) the presence of surface contamination sources near PALANQUIN or CABRIOLET that are upgradient of PM-3; (2) the downward head gradient of about 2 ft from PM-3-2 (shallow) to PM-3-1 (deep), indicating the potential for downward flow between these two intervals; (3) the ^3He concentrations are suggestive of less than 50-year travel times from the source to PM-3 and interchange with the vadose zone; and (4) there are higher ^3H concentrations observed in PM-3-2 (shallow) than PM-3-1 (deep).

The basic elements of this vertical flow and transport hypothesis include the following:

- Surface soils north of PM-3 are contaminated with high ^3H concentrations as a result of Plowshare tests conducted at PALANQUIN and CABRIOLET (Figure 3-1).
- Large precipitation event(s) could mix surface runoff with the ^3H in the soil near PALANQUIN and CABRIOLET and be transported down the ephemeral stream that runs about 400 m west of PM-3 (Figure 3-1).
- Ephemeral stream drainage could rapidly infiltrate along the trace of the drainage channel due to the high vertical permeability of alluvial materials in the wash.
- The alluvial aquifer and volcanic HSUs—notably the Thirsty Canyon volcanic aquifer and the Timber Mountain tuff aquifer—that occur at or near the land surface in the vicinity of PM-3 are sufficiently permeable and fractured to allow rapid vertical flow and transport of the tritiated water that infiltrates along the trace of the drainage channel.

These elements are further elaborated in the following discussion.

Two near-surface Plowshare tests were conducted in the 1960s upgradient of the location of PM-3 (Figure 3-1). The PALANQUIN test was a 4.3 kiloton (kt)-yield device detonated on April 14, 1965, located about 5.6 km northeast of PM-3; and the CABRIOLET test was a 2.3-kt-yield device detonated on January 26, 1968, and located east of PALANQUIN. Summaries of these tests are described in Hacker (1994) and Kirsch (2005). Both detonations resulted in surface contamination that could be mobilized and transported by surface runoff and or recharge. Although the general direction of the radioactive plume from the PALANQUIN test was toward the north away from the

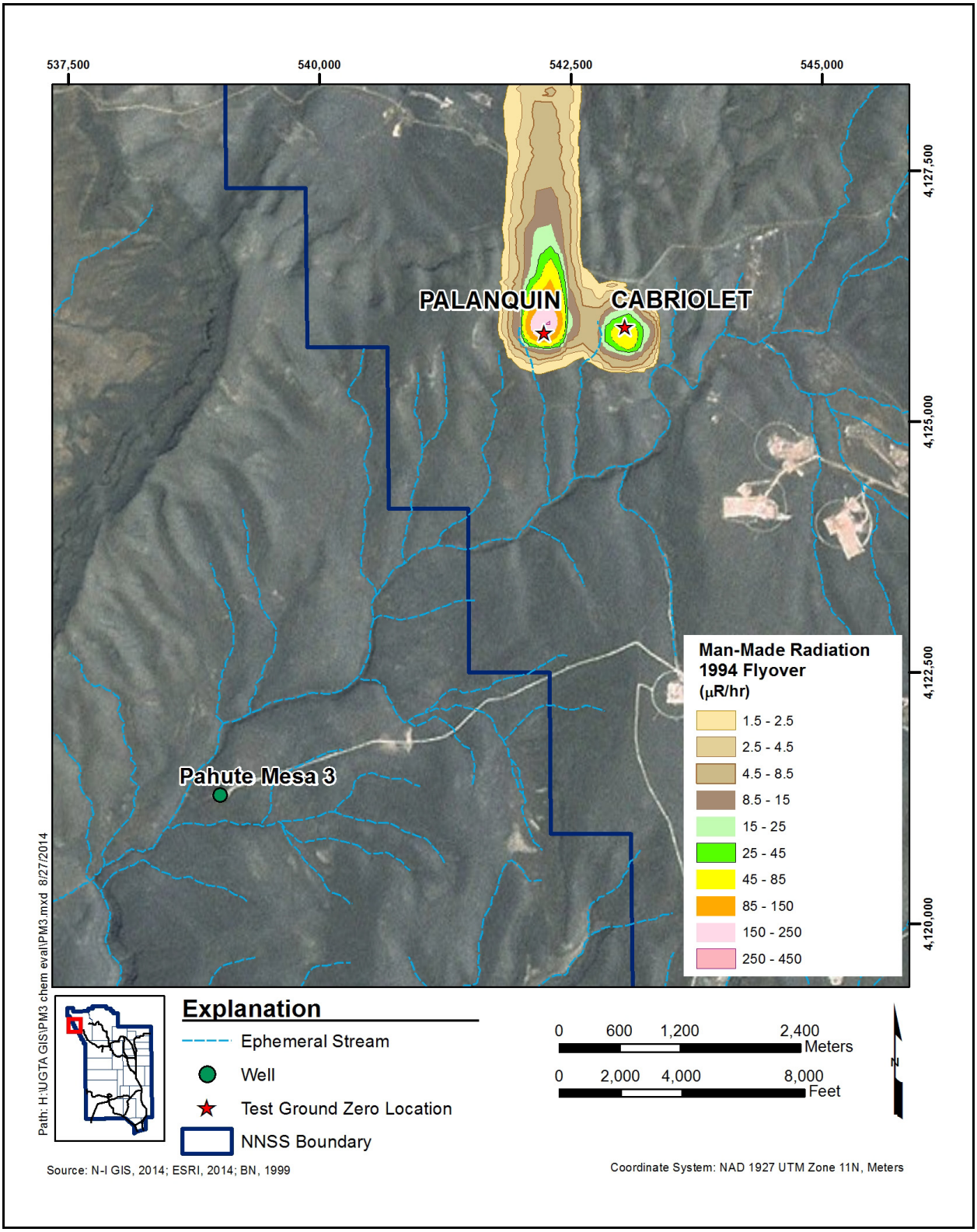

Figure 3-1
Surface Radiation Near PM-3 from 1994 Flyover

location of PM-3, there is significant uncertainty on the near-surface contamination in the vicinity of PALANQUIN resulting from this test. There is also uncertainty on the subsequent redistribution of the surface contamination that may exist in the vicinity of PALANQUIN and CABRIOLET by fluvial or eolian processes.

There are no direct observations of surface soil ^3H concentrations in the vicinity of PALANQUIN or CABRIOLET. Assuming these detonations are analogous to SEDAN and SCHOONER (although of a smaller magnitude and shallower), one can use observations from these other Plowshare tests to bound the possible extent of ^3H near PALANQUIN and CABRIOLET. The ^3H concentrations in soils and ejecta in the vicinity of the SEDAN test have been extensively reported by Koranda et al. (1967) based on observations made in 1965–1966, less than four years after the SEDAN detonation on July 6, 1962. This study evaluated the spatial and temporal distribution of tritiated water from the SEDAN crater lip to 5,000 ft from ground zero and from ground surface to a depth of 6 ft. The maximum ^3H concentrations observed were found at a depth of 5 ft, at the base of the ejecta material. The maximum fallback and crater-lip-ejecta ^3H concentrations were found to be in the range from 2.2 to 9.5 microcuries per milliliter (µCi/mL) of soil water (equivalent to 2.2E+09 to 9.5E+09 pCi/L). The ^3H soil water concentrations were found to decrease significantly at shallower depths, with the range of concentrations at 6 in. depth being about three orders of magnitude less than the values at 5-ft depth (i.e., approximately 0.004 µCi/mL of soil water or about 4.0E+06 pCi/L). The decrease at shallower depths has been attributed to dilution caused by rainfall events, especially large precipitation that occurred in the winter of 1965–1966.

Although no soil water ^3H measurements exist in the vicinity of PALANQUIN or CABRIOLET, it is reasonable to expect that the tritiated soil water at these locations may be similar to that observed near SEDAN, even though the SEDAN detonation was at a greater depth. However, it is also reasonable to expect that the soil water ^3H concentration will be reduced with time as precipitation events infiltrate the soil and mix with the residual ^3H.

Observations of ^3H in the air above the SEDAN and SCHOONER Plowshare tests are reported in the NNSS 2013 Environmental Report (Wills, 2014). The range of concentrations at SEDAN were from less than detection to about 6.7E-06 picocuries per milliliter (pCi/mL) with an average of about 2.1E-06 pCi/mL, while the range of concentrations at SCHOONER were from 5.3E-06 pCi/mL to 4.08E-04 pCi/mL with an average of 1.43E-04 pCi/mL. These results indicate that tritiated water in

the soil at these locations continues to diffuse to the surface decades after the test. Although no air sample measurements exist at PALANQUIN or CABRIOLET, it is reasonable to expect that the tritiated soil water at these locations would also continue to diffuse to the surface.

The contaminated soils at CABRIOLET and PALANQUIN may have provided a source of ^3H for surface water runoff events. While there have been no observations of significant ^3H concentrations in any surface discharge on or off the NNSS downgradient from Plowshare tests, the surface water could become contaminated when it is exposed to the tritiated soil water. The ^3H concentration in the surface water runoff would be expected to be orders of magnitude less than the concentration of the soil water based on the differences in the volumes and the observation that the highest soil water ^3H concentrations occur at depths below the ejecta and fallback material.

Surface water containing some amount of ^3H would be expected to drain quickly down the Thirsty Canyon drainage system if the storms are of sufficient magnitude and intensity. The lateral extent of the ephemeral drainage from the area of CABRIOLET and PALANQUIN would also be a function of the magnitude and intensity of the storm precipitation event. It is possible that the lateral extent could be as far as PM-3, located about 4 km downstream from these Plowshare tests.

A portion of the ephemeral stream drainage down the Thirsty Canyon drainage system could infiltrate into the permeable alluvial streambed materials and the underlying permeable volcanic units. Estimating how much water could infiltrate and the duration of the infiltration is uncertain, but a field-saturated hydraulic conductivity of 2,800 meters per day (m/day) has been measured by Ebel and Nimmo (2009) in Rainier Mesa while Mirus and Perkins (2012) have measured saturated hydraulic conductivity of 1.5 m/yr in surface exposures of the Thirsty Canyon/Timber Mountain volcanic aquifer and 1.8 m/yr in the Paintbrush volcanic aquifer in Pahute Mesa using an infiltrometer.

The potentially tritiated water that may infiltrate the permeable drainage wash materials would be expected to percolate through the unsaturated zone to the water table. Given the HSUs between the surface and the water table in the vicinity of PM-3 in part consist of fractured volcanic aquifers, notably the Thirsty Canyon volcanic aquifer (TCVA) and the Timber Mountain welded-tuff aquifer (TMWTA), it is possible that the water that infiltrates from the ephemeral drainage in the Thirsty Canyon could rapidly percolate to the water table and mix with groundwater that is derived from recharge further upgradient in the Black Mountain tributary flow system. The TCVA is about 500 ft

thick at PM-3 and consists of a preponderance of strongly welded ash-flow tuffs and dense lava flow units that are highly fractured (NSTec, 2014). The TMWTA is about 350 ft thick at PM-3 and consists mainly of welded ash-flow tuffs that are assumed to be highly fractured (NSTec, 2014). Beneath these two fractured rock aquifers lie the Timber Mountain lower vitric-tuff aquifer (TMLVTA), which is about 400 ft thick and consists mainly of nonwelded and bedded tuffs; and the Upper Paintbrush confining unit (UPCU), which generally consists of zeolitic bedded and nonwelded tuffs that have an unsaturated thickness of about 200 ft above the water table (which is located in the PM-3-2 [shallow] piezometer). Having rapid (i.e., decades) vertical transport of tritiated water in the approximately 850 ft of fractured rock units is possible; however, the nonwelded nature of the TMLVTA and would generally preclude rapid transport through the additional about 600 ft to the water table because these units are not significantly fractured. It is interesting to note that water levels at depth in other locations on the NNSS—most notably at WW-3 in Yucca Flat—have been postulated to respond to seepage from surface water ponds to depths of about 1,500 ft within a few years (Elliott and Fenelon, 2010). Although the conditions at WW-3 are different than the ephemeral events near PM-3, the possibility of some water being able to recharge the deep aquifer system within a few decades is at least plausible.

Given the paucity of direct field evidence to the contrary, the possibility of rapid vertical transport of potentially tritiated water from ephemeral infiltration in the Thirsty Canyon wash to the water table in the vicinity of PM-3 cannot be precluded. Although the major-ion and stable-isotope chemistry of the groundwater at PM-3 indicate that the majority of the water at this location is not derived from recent recharge (Section 2.2.2), only a small fraction (significantly less than 1 percent) of contaminated surface drainage water is necessary to provide the observed low ^3H concentrations. For example, only 0.001 percent of a 1.0E+07 pCi/L ^3H recharge water is necessary to yield an *in situ* concentration of 100 pCi/L. Such a low fraction would be undetectable from a major-ion and stable-isotope chemistry perspective. While there is no information to determine whether such an ephemeral event occurred and there have been no observations of any equivalent events on the NNSS, the available information cannot be used to preclude the vertical transport hypothesis.

3.2.5 Analysis of Possible Lateral Transport of ^3H from Underground Nuclear Tests

It is possible that the ^3H concentration in groundwater samples taken from the PM-3 piezometers is the result of lateral transport in the groundwater from known upgradient sources of ^3H contamination

on the NNSS resulting from underground nuclear testing. Although the nearest underground nuclear detonation to PM-3 is DELAMAR, located about 4.5 km northeast, the potentiometric surface in the area developed by Fenelon et al. (2010) (Figure 1-6) indicates that DELAMAR is downgradient of PM-3. The most likely candidate source of upgradient contamination for PM-3 is the HANDLEY detonation, a greater than 1 megaton (Mt)-yield detonation with a working point located about 7.2 km north–northeast and upgradient of PM-3 (see Figure B-1). Although it is also possible that the PURSE detonation, located about 7.2 km northeast of PM-3, could be a candidate source of contamination due to its proximity to the Purse fault, the analyses below assume the source was HANDLEY given its larger size, the fact the HANDLEY chimney intersects the BRA, and the perceived direction and magnitude of the hydraulic gradient between HANDLEY and PM-3 (Figure 1-6). A perspective view of the hydrostratigraphy between HANDLEY (U-20m) and PM-3 is illustrated in Figure 3-2.

There are several lines of reasoning that indicate that the source of the ^{3}H at PM-3 could be the result of lateral transport from upgradient contamination sources on the NNSS. First, PM-3 is located essentially along the inferred groundwater flow direction from upgradient sources of known contamination such as HANDLEY. Second, the major-ion and stable-isotope geochemistry observed at PM-3 is consistent with the geochemistry of other upgradient wells in the Thirsty Canyon area—including UE-20j WW, which was expended by the HANDLEY detonation (Section 2.2). Third, other mobile (i.e., ^{14}C, ^{36}Cl, and ^{129}I) radionuclide groundwater concentrations in PM-3-2 (shallow) water samples are in approximately the same concentration ratio with the assumed initial exchange volume concentrations at HANDLEY as ^{3}H (see Appendix C). Fourth, simple two-dimensional (2-D) numerical models of ^{3}H transport from HANDLEY to PM-3 indicate that for not unreasonable parameter values, it is possible to simulate ^{3}H concentrations that are similar to those observed at PM-3-2 (shallow) and PM-3-1 (deep) (see Appendix C). The results of the 2-D numerical models are summarized below.

HANDLEY is located along the inferred groundwater flow directions in the Black Mountain tributary flow system drawn by Fenelon et al. (2010) as illustrated in Figure 1-5. The hydraulic gradient between HANDLEY and PM-3 is about 0.01 m/m based on static water levels at UE-20j and U-20m of about 4,640 ft amsl, a static water level of about 4,365 ft amsl for PM-3, and a distance between these locations of about 7,200 m (about 24,000 ft). Analyses of the hydrogeology and hydraulic properties that affect the rate of groundwater movement and potential transport of ^{3}H downgradient of

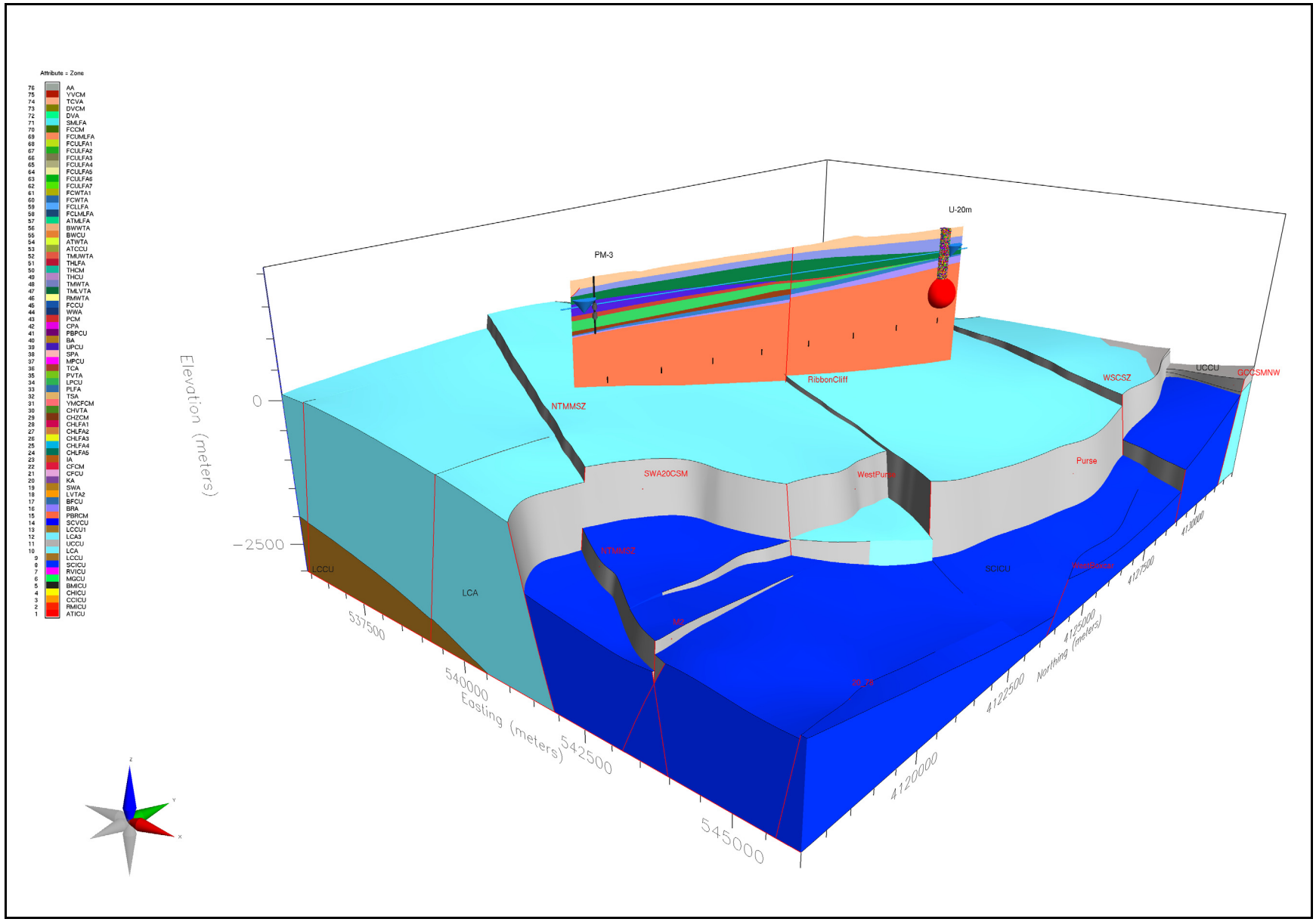

Figure 3-2

General Perspective View of Hydrostratigraphy and Major Structural Features in the Vicinity of PM-3

Note: Cavity radius based on maximum yield range identified in DOE/NV (2000) and Pawloski (1999). Positive Y-axis is to the north.

HANDLEY are summarized in Appendix B. This summary indicates that there is a large uncertainty with respect to the hydraulic properties and continuity of the HSUs through which groundwater is likely to flow and transport could occur between HANDLEY and PM-3.

Numerical modeling was used to quantitatively evaluate the feasibility of ^3H being transported from the HANDLEY detonation to PM-3. The models were vertical 2-D fences following streamlines originating at the HANDLEY detonation. The streamtube modeling included simulation of matrix diffusion, and all rock types are assumed to be fractured except alluvium, vitric tuff, and the intrusive confining units. The streamtube models along with the associated assumptions, parameter ranges and results are summarized in Appendix C.

The streamtube simulations of ^3H transport from the HANDLEY detonation to PM-3 presented in Appendix C used a range of flow and transport properties thought to bound possible radionuclide transport rates. Two streamlines were used to construct the HANDLEY streamtube models. The first streamline was from the Pahute Mesa potentiometric surface interpretation modified from Fenelon et al. (2010), and the second streamline was a straight line connection from HANDLEY to PM-3.

Three alternate hydraulic conductivity datasets are considered; notably, the Phase I hydrologic data document (HDD) (SNJV, 2004) and two interpretation methods based on recent USGS modeling (Halford et al., 2012). The USGS performed simultaneous numerical analysis of eight aquifer tests to estimate hydraulic properties on Pahute Mesa. The USGS analysis used simplified HSUs that were heterogeneous and calibrated the models by adjusting the hydraulic conductivity of pilot points and interpolating the pilot point values to model node locations. Hydraulic conductivity values for each streamtube model HSU were extracted from the USGS modeling using two interpretation methods. The first method calculated the volumetric average of all USGS model cells within each Phase II hydrostratigraphic framework model (HFM) HSU, and the second method calculated the thickness weighted average from vertical profiles at each Pahute Mesa detonation location.

The simulation of matrix diffusion in fractured rock requires the assumption of a fracture continuum with a specific geometry. The fracture continuum is assumed to consist of vertical parallel plates, and consistency between fracture properties is maintained by calculating the fracture porosity from the hydraulic conductivity and fracture spacing using the cubic law. The fracture properties of the permeable HSUs between HANDLEY and PM-3 significantly affect the lateral extent of ^3H transport. Alternate fracture spacings and an alternate fracture conceptual model were considered to address the

uncertainty in these properties. Streamtube simulations were performed using the mean fracture spacing as well as end points for a 95 percent confidence interval. These spacings are the 50, 2.5, and 97.5 percentile values assuming that the fracture spacing data are lognormal. The alternate conceptualization of matrix diffusion assumed three sets of orthogonal fractures that form cubic matrix blocks in combination with the HDD hydraulic conductivity parameterization.

An additional uncertainty explored in the streamtube model simulations presented in Appendix C was the location of the calculated ^3H concentration at PM-3. In addition to the two currently open intervals of PM-3-1 (deep) and PM-3-2 (shallow), there is a possibility that PM-3 allowed for hydraulic communication of all the permeable features intersecting the well for some time before the well was recompleted. For example, given the three years between drilling in 1998 and recompletion in 2002, a hypothetical hydraulic communication of 1 gpm would yield a total flow of more than one million gallons. If this is the case, it is possible that the deep BRA—which has a high permeability, a low effective fracture porosity, and is laterally continuous between HANDLEY and PM-3—could be a pathway for lateral ^3H transport. In addition, the smaller-than-expected drawdown during pump-jack sampling of PM-3-2 (shallow) suggests that the confining unit at PM-3 may have a higher hydraulic conductivity (about 0.2 feet per day [ft/day] as summarized in Section B.4.0) than is typical of a confining unit and may allow hydraulic communication with the deeper BRA. As a result, the additional location selected for comparing the observed and simulated ^3H concentrations was at the vertical location corresponding to the highest simulated ^3H concentration, which generally corresponds to where the BRA intersects PM-3.

The results of the simulated ^3H concentrations at PM-3 for the different permutations of flow fields, hydraulic conductivity distributions and fracture properties are presented in Appendix C. Representative results for the straight line streamline model with the results compared to the observations at PM-3-2 (shallow) are reproduced in Figure 3-3. These results indicate that for the HDD hydraulic conductivity case, the simulated concentrations would match the observed concentrations at PM-3-2 (shallow) if the fracture spacing is between the mean and 97.5 percentile. In addition, assuming the recent USGS modeling based hydraulic conductivity values, the simulated concentrations would match the observed concentrations at PM-3-2 (shallow) if the fracture spacing is about the 97.5 percentile. Also, when assuming the alternate fracture conceptual model with three sets of orthogonal fractures in combination with the HDD hydraulic conductivity values, the

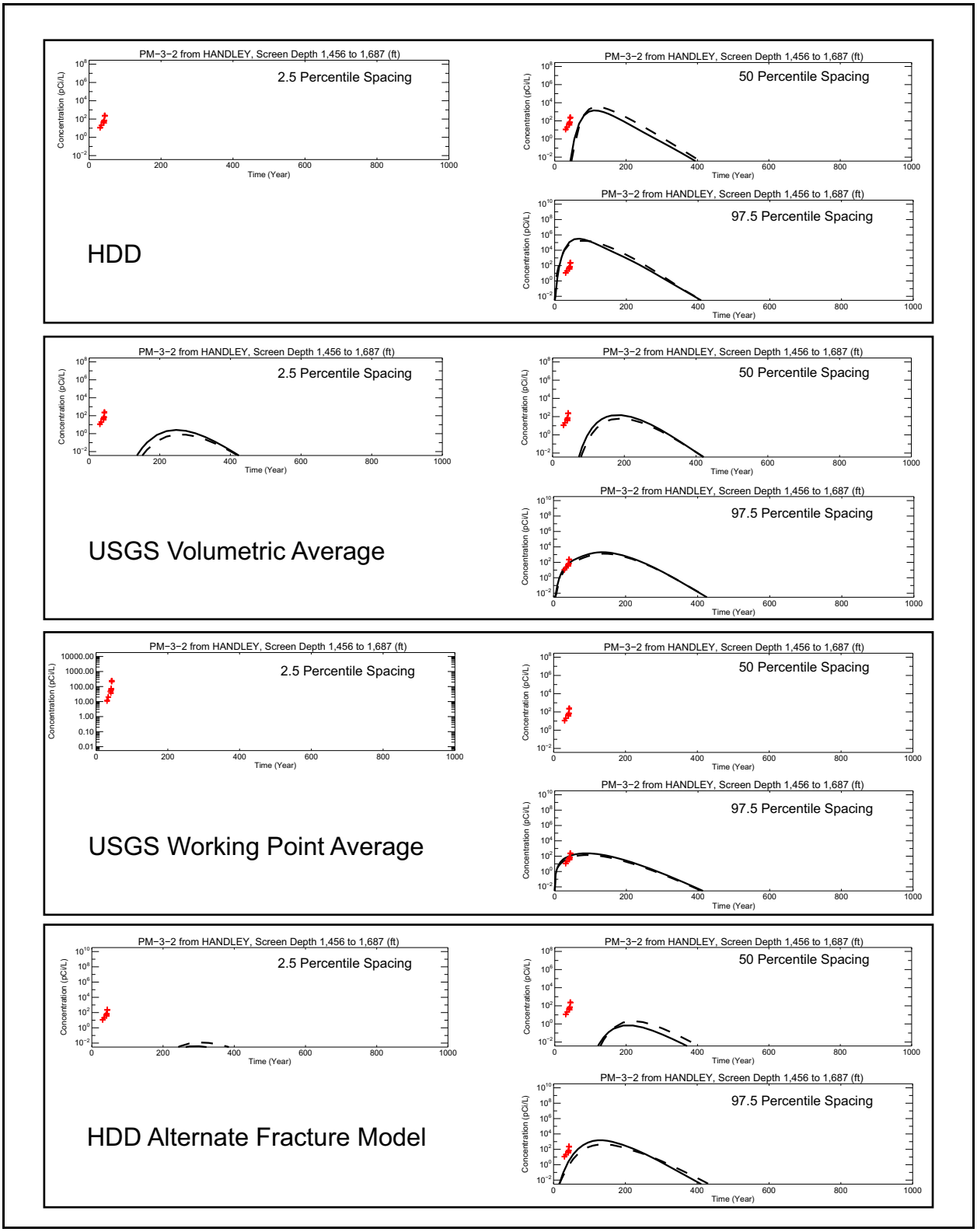

Figure 3-3
Straight Line Streamline Simulated Breakthrough and Observed ^3H Concentrations at PM-3-2

Note: Dashed line is maximum at any vertical location; solid line is well screen; red crosses are observations.

predicted breakthrough was coincident with observations only using the 97.5 percentile fracture spacing.

In summary, the streamtube simulations of ^3H transport from the HANDLEY detonation to PM-3—although they are uncalibrated and simply used a range of flow and transport properties thought to bound possible radionuclide transport rates—indicate that the ^3H observed in PM-3 may be from the HANDLEY detonation. The extent of lateral transport is likely significantly affected by the flow and transport properties of the BRA, which intersects the lowermost section of PM-3 as well as the chimney of the HANDLEY detonation.

3.3 Summary

Although the recent sampling and analyses have confirmed the presence of ^3H above the minimum detection limit at PM-3, there remains uncertainty on the source of the observed ^3H. Four alternative hypotheses for the ^3H observed at PM-3 have been evaluated. These alternative hypotheses are based on a range of assumptions that are not possible to independently confirm based on the paucity of information in this remote area of the NTTR, and the lack of information between PM-3 and possible sources of ^3H including nearby Plowshare tests or UGTA tests such as HANDLEY.

Based on mixing arguments, it is possible to rule out the hypotheses that the observed ^3H is the result of residual ^3H from drilling/recompletion activities or the result of percolation of atmospheric ^3H. If either hypothesis were correct, the observed water chemistry at PM-3 would have been more consistent with either the drilling/recompletion water or the average infiltration water.

There is insufficient information to rule out the hypothesis of vertical transport of tritiated groundwater that could have originated in ephemeral drainage from the upgradient Plowshare tests. Although it seems to require an implausible set of circumstances that starts with the runoff of ^3H surface water down the Thirsty Canyon wash followed by infiltration and subsequent transport through about 1,500 ft of variably saturated media to the water table, the local downward vertical hydraulic gradient from PM-3-2 (shallow) to PM-3-1 (deep) and the higher observed ^3H concentrations at PM-3-2 (shallow) favor this hypothesis.

There is insufficient information to confirm the hypothesis of lateral transport of tritiated groundwater from upgradient UGTA detonations, whether HANDLEY or PURSE. Although analyses summarized

in Section 3.2.5 indicate that it is conceivable for certain reasonable parameter values to yield simulated ^3H concentrations at PM-3 that are consistent with the observed concentrations assuming a ^3H source at HANDLEY, there remains uncertainty in the lateral continuity of the possible transport paths over the 7.2-km distance from HANDLEY to PM-3, and the local observations that indicate the shallow zones at PM-3-2 (shallow) have a higher concentration and higher head than deeper zones at PM-3-1 (deep). Although it is possible that the local ^3H and head observations reflect heterogeneous local features, there remains the possibility that they are indicative of vertical downward flow and transport at PM-3.

4.0 CONCLUSIONS

PM-3 was drilled and sampled to support the evaluation of the hydrogeology and geochemistry of the groundwater flow system west of the underground nuclear testing conducted in Western Pahute Mesa on the NNSS. Since the well was drilled in 1988 and recompleted as two separate isolated piezometers (PM-3-1 [deep] and PM-3-2 [shallow]) in 1992, the well has been sampled by DOE's RREMP and UGTA Activity to determine the chemistry of the groundwater at this location. The most recent sampling was conducted in August 2013, and a preliminary evaluation of the results of this sampling is summarized in N-I (2014b).

This report incorporates the additional chemical, radiochemical, stable-isotope, and noble gas data from samples taken in August 2013 that were analyzed after the completion of N-I (2014b). In addition, analyses of the hydrogeologic conditions in the vicinity of PM-3 and between PM-3 and possible sources of ^3H are summarized to evaluate the potential that the observed ^3H at PM-3 might be the result of either vertical transport of ^3H from the infiltration of ephemeral drainage from nearby Plowshare tests or lateral transport through the aquifers and confining units between possible UGTA sources and PM-3.

The conclusion of the additional chemical, radiochemical, stable-isotope, and noble gas data from PM-3 that are presented in Section 2.0 is that the groundwater at this location is similar to other groundwater upgradient and downgradient of this location, generally referred to as the Thirsty Canyon area in Rose et al. (2006). The additional data support the general flow-path directions identified by the geochemical flow-path analyses presented in Rose et al. (2006) and Kwicklis et al. (2005) as well as the groundwater flow system analyses presented in Fenelon et al. (2010)—i.e., that groundwater flow west of the Purse Fault is toward the south–southwest and discharges in the Oasis Valley area.

An additional effort was devoted to attempt to determine whether the noble gas data could fingerprint the source of the ^3H observed at PM-3. Although these data, summarized in Section 2.2.3, confirm the ^3H is of anthropogenic origin, it was not possible to determine whether the source of the ^3H was due to

lateral transport from upgradient sources, such as HANDLEY or PURSE, or from vertical transport from other sources of ^{3}H such as the nearby Plowshare tests, PALANQUIN, or CABRIOLET.

A range of possible hypotheses have been proffered to explain the observed ^{3}H at PM-3. These hypotheses range from the possibility that the observed concentrations are a result of either (1) downward percolation of surface water or precipitation with a higher ^{3}H concentration, or (2) lateral groundwater flow and ^{3}H transport from upgradient ^{3}H sources such as the HANDLEY detonation.

The vertical transport hypothesis relies on the possibility of vertical ^{3}H transport over the approximately 500 m to the PM-3-2 (shallow) open interval. Using average infiltration rates, it is not likely that anthropogenic ^{3}H would be transported this distance for the average transport properties. However, it is possible that localized higher infiltration rates are possible in areas where nearby ephemeral drainage channels intersect the permeable tuff aquifers. These areas of potentially higher infiltration could lead to more rapid vertical transport through the unsaturated zone.

Information that generally supports the vertical transport hypothesis includes (1) higher ^{3}H and other mobile radionuclide concentrations in PM-3-2 (shallow) than PM-3-1 (deep); (2) an apparent vertical hydraulic gradient between PM-3-2 (shallow) to PM-3-1 (deep), indicating the possibility of downward vertical flow; and (3) He concentrations suggesting less than a 50-year travel time.

The lateral transport hypothesis relies on the possibility of lateral ^{3}H transport over the 7.2-km distance from HANDLEY, or possibly PURSE, to PM-3 through aquifers and confining units between these locations. Information that generally supports the lateral transport hypothesis includes (1) a significant horizontal hydraulic gradient along the postulated groundwater flow path between HANDLEY and PM-3; (2) a similar groundwater geochemistry at HANDLEY (represented by UE-20j WW) and PM-3; (3) the presence of a continuous fractured HSU (i.e., the BRA) that is penetrated by the HANDLEY chimney and PM-3; and (4) observed concentrations of mobile radionuclides (i.e., ^{3}H, ^{14}C, ^{36}Cl and ^{129}I) at PM-3-2 (shallow) and PM-3-1 (deep) that have similar ratios to the HANDLEY cavity concentration when considering the effects of ^{3}H decay.

The lateral transport hypothesis was quantitatively evaluated using a simple quasi-three-dimensional (3-D) model developed along the possible flow path between HANDLEY and PM-3 (see Appendix C). The quasi-3-D model is along a 2-D profile from HANDLEY to PM-3 that has a

width equivalent to the diameter of the exchange volume at HANDLEY (assumed to have a radius of three times the cavity radius of 98 m, per the maximum announced yield of greater than 1 Mt [DOE/NV, 2000] and the depth- and yield-dependent cavity radius formula of Pawloski [1999]) with the width varying between HANDLEY and PM-3 to ensure that the volumetric flow rate is held constant along the flow path. Significant uncertainty exists in the hydrogeologic and source term conceptual models and parameters that could affect the rate of transport between HANDLEY and PM-3. These uncertainties include (1) the groundwater flow-path orientation, (2) the hydraulic gradient along this flow path, (3) the groundwater flow rate through this flow path that may intersect the ^3H sources at HANDLEY, (4) the distribution of this flow rate between the different HSUs between HANDLEY and PM-3, (5) the initial distribution of ^3H in the HANDLEY exchange volume and chimney, and (6) the transport properties (notably the effective fracture porosity and fracture spacing) that affect the rate of advective transport and matrix diffusion. These uncertainties were evaluated using a range of different parameter values in the analyses performed with the quasi-3-D model.

The results of the lateral transport hypothesis modeling, presented in Appendix C and summarized in Section 3.2.5, indicate it is possible to explain the observed ^3H concentrations measured in samples taken from PM-3-1 (deep) and PM-3-2 (shallow) by lateral transport from the HANDLEY exchange volume and chimney to PM-3. The likely transport path for the ^3H is through the BRA, which (1) intersects the HANDLEY chimney; (2) is continuous between HANDLEY and PM-3 (although offset at the Ribbon Cliff fault); (3) intersects the lower part of the PM-3 borehole (although this portion of the borehole has collapsed and was plugged during recompletion activities in 1992 that hydraulically separate PM-3-1 [deep] from the BRA); (4) has a high permeability; and (5) has a low effective porosity due to the fractured nature of this HSU.

In summary, although there remains uncertainty in the definitive interpretation of the PM-3 ^3H, it is possible that the ^3H observed at PM-3 is the leading edge of the plume resulting from lateral transport downgradient from HANDLEY. Disproving this hypothesis would be difficult even using other tracers indicative of rapid infiltration such as chlorofluorocarbons because of the possibility of some small amount of residual drilling/recompletion water contamination. If the lateral transport hypothesis is correct, one would expect that additional sampling of the two piezometers at this location over the next decades may show an increase of ^3H concentrations as illustrated in Figure 3-3. However, it is important to recognize that the ^3H at this location and other locations along the possible

transport path will also undergo decay. It is also worthwhile to note that if the observed concentrations are the result of lateral transport from HANDLEY, PM-3 serves as an excellent monitoring location.

5.0 REFERENCES

BN, see Bechtel Nevada.

Bechtel Nevada. 1999. *An Aerial Radiological Survey of the Nevada Test Site, Nevada Test Site, Nevada,* DOE/NV/11718--324. Las Vegas, NV.

Bechtel Nevada. 2002. *A Hydrostratigraphic Model and Alternatives for the Groundwater Flow and Contaminant Transport Model of Corrective Action Units 101 and 102: Central and Western Pahute Mesa, Nye County, Nevada*, DOE/NV/11718--706. Las Vegas, NV.

Belcher, W.R., J.B. Blainey, F.A. D'Agnese, C.C. Faunt, M.C. Hill, R.J. Laczniak, G.M. O'Brien, C.J. Potter, H.M. Putnam, C.A. San Juan, and D.S. Sweetkind. 2004. *Death Valley Regional Ground-Water Flow System, Nevada and California–Hydrogeologic Framework and Transient Ground-Water Flow Model,* Scientific Investigations Report 2004-5205. Reston, VA: U.S. Geological Survey.

Craig, H. 1961. "Isotopic Variations in Meteoric Waters." In *Science*, Vol. 133(3465): 1702–1703. Washington, DC: American Association for the Advancement of Science.

Criss, R.E. 1999. *Principles of Stable Isotope Distribution*. New York, NY: Oxford University Press.

DOE/NV, see U.S. Department of Energy, Nevada Operations Office.

ESRI, see ESRI, i-cubed, USDA FSA, USGS, AEX, GeoEye, Getmapping, Aerogrid, and IGP.

Ebel, B.A., and J.R. Nimmo. 2009. *Hydraulic Property and Soil Textural Classification Measurements for Rainier Mesa, Nevada Test Site, Nevada*, Open-File Report 2009–1264. Reston, VA: U.S. Geological Survey.

Elliott, P.E., and J.M. Fenelon. 2010. *Database of Groundwater Levels and Hydrograph Descriptions for the Nevada Test Site Area, Nye County, Nevada*, *1941–2010,* Data Series 533. Reston, VA: U.S. Geological Survey. (Version 5.0 released in October 2014).

ESRI, i-cubed, USDA FSA, USGS, AEX, GeoEye, Getmapping, Aerogrid, and IGP. 2014. ArcGIS Online website. As accessed at http://www.arcgis.com/home/gallery.html on 27 August.

Fenelon, J.M., D.S. Sweetkind, and R.J. Laczniak. 2010. *Groundwater Flow Systems at the Nevada Test Site, Nevada: A Synthesis of Potentiometric Contours, Hydrostratigraphy, and Geologic Structures*, Professional Paper 1771. Reston, VA: U.S. Geological Survey.

Hacker, B.C. 1994. *Elements of Controversy: The Atomic Energy Commission and Radiation Safety in Nuclear Weapons Testing 1947-1974*. Berkeley, CA: University of California Press.

Halford, K., J. F. Fenelon, and S. Reiner, U.S. Geological Survey. 2012. Memorandum to D. Galloway (USGS) titled, "Aquifer-Test Package - Simultaneous Numerical Analysis of Eight Aquifer Tests To Estimate Hydraulic Properties on Pahute Mesa, Nevada National Security Site." Henderson, NV. As accessed at http://nevada.usgs.gov/water/AquiferTests /Pahute_Mesa_8.cfm?studyname=Pahute_Mesa_8 on 11 August 2014.

Ingraham, N.L., R.L. Jacobson, J.W. Hess, and B.F. Lyles. 1990. *Stable Isotopic Study of Precipitation and Spring Discharge on the Nevada Test Site*, DOE/NV/10845--03; Publication No. 45078. Las Vegas, NV: Desert Research Institute.

Kilroy, K.C., and C.S. Savard. 1996. *Geohydrology of Pahute Mesa-3 Test Well, Nye County, Nevada*, Water-Resources Investigations Report 95-4239. Carson City, NV: U.S. Geological Survey.

Kirsch, S. 2005. *Proving Grounds: Project Plowshare and the Unrealized Dream of Earthmoving.* Piscataway, NJ: Rutgers University Press.

Koranda, J.J., J.R. Martin, and R. Wikkerink. 1967. *Residual Tritium at Sedan Crater Part II: Soil and Ejecta Studies*, UCRL-50360. Livermore, CA: Lawrence Radiation Laboratory, University of California.

Kwicklis, E.M., T.P. Rose, and F.C. Benedict. 2005. *Evaluation of Groundwater Flow in the Pahute Mesa – Oasis Valley Flow System Using Groundwater Chemical and Isotopic Data*, LA-UR 05-4344. Los Alamos, NM: Los Alamos National Laboratory.

Merlivat, L., and J. Jouzel. 1979. "Global Climatic Interpretation of the Deuterium Oxygen-18 Relationship for Precipitation." In *Journal of Geophysical Research: Oceans,* Vol. 84(C8): pp. 5029–5033.

Mirus, B.B., and K.S. Perkins, 2012. "Practical Estimates of Field-Saturated Hydraulic Conductivity of Bedrock Outcrops Using a Modified Bottomless Bucket Method." In *Water Resources Research*, Vol. 48(9).

N-I, see Navarro-Intera, LLC.

N-I GIS, see Navarro-Intera Geographic Information Systems.

NNSA/NSO, see U.S. Department of Energy, National Nuclear Security Administration Nevada Site Office.

NNSA/NV, see U.S. Department of Energy, National Nuclear Security Administration Nevada Operations Office.

NSTec, see National Security Technologies, LLC.

National Security Technologies, LLC. 2014. Written communication. Subject: *Phase II Hydrostratigraphic Framework Model for Corrective Action Units 101 and 102: Central and Western Pahute Mesa, Nye County, Nevada*. Las Vegas, NV.

Navarro-Intera, LLC. 2011. Written communication. Subject: *Data Report for Well Pahute Mesa #3 (PM-3) Groundwater Sampling*. Las Vegas, NV.

Navarro-Intera, LLC. 2014a. Written communication. Subject: "UGTA Geochemistry Database," UGTA Technical Data Repository Database Identification Number UGTA-4-129. Las Vegas, NV. As accessed on 15 August.

Navarro-Intera, LLC. 2014b. Written communication. Subject: *Well Pahute Mesa #3 (PM-3) Well Development and Sampling Data Report*. Las Vegas, NV.

Navarro-Intera Geographic Information Systems. 2011–2014. ESRI ArcGIS Software.

Pawloski, G.A. 1999. *Development of Phenomenological Models of Underground Nuclear Tests on Pahute Mesa, Nevada Test Site-Benham and TYBO,* UCRL-ID-136003. Livermore, CA. Lawrence Livermore National Laboratory.

Rose, T.P., F.C. Benedict, Jr., J.M. Thomas, W.S. Sicke, R.L. Hershey, J.B. Paces, I.M. Farnham, and Z.E. Peterman. 2006. *Geochemical Data Analysis and Interpretation of the Pahute Mesa - Oasis Valley Groundwater Flow System, Nye County, Nevada, August 2002*, UCRL-TR-224559. Livermore, CA: Lawrence Livermore National Laboratory; Reno, NV: GeoTrans Inc. and Desert Research Institute; Denver, CO: U.S. Geological Survey; and Las Vegas, NV: Harry Reid Center for Environmental Studies.

Russell, G.M., and G.L. Locke. 1997. *Summary of Data Concerning Radiological Contamination at Well PM-2, Nevada Test Site, Nye County, Nevada*, Open-File Report 96-599. Carson City, NV: U.S. Geological Survey.

SNJV, see Stoller-Navarro Joint Venture.

Slate, J.L., M.E. Berry, P.D. Rowley, C.J. Fridrich, K.S. Morgan, J.B. Workman, O.D. Young, G.L. Dixon, V.S. Williams, E.H. McKee, D.A. Ponce, T.G. Hildenbrand, W.C. Swadley, S.C. Lundstrom, E.B. Ekren, R.G. Warren, J.C. Cole, R.J. Fleck, M.A. Lanphere, D.A. Sawyer, S.A. Minor, D.J. Grunwald, R.J. Laczniak, C.M. Menges, J.C. Yount, and A.S. Jayko. 1999. *Part A. Digital Geologic Map of the Nevada Test Site and Vicinity, Nye, Lincoln, and Clark Counties, Nevada, and Inyo County, California, Revision 4*, Open-File Report 99-554-A, scale 1:120,000. Denver, CO: U.S. Geological Survey.

Stoller-Navarro Joint Venture. 2004. *Hydrologic Data for the Groundwater Flow and Contaminant Transport Model of Corrective Action Units 101 and 102: Central and Western Pahute Mesa, Nye County, Nevada*, Rev. 0, S-N/99205-002; Shaw/13052-204. Las Vegas, NV.

Stoller-Navarro Joint Venture. 2006. *Geochemical and Isotopic Evaluation of Groundwater Movement in Corrective Action Unit 97: Yucca Flat/Climax Mine, Nevada Test Site, Nevada,* Rev. 0, S-N/99205--070. Las Vegas, NV.

Stoller-Navarro Joint Venture. 2009. *Phase I Transport Model of Corrective Action Units 101 and 102: Central and Western Pahute Mesa, Nevada Test Site, Nye County, Nevada,* Rev. 1, S-N/99205--111. Las Vegas, NV.

Thomas, J.M., F.C.Benedict, Jr., T.P. Rose, R.L. Hershey, J.B. Paces, Z.E. Peterman, I.M. Farnham, K.H. Johannesson, A.K. Singh, K.J. Stetzenbach, G.B. Hudson, J.M. Kenneally, G.F. Eaton, and D.K. Smith. 2002. *Geochemical and Isotopic Interpretations of Groundwater Flow in the Oasis Valley Flow System, Southern Nevada*, DOE/NV/11508-56; Publication No. 45190. Las Vegas, NV: Desert Research Institute.

USC, see *United States Code*.

United States Code. 2012. Title 42 USC 300f et seq., "Safe Drinking Water Act of 1974," as amended. Washington, DC: U.S. Government Printing Office.

U.S. Department of Energy, National Nuclear Security Administration Nevada Operations Office. 2002. *Nevada Test Site Orthophoto Site Atlas,* DOE/NV/11718--604. Aerial photos acquired Summer 1998. Prepared by Bechtel Nevada. Las Vegas, NV.

U.S. Department of Energy, National Nuclear Security Administration Nevada Site Office. 2009. *Phase II Corrective Action Investigation Plan for Correction Action Units 101 and 102: Central and Western Pahute Mesa, Nevada Test Site, Nye County, Nevada,* DOE/NV--1312- Rev. 2. Las Vegas, NV.

U.S. Department of Energy, Nevada Operations Office. 1991. Written communication. Subject: *Hydrology Radionuclide Migration Program, Final Draft Well Completion Report Well PM-3, Nevada Test Site, Nevada*. Las Vegas, NV.

U.S. Department of Energy, Nevada Operations Office. 1992. *PM-3 Well Recompletion Summary for the Groundwater Characterization Project (GCP).* Las Vegas, NV.

U.S. Department of Energy, Nevada Operations Office. 1996. *Recompletion Report and Summary of Well History for Well PM-3,* DOE/NV--437 UC-700. Las Vegas, NV.

U.S. Department of Energy, Nevada Operations Office. 2000. *United States Nuclear Tests, July 1945 through September 1992*, DOE/NV--209-REV 15. Las Vegas, NV.

Wahl, R.R., D.A. Sawyer, S.A. Minor, M.D. Carr, J.C. Cole, W.C. Swadley, R.J. Laczniak, R.G. Warren, K.S. Green, and C.M. Engle. 1997. *Digital Geologic Map Database of the Nevada Test Site, Nevada*, Open-File Report 97-140, scale 1:120,000. Denver, CO: U.S. Geological Survey.

Warren, R.G., G.L. Cole, and D. Walther. 2000. *A Structural Block Model for the Three-Dimensional Geology of the Southwestern Nevada Volcanic Field,* LA-UR-00-5866. Los Alamos, NM: Los Alamos National Laboratory.

Wassenaar, L., R. Aravena, J. Hendry, and P. Fritz. 1991. "Radiocarbon in Dissolved Organic Carbon, A Possible Groundwater Dating Method: Case Studies from Western Canada." In *Water Resources Research,* Vol. 27(8): pp. 1975–1986.

White, A.F., and N.J. Chuma. 1987. "Carbon and Isotopic Mass Balance Models of Oasis Valley–Fortymile Canyon Groundwater Basin, Southern Nevada." In *Water Resources Research*, Vol. 23(4): pp. 571–582. Washington, DC: American Geophysical Union.

Wills, C., ed. 2014. *Nevada National Security Site Environmental Report 2013*, DOE/NV/25946--2182. Prepared for the U.S. Department of Energy, National Nuclear Security Administration Nevada Site Office. Las Vegas, NV: National Security Technologies, LLC.

Wycoff, R.C., U.S. Department of Energy, Nevada Operations Office. 2000. Letter to P.J. Liebendorfer (NDEP) titled "Analytical Sampling at Well PM-3," 28 February. Las Vegas, NV. (Also included as Appendix A of N-I [2011]).

Zavarin, M., A.B. Kersting, R.E. Lindvall, and T.P. Rose eds. 2008. *Hydrologic Resources Management Program and Underground Test Area Project FY2006 Progress Report,* LLNL-TR-404620. Livermore, CA: Lawrence Livermore National Laboratory.

Appendix A

PM-3 Analytical Chemistry and Radiochemistry Results

A.1.0 INTRODUCTION

Groundwater characterization samples were collected from both PM-3-1 (deep) and PM-3-2 (shallow) after water-quality parameters stabilized. The sampling methods and stabilization achieved are summarized in the *Well Pahute Mesa #3 (PM-3) Well Development and Sampling Data Report* (N-I, 2014b). The samples were collected from the wellhead manifold sampling port.

Groundwater characterization samples were collected from PM-3-1 (deep) over the two-day period of August 11 and 12, 2013. Samples were collected on August 11, 2013, after purging approximately 24,200 gal and water-quality parameters had stabilized; and on August 12, 2013, after purging approximately 28,800 gal and water-quality parameters had stabilized.

Groundwater characterization samples were collected from PM-3-2 (shallow) over the two-day period of August 22 and 23, 2013. Samples were collected on August 22, 2013, after purging approximately 31,800 gal and water-quality parameters had stabilized; and on August 23, 2013, after purging approximately 36,000 gal and water-quality parameters had stabilized.

Samples were collected and analyzed in accordance with the UGTA Quality Assurance Plan (NNSA/NSO, 2012) and sent to ALS Laboratory and ARS International, commercial laboratories certified by the State of Nevada for a large suite of analytical parameters. In addition, samples were sent to LLNL, USGS, and DRI for analyses not available from the commercial laboratory. With a few exceptions, the specific analytes are consistent with the Record of Technical Change dated January 30, 2014, for the *Pahute Mesa Phase II Corrective Action Investigation Plan for Corrective Action Units 101 and 102: Central and Western Pahute Mesa, Nevada Test Site, Nye County, Nevada* (NNSA/NSO, 2009). The exceptions are that LLNL rather than a commercial laboratory analyzed samples for ^{14}C and ^{36}Cl as age and migration parameters because the concentrations of these analytes are significantly below the levels detectable by the commercial laboratory's analytical instrumentation. LLNL uses an AMS capable of achieving superior detection limits for these analytes.

A.2.0 ANALYTICAL RESULTS

The analytical results for the PM-3-1 (deep) and PM-3-2 (shallow) samples collected in August 2013 are presented in Table A-1. In addition, ranges reported by Rose et al. (2006) for the analytes in the Thirsty Canyon geochemical group (ER-EC-1, ER-EC-2A, ER-EC-4, ER-EC-6, ER-EC-8, ER-OV-1, and ER-OV-6a) are presented in Table A-1.

Table A-1
Chemistry Data for PM-3-1 (Deep) and PM-3-2 (Shallow) from August 2013 Sampling
(Page 1 of 5)

Analyte	Laboratory	Detection Limit	PM-3-1 (Deep) 08/11/2013–08/12/2013	PM-3-2 (Shallow) 08/22/2013–08/23/2013	Range of Results for Thirsty Canyon Wells [a]
Water-Quality and Major-Ion Data (mg/L unless noted)					
T (°C)	Field	--	26.6–27.4	26.4–27.0	26.4–40.4
pH (-)	ALS	0.1	J 7.8	J 8.0	7.8–8.35
			J 7.8	J 8.0	
EC (µmhos/cm)	ALS	1.0	840	820	613–818
			850	810	
Total Dissolved Solids	ALS	20	550	530	--
			550	540	
Total Organic Carbon	ALS	1.0	<1	<1	--
			<1	<1	
Total Sulfide	ALS	2.0	<2	<2	--
			<2	<2	
Total Suspended Solids	ALS	20	<20	<20	--
			<20	<20	
HCO_3	Field	--	104.4	106.8	144–198
	ALS	24	146	146	
			146	146	
CO_3	ALS	12	<12	<12	0.6–1.9
			<12	<12	
Cl	ALS	2.0	110	95	47.5–95
			110	94	
SO_4	ALS	10	120	120	77–120
			130	120	
Br	ALS	0.2	0.55	0.56	--
			0.50	0.68	

Table A-1
Chemistry Data for PM-3-1 (Deep) and PM-3-2 (Shallow) from August 2013 Sampling
(Page 2 of 5)

Analyte	Laboratory	Detection Limit	PM-3-1 (Deep) 08/11/2013–08/12/2013	PM-3-2 (Shallow) 08/22/2013–08/23/2013	Range of Results for Thirsty Canyon Wells [a]
Water-Quality and Major-Ion Data (mg/L unless noted) *(continued)*					
F	ALS	0.1	2.7	2.4	2.04–5.6
			2.8	2.4	
Na	ALS	1–5	130 | 130	130 | 130	120–150
			120 | 120	130 | 130	
K	ALS	1.0	J 11 | J 11	J 14 | J 15	2.1–12.3
			J 11 | J 11	J 15 | J 15	
Ca	ALS	1	32 | 32	28 | 29	2.3–27
			32 | 32	29 | 28	
Mg	ALS	1.0	2.5 | 2.5	1.7 | 1.7	0.09–4.1
			2.4 | 2.4	1.7 | 1.7	
SiO_2	ALS	0.11	55.6 | 55.6	55.6 | 57.8	32.1–70
			55.6 | 53.5	57.8 | 55.6	
Environmental Isotope and DIC and DOC ^{14}C Data					
δD (‰)	LLNL	--	-116.7 ± 0.6	-115.6 ± 0.2	-116 to -112
$\delta^{18}O$ (‰)	LLNL	--	-14.71 ± 0.06	-14.5 ± 5.5	-15.0 to -14.6
$\delta^{13}C$ DIC (‰)	LLNL	--	-3.57 ± 0.03 | -3.44 ± 0.05	-2.83 ± 0.01 | -3.39 ± 0.02	-4.0 to -1.0
^{14}C (pmc)	LLNL	3.2	68.4 ± 1.4	82.9 ± 1.2	5.0–8.7
DOC (mg/L)	DRI	--	0.23	0.29	0.1–0.2
$\delta^{13}C$ DOC (‰)	DRI	--	-26.6	-27.4	-32.0 to -22.2
^{14}C DOC (pmc)	DRI	--	55.9	51.5	10–74
$^{36}Cl/Cl$ ($\times 10^{-13}$)	LLNL	--	5.57 ± 0.08	6.64 ± 0.08	4.63–5.61
$^{129}I/^{127}I$	LLNL	--	3.52E-09 ± 2.05E-10	2.02E-08 ± 1.09E-09	--
$^{87}Sr/^{86}Sr$	USGS	--	0.710547 ± 0.000006	0.710606 ± 0.000010	0.70882–0.71058
$^{234}U/^{238}U$ Activity Ratio	LLNL	--	3.255 ± 0.011	3.787 ± 0.013	2.84–5.06
	USGS	--	3.264 ± 0.010	3.801 ± 0.006	
$^{34/32}S$ (‰)	USGS	--	20.0 ± 0.5	20.0 ± 0.9	--
Dissolved Noble Gas Data (all in atoms/g except R/R_a*)					
^{3}He	LLNL	--	7.87E+06 ± 2.8E+05	7.35E+06 ± 2.65E+05	--
^{4}He	LLNL	--	7.60E+12 ± 1.5E+11	3.92E+12 ± 7.84E+10	3.69E+12–1.75E+13
R/R_a^*	LLNL	--	0.751 ± 0.0224	1.36 ± 0.04	0.71–1.26
Ne Total	LLNL	--	7.27E+12 ± 1.5E+11	4.17E+12 ± 8.35E+10	--
^{20}Ne	LLNL	--	6.58E+12 ± 1.3E+11	3.78E+12 ± 7.55E+10	5.16E+12–1.07E+13
Ar Total	LLNL	--	7.40E+15 ± 1.5E+14	6.11E+15 ± 1.22E+14	--
^{40}Ar	LLNL	--	7.38E+15 ± 1.5E+14	6.09E+15 ± 1.22E+14	5.8E+15–1.02E+16
Kr	LLNL	--	1.49E+12 ± 4.5E+10	1.33E+12 ± 3.99E+10	--
Xe Total	LLNL	--	1.91E+11 ± 7.1E+09	1.94E+11 ± 7.23E+09	--
^{130}Xe	LLNL		7.83E+09 ± 2.9E+08	7.94E+09 ± 2.97E+08	--

Table A-1
Chemistry Data for PM-3-1 (Deep) and PM-3-2 (Shallow) from August 2013 Sampling
(Page 3 of 5)

Analyte	Laboratory	Detection Limit	PM-3-1 (Deep) 08/11/2013–08/12/2013	PM-3-2 (Shallow) 08/22/2013–08/23/2013	Range of Results for Thirsty Canyon Wells [a]
Trace Element (µg/L)					
Al	ALS	200	<200 | <200	<200 | <200	--
			<200 | <200	<200 | <200	
Ag	ALS	10	<10 | <10	<10 | <10	--
			<10 | <10	<10 | <10	
As	ALS	10	<10 | <10	15 | <10	2.11–12.9
			<10 | 8.5	13 | 4.8	
Ba	ALS	100	4.5 | 4.2	J- 4.2 | J- 3.8	0.49–6.43
			4.4 | 4.0	J- 4.2 | J- 3.5	
Cd	ALS	5	<5 | <5	<5 | <5	0.012–0.034
			<5 | <5	<5 | <5	
Cr	ALS	10	J- 1.6 | <10	<10 | <10	0.62–1.48
			J- 2.4 | J- 1	<10 | <10	
Fe	ALS	100	4,900 | 3,400	J 4,000 | J 1,900	--
			4,700 | 3,100	J 3,700 | J 1,800	
Hg	ALS	0.2	<0.2 |<0.2	<0.2 | <0.2	--
			<0.2 |<0.2	<0.2 | <0.2	
Li	ALS	10	J 160 | J 150	J 130 | J 130	114–177
			J 150 | J 150	J 130 | J 130	
Mn	ALS	10	170 | 160	120 | 110	0.52–60.9
			160 | 160	120 | 110	
Pb	ALS	3	<3 |<3	<3 |<3	--
			<3 |<3	1.3 | <3	
Se	ALS	5	5.1 | <5	J+ 6 | <5	0.37–2.02
			<5 | <5	<5 | <5	
Sr	ALS	10	110 | 110	50 | 52	2.6–150
			100 | 100	52 | 51	
U	ALS	0.1	0.54 | 0.46	1.3 | 1.2	4.13–8.63
			0.54 | 0.47	1.2 | 1.1	
Radioisotope Data (all in pCi/L)					
Gross Alpha	ALS	1.3–1.8	<1.8	2.3 ± 0.97	--
			U 1.5 ± 1	<1.6	
Gross Beta	ALS	1.9–2.4	9.9 ± 2.2	11.9 ± 2.4	--
			11.4 ± 2.4	10.8 ± 2.2	
^3H	ALS	290–340	<290	<340	--
			<300	<340	
^3H	ARS	2.1–4.5	37.0 ± 11.1	225 ± 66	--
			43.7 ± 13.1	249 ± 74	
^3H	LLNL	284–289	<289	462 ± 175	--
		6.5–25.2	87.8 ± 3.3	355 ± 13	

Table A-1
Chemistry Data for PM-3-1 (Deep) and PM-3-2 (Shallow) from August 2013 Sampling
(Page 4 of 5)

Analyte	Laboratory	Detection Limit	PM-3-1 (Deep) 08/11/2013–08/12/2013	PM-3-2 (Shallow) 08/22/2013–08/23/2013	Range of Results for Thirsty Canyon Wells [a]
Radioisotope Data (all in pCi/L) *(continued)*					
^{7}Be	ALS	54–67	<60	<54	--
			<67	<59	
^{14}C	ALS	410–460	<460	<410	--
			<460	<420	
^{14}C	LLNL	1E-04	J+ 0.124 ± 0.003 [b]	J+ 0.153 ± 0.002 [b]	--
^{36}Cl	LLNL	1E-08	1.86E-03 ± 0.03E-03	2.07E-03 ± 0.02E-03	--
^{26}Al	ALS	6.9–11.3	<6.9	<11.3	--
			<11	<9.5	
^{40}K	ALS	142–180	<151	<142	--
			<180	<154	
^{58}Co	ALS	7.1–9.0	<7.1	<8.9	--
			<9.0	<7.6	
^{60}Co	ALS	7.5–9.8	<7.5	<8.5	--
			<9.7	<9.8	
^{90}Sr	ALS	0.39–0.52	<0.39	<0.51	--
			<0.39	<0.52	
^{94}Nb	ALS	7.3–9.3	<7.3	<9.3	--
			<7.9	<8.0	
^{99}Tc	ALS	5.7–6.1	<5.7	<5.7	--
			<6.0	<6.1	
^{125}Sb	ALS	18.0–19.1	<18.0	<18.6	--
			<19.0	<19.1	
^{129}I	LLNL	1E-07	1.61E-05 ± 0.10E-05	8.82E-05 ± 0.48E-05	--
^{134}Cs	ALS	7.1–8.6	<7.1	<8.4	--
			<8.6	<8.4	
^{137}Cs	ALS	7.2–8.6	<7.2	<7.8	--
			<8.6	<7.2	
^{152}Eu	ALS	40–49	<40	<49	--
			<46	<38	
^{154}Eu	ALS	47–53	<53	<52	--
			<47	<47	
^{155}Eu	ALS	13.6–32	<32	<13.6	--
			<20	<19	
^{208}Tl	ALS	7.7–13.1	<10.0	<11.2	--
			<13.1	<7.7	
^{212}Bi	ALS	104–180	<104	<180	--
			<124	<111	
^{214}Bi	ALS	23–30	U 41 ± 16	<23	--
			U 38 ± 16	<30	

Table A-1
Chemistry Data for PM-3-1 (Deep) and PM-3-2 (Shallow) from August 2013 Sampling
(Page 5 of 5)

Analyte	Laboratory	Detection Limit	PM-3-1 (Deep) 08/11/2013–08/12/2013	PM-3-2 (Shallow) 08/22/2013–08/23/2013	Range of Results for Thirsty Canyon Wells [a]
Radioisotope Data (all in pCi/L) *(continued)*					
^{214}Pb	ALS	21–23	J 36 ± 12	<22	--
			U 28 ± 12	<23	
^{227}Th	ALS	34–57	<57	<34	--
			<57	<37	
^{228}Ac	ALS	38–47	<42	<38	--
			<46	<47	
^{234}Th	ALS	97–270	<270	<97	--
			<144	<159	
^{234}U	LLNL	--	0.517 ± 0.011	1.64 ± 0.03	--
^{235}U	LLNL	--	7.32E-03 ± 0.16E-03	0.02 ± 0.0004	--
^{235}U	ALS	37–42	<42	<38	--
			<37	<41	
^{236}U	LLNL	--	<4.07E-05	<4.07E-05	--
^{238}U	LLNL	--	0.159 ± 0.004	0.434 ± 0.008	--
^{238}Pu	ALS	0.024–0.034	<0.024	<0.026	--
			<0.029	<0.034	
$^{239/240}Pu$	ALS	0.009–0.034	U 0.01 ± 0.013	<0.033	--
			<0.021	<0.034	
^{241}Am	ALS	9.8–250	<250	<9.8	--
			<48	<39	

[a] Wells indicated in Rose et al. (2006) as being in the Thirsty Canyon geochemical group include ER-EC-1, ER-EC-2A, ER-EC-4, ER-EC-6, ER-EC-8, ER-OV-1, and ER-OV-6a. The water-quality, environmental isotope, dissolved gases, and trace element data for these wells are presented in Tables A.1-2 through A.1-5, respectively, of Rose et al. (2006). The well location is shown in Figure 1-7.

[b] High reported ^{14}C likely represents contamination from analytical procedure (e.g., vacuum line contamination, environmental sample analyzed by high level ^{14}C "hot" AMS).

* R/R_a is the $^{3}He/^{4}He$ ratio of the sample relative to the $^{3}He/^{4}He$ ratio of air.

Note: Shaded cells indicate field duplicate results, and "|" indicates analysis results from unfiltered | filtered samples.

J = Estimated value
J+ = Estimated value, biased high
J- = Estimated value, biased low
U = Analyte was not detected. Measured value is less than the detection limit plus error.
< = Value is less

Historical analytical results for PM-3 are reported in the UGTA Geochemistry Database (N-I, 2014a). These results represent samples collected using different methods (pumped, air-lifted, bailed) by multiple organizations including the management and operating (M&O) contractors, DRI, Los Alamos National Laboratory (LANL), LLNL, and USGS. Historical PM-3 ^3H results reported above the MDCs are presented in Table A-2. Table A-2 also lists the type and the collection method for the samples.

Table A-2
PM-3 Laboratory Analyses of ^3H
(Page 1 of 2)

Sample Number	Date	Result (pCi/L)	Error (+/-) (pCi/L)	Detection Limit (pCi/L)	Sample Type	Sample Description
PM-3-1						
127-081213-9	08/12/2013	87.7	3.3	6.5	Field	Pumped (29,313 gal purged)
127-081113-3	08/11/2013	37.04	11.12	2.12	Field	Pumped (24,200 gal purged)
127-081113-4	08/11/2013	43.67	13.06	2.12	Duplicate	Pumped (24,200 gal purged)
127-080613-1	08/06/2013	37.17	11.14	1.95	Field	Pumped (260 gal purged)
127-073013-1	07/30/2013	11.44	3.72	2.08	Field	Bailer (before pumping)
127-073013-2	07/30/2013	16.16	5.04	1.99	Duplicate	Bailer (before pumping)
EM11953	03/13/2012	52.9	17.4	24.1	Field	Bailer (before pumping)
EM11954	03/13/2012	39.0	15.1	22.1	Duplicate	Bailer (before pumping)
PM-3-072211-1	07/22/2011	18.64	5.87	2.54	Field	Depth-Discrete Bailer (depth = 1,983 ft bgs)
PM-3-072211-2	07/22/2011	33.17	10.12	2.86	Duplicate	Depth-Discrete Bailer (depth = 1,983 ft bgs)
EM8481	07/20/2011	33.8	18.2	28.1	Duplicate	Depth-Discrete Bailer (depth = 1,984 ft bgs)
EM8483	07/20/2011	19.5	17.5	28.0	Field	Depth-Discrete Bailer (depth = 1,984 ft bgs)
PM-3-2						
127-082213-9	08/22/2013	355.2	12.6	25.2	Field	Pumped (31,802 gal purged)
127-082213-4	08/22/2013	248.95	73.63	4.53	Duplicate	Pumped (31,802 gal purged)
127-082213-3	08/22/2013	224.68	66.48	4.35	Field	Pumped (31,802 gal purged)
EM11956	03/13/2012	64.6	18.3	23.9	Field	Bailer (before pumping)
EM11957	03/13/2012	73.4	18.4	22.2	Duplicate	Bailer (before pumping)
PM-3-072211-4	07/22/2011	36.73	11.11	2.59	Field	Depth-Discrete Bailer (depth = 1,560 ft bgs)
PM-3-072211-5	07/22/2011	56.65	17.01	3.16	Field	Depth-Discrete Bailer (depth = 1,560 ft bgs)
EM8484	07/20/2011	63.2	20.4	27.9	Duplicate	Depth-Discrete Bailer (depth = 1,560 ft bgs)
EM8486	07/20/2011	58.0	20.0	27.9	Field	Depth-Discrete Bailer (depth = 1,560 ft bgs)
--	05/18/2010	48.3	17.9	25.5	Field	Depth-Discrete Bailer (depth = 1,560 ft bgs)
--	05/18/2010	46.8	16.1	22.7	Duplicate	Depth-Discrete Bailer (depth = 1,560 ft bgs)

Table A-2
PM-3 Laboratory Analyses of ^3H
(Page 2 of 2)

Sample Number	Date	Result (pCi/L)	Error (+/-) (pCi/L)	Detection Limit (pCi/L)	Sample Type	Sample Description
PM-3-2 (continued)						
EM00007629	05/25/2004	20.2	11.6	18.3	Field	Depth-Discrete Bailer (depth = 1,560 ft bgs)
--	10/12/2000	12.1 [a]	5.13	6.39	Field	Bennett Pump
--	09/25/2000	10.7 [a]	5.07	6.45	Field	Depth-Discrete Bailer (depth = 1,554 ft bgs)

Source: N-I, 2011, 2014a, and 2014b; Townsend and Grossman, 2001

[a] Results of field quality assurance samples demonstrated a large degree of variability and overestimated ^3H concentrations. There is a low degree of confidence associated with these results and the actual amount of ^3H present may be overestimated (Townsend and Grossman, 2001, p. 8-40).

A.3.0 REFERENCES

N-I, see Navarro-Intera, LLC.

NNSA/NSO, see U.S. Department of Energy, National Nuclear Security Administration Nevada Site Office.

Navarro-Intera, LLC. 2011. Written communication. Subject: *Data Report for Well Pahute Mesa #3 (PM-3) Groundwater Sampling*. Las Vegas, NV.

Navarro-Intera, LLC. 2014a. Written communication. Subject: "UGTA Geochemistry Database," UGTA Technical Data Repository Database Identification Number UGTA-4-129. Las Vegas, NV. As accessed on 15 August.

Navarro-Intera, LLC. 2014b. Written communication. Subject: *Well Pahute Mesa #3 (PM-3) Well Development and Sampling Data Report*. Las Vegas, NV.

Rose, T.P., F.C. Benedict, Jr., J.M. Thomas, W.S. Sicke, R.L. Hershey, J.B. Paces, I.M. Farnham, and Z.E. Peterman. 2006. *Geochemical Data Analysis and Interpretation of the Pahute Mesa - Oasis Valley Groundwater Flow System, Nye County, Nevada, August 2002*, UCRL-TR-224559. Livermore, CA: Lawrence Livermore National Laboratory; Reno, NV: GeoTrans Inc. and Desert Research Institute; Denver, CO: U.S. Geological Survey; and Las Vegas, NV: Harry Reid Center for Environmental Studies.

Townsend, Y., and R. Grossman ed. 2001. *Nevada Test Site Annual Environmental Report for Calendar Year 2000*, DOE/NV/11718-605. Las Vegas, NV: Bechtel Nevada.

U.S. Department of Energy, National Nuclear Security Administration Nevada Site Office. 2009. *Phase II Corrective Action Investigation Plan for Correction Action Units 101 and 102: Central and Western Pahute Mesa, Nevada Test Site, Nye County, Nevada,* DOE/NV--1312-Rev. 2. Las Vegas, NV.

U.S. Department of Energy, National Nuclear Security Administration Nevada Site Office. 2012. *Underground Test Area Activity Quality Assurance Plan, Nevada National Security Site, Nevada*, Rev. 1, DOE/NV--1450-REV. 1. Las Vegas, NV.

Appendix B

Hydrogeology and Hydraulic Properties of HSUs in the Vicinity of PM-3

B.1.0 INTRODUCTION

As a precursor to evaluating the possible hydraulic communication between upgradient contaminant sources and PM-3, it is relevant to summarize the available hydrogeologic information and the hydraulic properties in the area of interest. As indicated in Figure 1-1, there is very little borehole control of geologic and hydrogeologic information in the vicinity of PM-3. The nearest wells are about 4.5 km away on the other side of the Purse fault and the NTMMSZ at ER-EC-1 and about 7.2 km away in the vicinity of the HANDLEY detonation (notably, U-20m and UE-20j).

B.2.0 GEOLOGIC INFORMATION

The detailed hydrostratigraphy at PM-3 is illustrated in the well completion diagram shown in Figure 1-2. The saturated aquifers intersected by PM-3 include, from top to bottom, the TCA and the BRA. The TCA occurs from a depth of about 1,880 to 2,140 ft bgs. The UPCU and LPCU confining units overlie and underlie the TCA, respectively. The BRA, which intersects PM-3 from a depth of 2,950 to 2,990 ft bgs, occurs below the zone of collapsed borehole at a depth of about 2,600 ft bgs. The degree to which the BRA is in hydraulic communication with the rest of the borehole is unknown, although this is assumed to be insignificant due to the low transmissivity observed in the bottom single-packer test in test interval G (see Section B.4.1).

Figure B-1 illustrates a map view of the major structural features included in the Phase II Pahute Mesa HFM along with detonations in the vicinity of PM-3. This figure was drawn by removing all the Tertiary units above the lower carbonate aquifer (LCA) where the LCA is present in the area of interest, and removing all the volcanic units above the Subcaldera volcanic confining unit (SCVCU) to the west and Silent Canyon intrusive confining unit (SCICU) to the east where the LCA is not present. The structural features illustrated on this figure include (1) the NTMMSZ south of PM-3, (2) the Black Mountain Caldera structural margin (BMCSM) west of PM-3 and U-20m (HANDLEY), (3) the Western Silent Canyon structural zone (WSCSZ) north of U-20m, (4) the southwest Area 20 structural margin (SWA20SM) east of PM-3, (5) the Purse fault east of U-20m, (6) the West Purse fault east of PM-3, (7) the Handley fault west of U-20m (HANDLEY), and the West Boxcar fault. The extent of any other structural features in this area is unknown due to the paucity of borehole control. This figure also illustrates the presence of the HANDLEY detonation with a working point in the PBRCM with the exchange volume drawn to three times the 98-m radius of the cavity (assuming the maximum announced yield of greater than 1 Mt [DOE/NV, 2000] and the depth- and yield-dependent cavity radius formula of Pawloski [1999]).

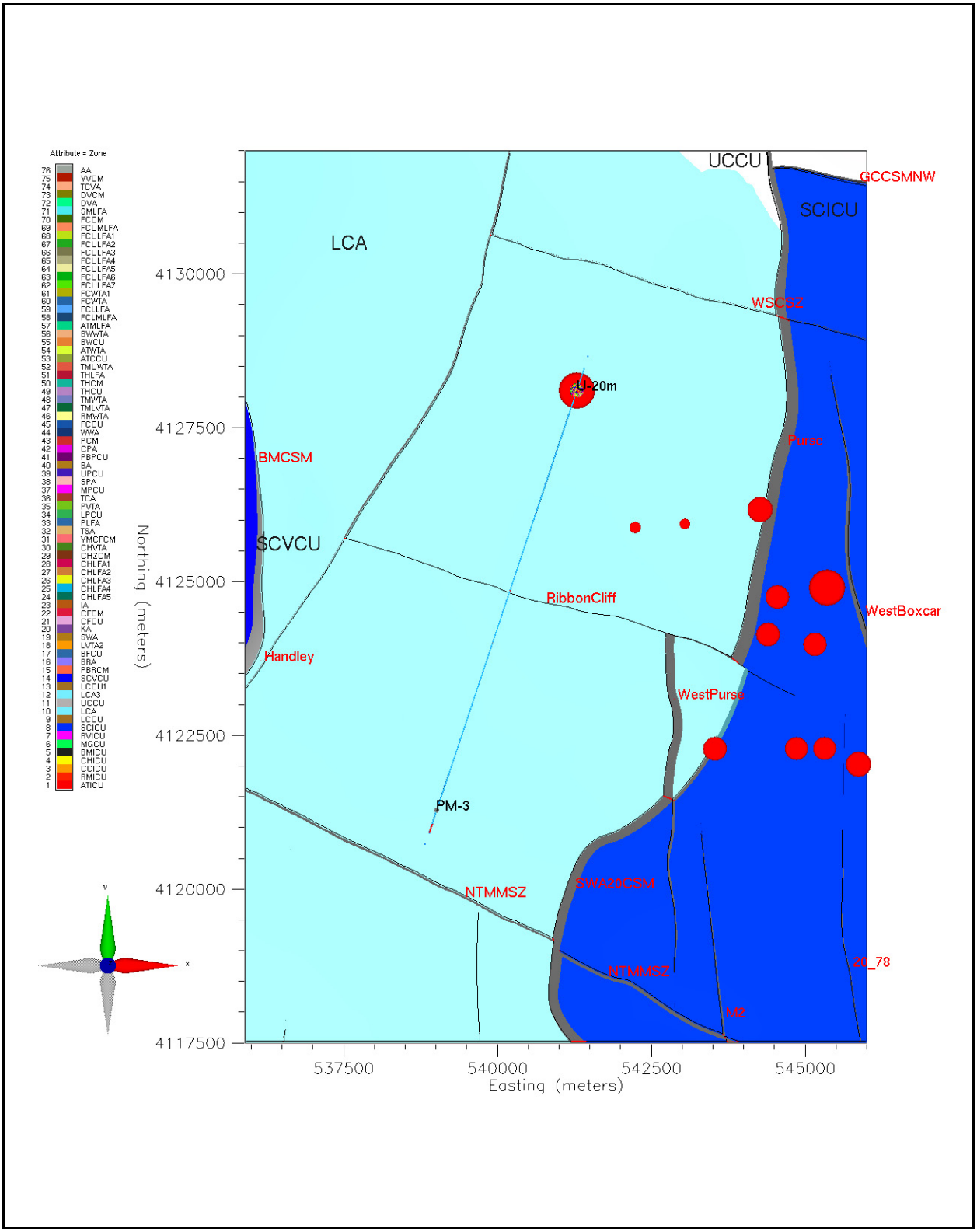

Figure B-1
Map View of Major Structures and Detonations in the Vicinity of PM-3

Note: Cavity radius based on maximum yield range identified in DOE/NV (2000) and Pawloski (1999).

The Phase II HFM in the vicinity of PM-3 and between HANDLEY (U-20m) and PM-3 is shown in perspective views in Figures B-2 and B-3, and in a northeast–southwest cross section in Figure B-4. The perspective views again have removed the Tertiary volcanics above the LCA where the LCA is present and above the SCICU where the LCA is not present in order to illustrate the major structural features in the area. The HANDLEY exchange volume and chimney are also illustrated where the chimney is assumed to have a radius of 92 m equivalent to the assumed cavity radius.

Figure B-4 present a hydrostratigraphic cross section drawn between HANDLEY (U-20m) and PM-3. It is apparent from this section that the PBRCM is continuous from HANDLEY to PM-3. Although there is uncertainty in the continuity of the HSUs in the vicinity of PM-3 and between PM-3 and HANDLEY, due to the noted paucity of borehole control between U-20m (and UE-20j) and PM-3, based on the current interpretation, the BRA appears to be continuous over the 7 km between the two boreholes with the exception of the offset along the Ribbon Cliff fault located about halfway between U-20m and PM-3.The confining units overlying the BRA—notably, the BFCU, CHZCM, and LPCU—are of variable continuity between HANDLEY and PM-3. While the TCA exists at PM-3, it has not been observed in either U-20m or UE-20j. However, the lateral extent of the TCA is uncertain due to the paucity of well control in this area. The UPCU and TMLVTA are continuous between U-20m/UE-20j and PM-3. As illustrated in Figure B-4, the water table is in the TMLVTA at U-20m/UE-20j and in the UPCU at PM-3.

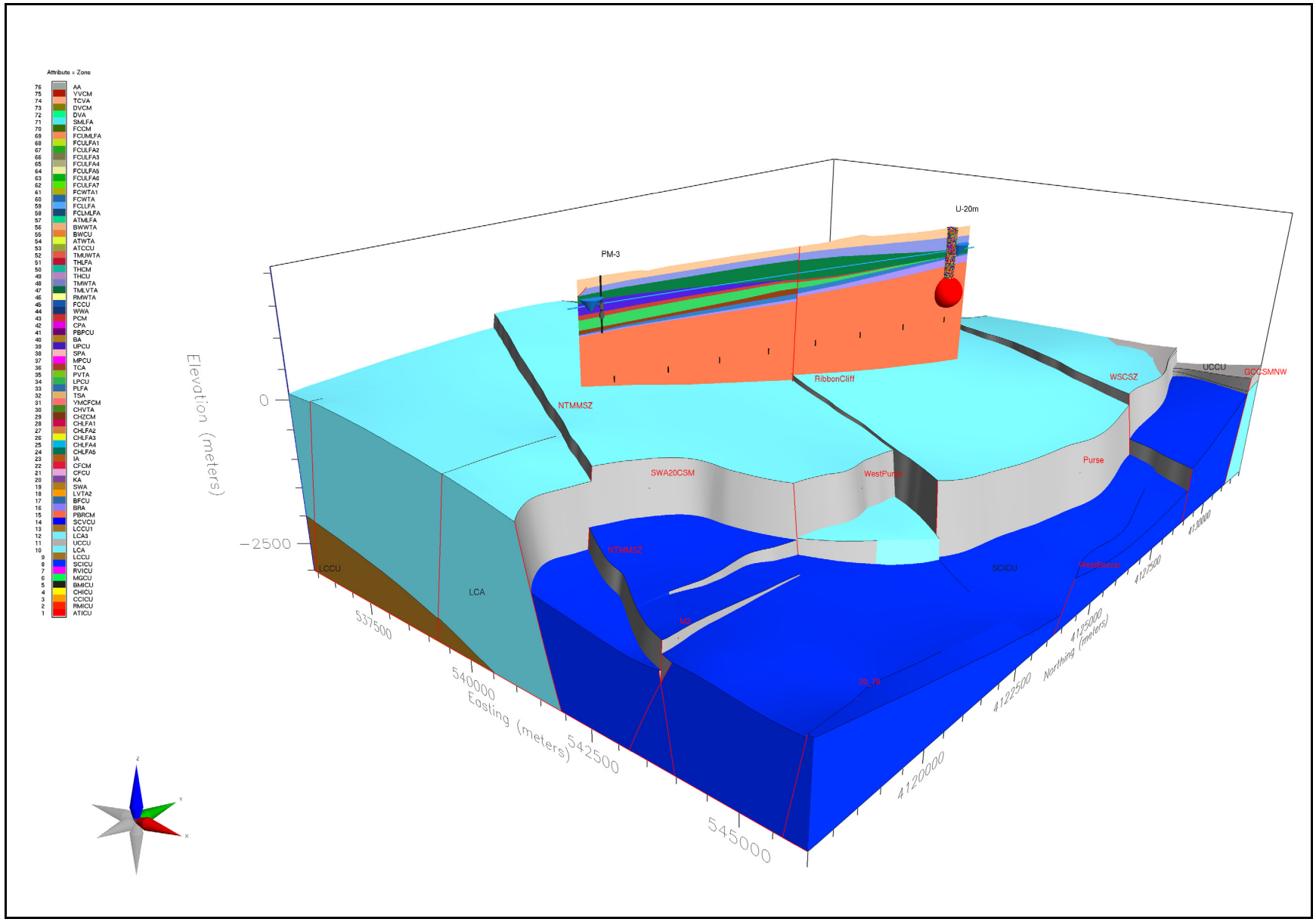

Figure B-2

General Perspective View of Hydrostratigraphy and Major Structural Features in the Vicinity of PM-3

Note: Cavity radius based on maximum yield range identified in DOE/NV (2000) and Pawloski (1999). Positive Y-axis is to the north.

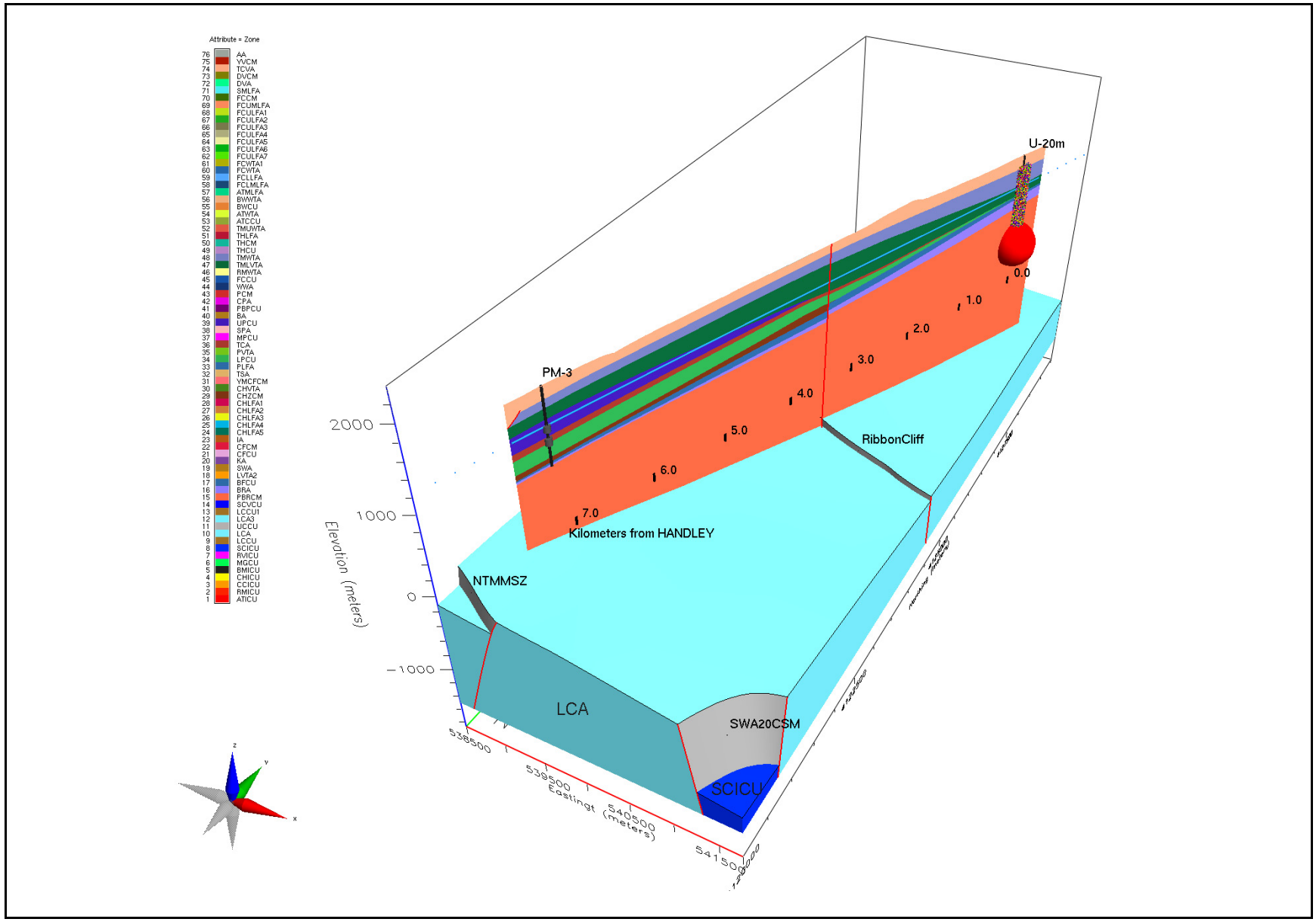

Figure B-3

Detailed Perspective View of Hydrostratigraphy and Major Structural Features in the Vicinity of PM-3

Note: Cavity radius based on maximum yield range identified in DOE/NV (2000) and Pawloski (1999). Positive Y-axis is to the north.

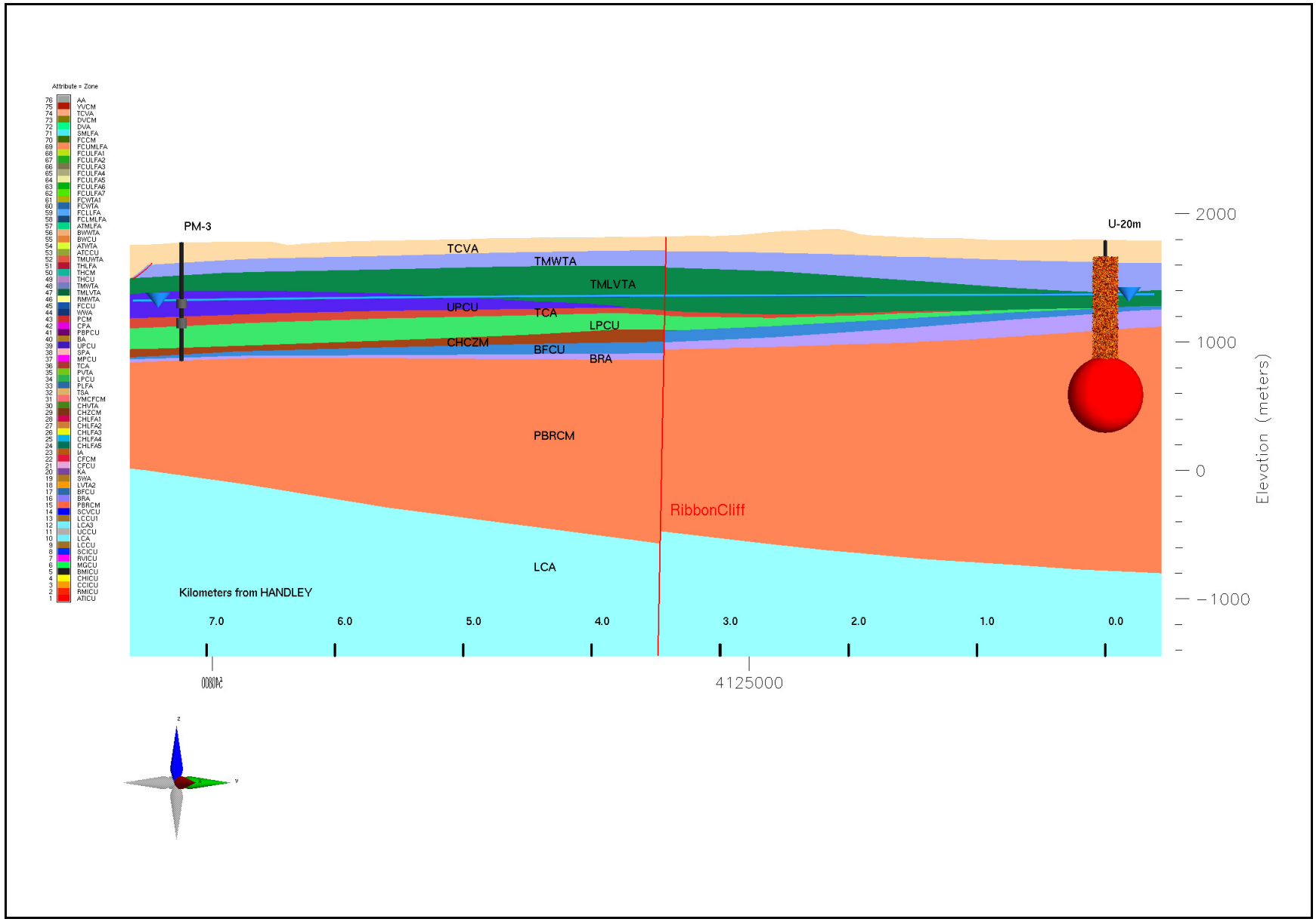

Figure B-4
Cross Section of HSUs between HANDLEY and PM-3

Note: Cavity radius based on maximum yield range identified in DOE/NV (2000) and Pawloski (1999).

B.3.0 WATER-LEVEL INFORMATION

The water levels on the western side of the northwestern boundary of the SCCC (which approximately parallels the trace of the Purse fault to the north and the Thirsty Canyon lineament to the south) are several hundred feet above the water levels on the eastern side of this boundary (Fenelon et al., 2010). This discontinuity in the water-level surface is illustrated in Figure 1-6 and results in the boundary between the Black Mountain tributary flow system and the Pahute Mesa tributary flow system identified by Fenelon et al. (2010).

The hydraulic gradient inferred from the water-level contours on the east side of Purse fault is about 0.002 (100 ft/8 mi) to the southwest, while on the west side of Purse fault between HANDLEY and PM-3 the gradient is about 0.01 (200 ft/4 mi) to the south.

The hydraulic discontinuity between the flow systems west and east of the Purse fault inferred by Fenelon et al. (2010) is consistent with the differences in the geochemistry summarized by Kilroy and Savard (1996), who noted the similar geochemical signature (high SO_4, high Cl, low HCO_3 in terms of milliequivalents per liter) at UE-20j and PM-3 in comparison to the other Pahute Mesa and Oasis Valley wells. A similar comparison was made by Blankennagel and Weir (1965, Figure 11). More recent analyses performed by Rose et al. (2006) have indicated the PM-3 geochemical signature is similar to the groundwater characteristics of other wells in the Thirsty Canyon area (notably ER-EC-1, ER-EC-2A, ER-EC-4, ER-EC-6, ER-EC-8, ER-OV-1, and ER-OV-6a) as illustrated in Figure B-5. Several of these wells (notably ER-EC-1 and ER-EC-6) have been interpreted to be along the possible flow path from PM-3, indicated by the question mark in Figure 1-8.

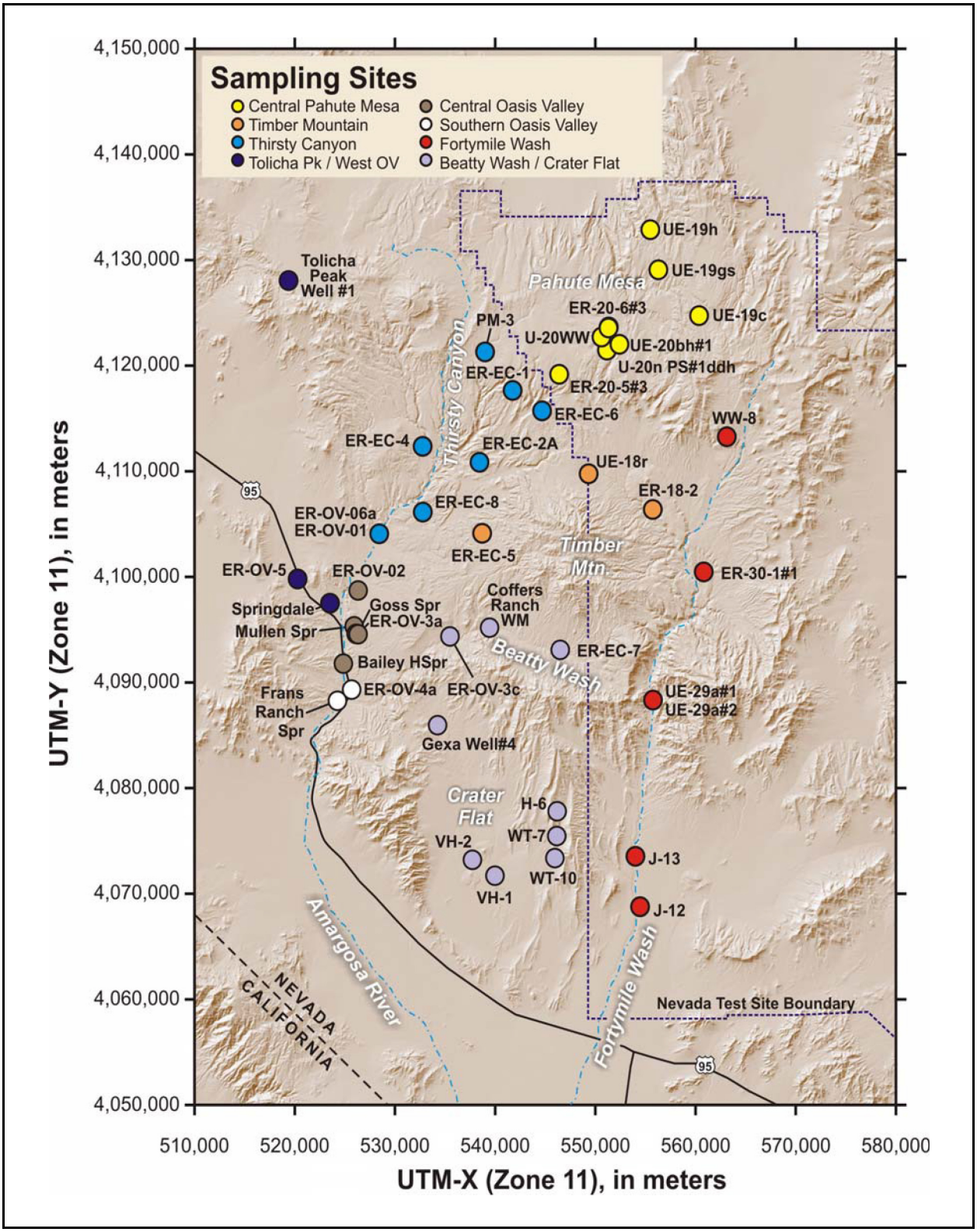

Figure B-5
Geochemical Groups in Pahute Mesa–Oasis Valley Groundwater Flow Domain
Source: Rose et al., 2006

B.4.0 HYDRAULIC PROPERTIES

Limited information exists on the hydraulic properties—notably, the transmissivity or hydraulic conductivity—of the HSUs in the vicinity of PM-3. The results of pump and slug tests of PM-3 are summarized in Section B.4.1. The results of pump tests conducted in UE-20j are summarized in Section B.4.2. The results of hydraulic test interpretations for recent UGTA testing in similar HSUs in southwest Area 20 and the NTTR are summarized in Section B.4.3.

B.4.1 PM-3 Hydraulic Testing Results

PM-3 was drilled from September 1 to 19, 1988 to a TD of 3,019 ft bgs. The bottom 1,546 ft of the test well (from 1,473 to 3,019 ft bgs) was left uncased to allow for hydraulic testing of the saturated HSUs. The static water level in this hole was at a depth of about 1,455 ft bgs. The saturated HSUs, from top to bottom in the hole, consist of the TMLVTA, UPCU, TCA, LPCU, CHZCM, BFCU, BRA, and PBRCM.

Injection tests were performed in six discrete depth intervals from September 23 to 26, 1988. The hydraulic testing and results of the PM-3 test well are summarized by Kilroy and Savard (1996). At some point during the injection testing, material in the bottom almost 500 ft of open borehole collapsed. After the collapse, it was not clear what, if any, hydraulic communication existed between the test intervals and the bottom of the borehole, but it was assumed there was no communication below the collapse depth of 2,605 ft bgs. This assumption was believed appropriate due to the low interpreted transmissivity for this portion of the borehole in test interval G. The results of these short-duration slug injection tests are summarized in Table B-1.

A pumping test was performed on September 27 and 28, 1988 over the entire open interval by pumping at the rate of 169 gpm for about 31 hours followed by about 9.5 hours of recovery. The open interval at this time was assumed to be from 1,473 to 2,605 ft bgs. The drawdown at the end of the pumping was 78 ft and the drawdown recovered to prepumping levels within about 100 minutes (min) (Kilroy and Savard, 1996). Both the drawdown and recovery phases of the aquifer test were interpreted by Kilroy and Savard (1996) using (1) different assumptions regarding whether the response was the result of unconfined or confined conditions, (2) whether the response was or was not

Table B-1
Summary of PM-3 Injection Testing Results

Tested Interval	Depth Interval (ft bgs)	Total Duration of Injection Test (min)	Time to 50% Recovery (min)	Transmissivity (ft^2/day)	Hydraulic Conductivity (ft/day)	Phase II HFM Equivalent HSU
A	1,473 - 1,667	20	~10	3.0	1.5×10^{-2}	UPCU
B	1,665 - 1,865	200	NR	1.2×10^{-2}	6×10^{-5}	UPCU
C	1,886 - 1,933	100	NR	3.1×10^{-3}	6.6×10^{-5}	TCA
D	1,934 - 2,134	20	~0.3	25	0.12	TCA
E	2,134 - 2,390	NA	NA	Not tested	NA	LPCU
F	2,390 - 2,550	400	~60	0.18	1.1×10^{-3}	LPCU
G	2,550 - 2,605	250	~60	0.15	2.7×10^{-3}	LPCU

Source: Modified from Kilroy and Savard, 1996 (Table 5)

ft/day = Feet per day
ft^2/day = Square feet per day
NA = Not available
NR = Not recorded

affected by well-bore storage and (3) two different methods for analyzing the effects of well-bore storage.

Assuming an unconfined aquifer response the range of transmissivities interpreted by Kilroy and Savard (1996) was from 38 to 70 ft^2/day, corresponding to an average hydraulic conductivity over the 1,132 ft of open hole of 3.4E-02 to 6.2E-02 ft/day. Assuming a confined aquifer response without well-bore storage effects, the range of transmissivities interpreted by Kilroy and Savard (1996) was from 52 to 76 ft^2/day, corresponding to an average hydraulic conductivity over the 1,132 ft of open hole of 4.6E-02 to 6.7E-02 ft/day. Assuming a confined aquifer response and removing the effects of well-bore storage, the range of transmissivities interpreted by Kilroy and Savard (1996) was from 360 to 840 ft^2/day, corresponding to an average hydraulic conductivity over the 1,132 ft of open hole of 3.2E-01 to 7.4E-01 ft/day.

Subsequent to the individual slug tests and the longer duration pumping test, PM-3 was recompleted with separate isolated zones in the upper (PM-3-2 [shallow]) and lower (PM-3-1 [deep]) zones. PM-3-2 (shallow) is open over test interval A and is open to the UPCU, while PM-3-1 (deep) is open over test interval D and is open to the TCA. Continual monitoring of pressure changes in the PM-3-2 (shallow) zone has allowed for an interpretation of specific storage using the earth-tide fluctuation data and the method proposed by Cutillo and Bredehoeft (2011). The interpreted specific storage was

about 3E-06 m^{-1} consistent with semi-confined to confined conditions, implying the higher estimated transmissivities under confined conditions from Kilroy and Savard (1996) are be more representative.

Additionally, it is noted that during the pump-jack sampling of PM-3-2 (shallow), the water level did not drop below the pump seal located about 17 ft below the static water level. Assuming a maximum drawdown of 17 ft for a pumping rate of 3.5 gpm yields a minimum transmissivity of the open interval of PM-3-2 (shallow) of between 40 and 55 ft^2/day, corresponding to a hydraulic conductivity of about 0.2 ft/day over the 250 ft of the gravel-packed open interval in PM-3-2 (shallow). Thus, the transmissivity and hydraulic conductivity of this limited portion of the UPCU is estimated to be at least a factor of 10 greater than that estimated from the short-duration slug injection tests performed immediately after drilling. This difference may be the result of the shorter duration of the slug injection test (20 min) compared to the duration of pumping using the pump jack (12 days) or to the fact the well was not fully developed at the time of the slug injection test.

In conclusion, the transmissivity of the HSUs intersected by PM-3 is in the range of 50 to 500 ft^2/day. While it is likely that the greatest fraction of that transmissivity is contributed by the approximately 200-ft-thick TCA, the contribution from the UPCU is not insignificant and it appears at least in some places the UPCU does not behave as an aquitard or a typical tuff confining unit. The lateral continuity of the permeable features encountered in the upper portion of the UPCU at PM-3 cannot be determined from the limited observations available.

B.4.2 U-20m and UE-20j Hydraulic Testing Results

U-20m is the emplacement borehole and shaft for the HANDLEY detonation located about 7 km north of PM-3. Exploratory well UE-20j is located about 80 ft south of U-20m. Hydraulic testing was performed in both U-20m and UE-20j to characterize the hydraulic properties of the rocks before the HANDLEY detonation, which occurred on March 26, 1970.

U-20m was drilled in 1968 to a TD of 4,147 ft bgs. The static water level in this hole was estimated at a depth of 1,263 ft bgs. The saturated HSUs, from top to bottom in the hole, consist of the TMWTA, LPCU, BFCU, BRA, and PBRCM. A series of injection and swabbing packer tests were performed in 1968. The results of these tests yielded very low specific capacities ranging from 0.014 to 4.5E-05 gpm per foot of drawdown as summarized by Orkild (1969). The data from these packer tests are available in Wood (2007). Of the tests performed in U-20m, only the test in the

uppermost tested interval from a depth of 3,493 to 3,703 ft bgs in the PBRCM had sufficient quality data for reanalysis. This test applied a slug of water of 1,200 ft that dissipated to the pre-injection static water level in 70 min and had a 50 percent recovery in the first 15 min. The reanalyzed transmissivity of this test was 360 ft^2/day, or an average hydraulic conductivity of 1.7 ft/day over the tested interval of 210 ft. Although the test data appear of reasonable quality, the field interpretation by Orkild (1969) was that this test may have been affected by leakage around the casing shoe, which probably accounts for the total measured specific capacity. As a result, there are no data of sufficient quality for analysis of hydraulic properties from U-20m.

UE-20j was drilled in 1964 to a TD of 5,690 ft bgs. The static water level in this hole was estimated at a depth of 1,271 ft bgs. The saturated HSUs, from top to bottom in the hole, consist of the TMWTA, TMLVTA, BFCU, BRA, and PBRCM. The hydraulic testing and results of testing the UE-20j exploratory borehole are summarized by Blankennagel and Weir (1973). The bottom 3,950 ft of the test well (from 1,740 to 5,690 ft bgs) was left uncased to allow for hydraulic testing of the saturated HSUs. A pumping test was conducted by pumping at 56 gpm for 23 hours with a reported drawdown of greater than 3 ft. The interpreted transmissivity of this test was 7,900 ft^2/day, or an average hydraulic conductivity of 2 ft/day over the 3,950 ft of open borehole (Blankennagel and Weir, 1973, Table 3). The water production from this well was noted by Blankennagel and Weir (1973) to be contributed from highly fractured WTAs.

The different result in the hydraulic testing between U-20m (low to very low specific capacity estimated from slug injection and withdrawal packer tests) and UE-20j (very high transmissivity estimated from a pump test) is anomalous given these two holes intercept the same HSUs only 80 ft apart. A possible explanation could be the lack of development of U-20m and the packer tests being impacted by drilling fluid and other skin effects, while the developed well, UE-20j, yielded properties more consistent with the expected conditions; however, this is speculation given the paucity of information available on the test conditions.

B.4.3 Recent Hydraulic Testing in Southwest Area 20 and the NTTR

Several of the HSUs of importance to the interpretation of the groundwater flow domain in the vicinity of PM-3 have been tested in wells drilled by the UGTA Activity during the Phase II

characterization of the Pahute Mesa. This has included single well testing of the following test intervals (and their corresponding HSUs):

- ER-20-4 (CHZCM-Crater Flat confining unit [CFCU])
- ER-20-7 (TSA)
- ER-20-8 (upper) (TSA)
- ER-20-8 (lower) (TCA)
- ER-20-8#2 (Scrugham Peak aquifer [SPA])
- ER-EC-11 (TCA/TSA)
- ER-EC-12 (lower) (TSA)
- ER-EC-12 (upper) (TCA)
- ER-EC-13 (deep)
- ER-EC-13 (intermediate)
- ER-EC-14
- ER-EC-15
- ER-20-11

Although the analyses of these tests is ongoing, several of the hydraulic tests performed in these wells during well development and testing have been interpreted using both single-well aquifer test (SWAT) and multiple-well aquifer test (MWAT) interpretations by both N-I and USGS (N-I, 2012 and 2014), Halford et al. (2012), and Jackson et al. (2014b). A summary of these interpretations is provided in Table B-2.

It is useful to note that the USGS interpretations of transmissivities identified in Table B-2 have the advantage of basing the calibrated estimates to MWAT hydraulic responses from several combinations of pumping and observation wells in the area of study in southwest Area 20 and the nearby wells in the adjacent NTTR. In addition, this calibration includes calibration within the groundwater subbasin using independent observations of total discharge from the subbasin to Oasis Valley combined with the observed steady-state water levels in this area (i.e., the calibrated transmissivity values are derived from best fits to several transient MWATs conducted over periods of 10 to 20 days while maintaining a reasonable fit to the total discharge and observed steady-state heads in the area). That said, the estimates of Halford et al. (2012) did not consider the role that faults might have in creating areas of enhanced transmissivity along the fault trace or providing vertical conduits through aquitards as was evaluated in the volcanic rocks south of Yucca Mountain (Geldon et al., 2002). In addition, the transmissivity estimates derived from Halford et al. (2012) lumped several confining units and aquifers into a composite unit. For example, the UPCU, Middle Paintbrush confining unit (MPCU), TCA, LPCU, and TSA were lumped into a single composite unit called

Table B-2
Comparison of N-I and USGS Interpretations of Phase II Pahute Mesa Single-Well and Multiple-Well Aquifer Tests

Well	HSU Tested	USGS SWAT (ft^2/day)	N-I SWAT (ft^2/day)	N-I SWAT nSIGHTS (ft^2/day)	USGS MWAT (ft^2/day)
ER-20-4	CHZCM-CFCU	2,000	3,100–4,400	1,560–2,180	1,700
ER-20-7	TSA	ND	5,000–40,000	31,000	18,000
ER-20-8 (upper)	TSA	ND	ND	> 90,000	140,000
ER-20-8 (lower)	TCA	ND	3,100–5,400	1,900	
ER-20-8#2	BA/SPA	30,000–100,000	ND	6,700–45,000	110,000
ER-EC-11	TCA/SPA	ND	ND	3,650 - > 14,000	25,000
ER-EC-12 (lower)	TSA	0.1	0.16–0.47	0.0019	ND
ER-EC-12 (upper)	TCA	50	37	37–43	940
ER-EC-13 (deep)	FCCU	ND	1,500	1,810	5,000
ER-EC-13 (intermediate)	FCCU	ND	6,700	2,200	

BA = Benham aquifer
FCCU = Fluorspar Canyon confining unit

ND = Not determined

Paintbrush tuffs while the CHZCM, BRA, and Inlet aquifer (IA) were combined into a single composite unit called the sCHZCM. The calibrated transmissivities of the Paintbrush tuffs ranged from 140 to 16,000 ft^2/day, while the calibrated transmissivities of the sCHZCM ranged from 7 to 3,000 ft^2/day over the area interrogated by the MWATs.

Although analyses of the hydraulic property distributions in the vicinity of PM-3 are still ongoing, the most current map of a possible transmissivity field in the area has been developed by Jackson et al. (2014b). The portion of this transmissivity field in the vicinity of PM-3 is illustrated in Figure B-6 and shows a best-estimate transmissivity in the vicinity of PM-3 of less than 100 ft^2/day with the transmissivity values increasing to between 3,000 and 10,000 ft^2/day at UE-10j. These values are approximately consistent with the interpreted transmissivities from aquifer testing at PM-3 and UE-20j summarized in Sections B.4.1 and B.4.2, respectively; however, the transmissivity derived from the SWATs in PM-3 would indicate values more in the range of 300 to 1,000 ft^2/day.

B.4.4 Summary of Hydraulic Testing Results

There is significant uncertainty associated with the hydraulic properties of the HSUs in the vicinity of PM-3. There is additional uncertainty associated with the hydraulic continuity of the HSUs upgradient of PM-3 toward HANDLEY. However, there appears to be less uncertainty that the general groundwater flow direction is from HANDLEY toward PM-3.

The conceptual model that the TCA is the most transmissive unit at PM-3 is confirmed by the available packer testing results. The magnitude of the transmissivity in the TCA is uncertain as the short-duration slug injection tests tend to underrepresent the total borehole transmissivity estimated from pumping tests of longer duration. Transmissivities of 100 to 1,000 ft^2/day seem plausible in the area of PM-3. The lateral extent of the TCA north of PM-3 is unknown. It is possible that it extends almost to the location of the HANDLEY exchange volume as conceptualized in the current Phase II HFM (Figure B-4), but that is uncertain given the paucity of data in the area between PM-3 and UE-20j.

The hydraulic properties of the UPCU inferred from the ability to pump PM-3-2 (shallow) at 3.5 gpm for several days without inducing a drawdown of greater 17 ft (yielding a transmissivity of this interval in the UPCU of between 40 and 55 ft^2/day) are not consistent with the conceptual model of the UPCU being analogous to a typical tuff confining unit. The UPCU has been combined with other confining units and aquifers in the USGS interpretation of the MWAT responses, which does not allow for a unique determination of the hydraulic properties of this HSU. The extent to which the hydraulic properties of the UPCU in the vicinity of PM-3 may be affected by joints or other structural discontinuities, thus allowing this unit to be more permeable than what the conceptual model may indicate is indeterminate. The lateral continuity of the UPCU to north of PM-3 is unknown.

The BRA is also a potential conduit for groundwater flow and radionuclide transport between HANDLEY and PM-3. There are no direct observations of the hydraulic properties of the BRA in either location. Although it is likely that this permeable fractured tuff aquifer contributed significantly to the large transmissivity estimated from the pumping test conducted in UE-20j, which intersected the BRA, this cannot be confirmed. While the BRA was intercepted near the bottom of the PM-3 borehole, the borehole collapsed above this HSU and this HSU was never directly tested. The low transmissivity estimated for the bottom single packer test at PM-3 (conducted after the borehole had collapsed) tends to confirm that there was likely only very limited hydraulic communication between

the BRA and the borehole. This may be a result of the low permeability of the collapsed material or the low permeability of the BRA. The role the BRA has in affecting lateral groundwater flow and radionuclide transport from HANDLEY or other detonations in the area is indeterminate from the information available in the vicinity of PM-3.

The role of faults in affecting the hydraulic properties in the vicinity of PM-3 and between PM-3 and HANDLEY is also unknown. There are several major structures in the vicinity of PM-3 (notably, the Ribbon Cliff and Purse faults, and potentially other unnamed faults) that may provide for hydraulic communication. Northerly trending faults and their intersection with northwesterly trending faults similar to the structural trends between PM-3 and HANDLEY have been interpreted to have a significant control on groundwater flow and the spatial distribution of transmissive features in the analysis of the C-well complex near Yucca Mountain (Geldon et al., 2002). However, the hydraulic properties of structural features in the area or the lateral hydraulic continuity of those features cannot be inferred from the available information.

B.5.0 ANALYSIS OF GROUNDWATER FLOW BUDGET IN THE VICINITY OF PM-3

The HANDLEY-to-PM-3 flow path is part of the Black Mountain tributary flow system, which along with the Pahute Mesa tributary flow system feeds the Oasis Valley flow system (Fenelon et al., 2010, Figure 6). Groundwater discharge in Oasis Valley has been estimated as 6,200 ac-ft/yr (7.6E+06 cubic meters per year [m^3/yr]) (Laczniak et al., 2001). Fenelon et al. (2010) interpret that the Black Mountain tributary system has minor amounts of flow relative to the Pahute Mesa tributary flow system. Thus, a reasonableness check is to estimate how much water flows through the Black Mountain tributary flow system as a fraction of the total Oasis Valley discharge and to compare this estimate to the average hydraulic properties derived using Darcy's Law.

Darcy's Law can be written as

$$Q = T\,i\,W \qquad \textit{(B-1)}$$

where

Q = total volumetric discharge (L^3/T)

T = transmissivity (L^2/T)

i = hydraulic gradient (L/L)

W = the width of the flow path perpendicular to groundwater flow direction (L)

Assuming flow in the Black Mountain tributary flow system is confined to the area between the Purse and Handley faults, the width of the flow path would be about is 4,000 m. Assuming the groundwater flow in the Black Mountain tributary flow system is about 8.0E+05 m^3/yr (assuming about 10 percent of the total discharge to Oasis Valley is provided by flow west of the Purse fault based on geochemical mixing models presented in Kwicklis et al. (2005, Table 13 and Figure E-10) and a hydraulic gradient of about 0.01 between HANDLEY and PM-3 (based on the head difference of about 265 ft between U-20m with a static water level of about 4,640 ft amsl and PM-3 with a static water level of about 4,365 ft amsl [Fenelon et al., 2010] and a distance of about 26,000 ft [7,200 m]), the total transmissivity of the flow system would be about 20,000 square meters per year (m^2/yr), or about 600 ft^2/day. This value is well within the estimated transmissivity in the vicinity of PM-3

(Section B.4.1) and the transmissivity map developed by Jackson et al. (2014a) illustrated in Figure B-6. Considering that the groundwater would most likely flow through the more transmissive HSUs and that the total saturated thickness of the transmissive HSUs at U-20m is about 260 m (consisting of about 30 m for the TMWTA, about 100 m of TMLVTA, and about 130 m of welded BRA) the average hydraulic conductivity corresponding to this average transmissivity would be about 0.1 m/day or about 0.3 ft/day. These saturated thicknesses of transmissive units at U-20m assumes the PBRCM at U-20m is non-transmissive and hence considers the 140-m-thick lava unit in the PBRCM at PBRCM of being of limited areal extent and not significantly contributing to the overall transmissivity at U-20m. Again, this average hydraulic conductivity is within the expected range for these aquifers.

The simple water budget analysis in the vicinity of PM-3 indicates that the estimated transmissivities and hydraulic conductivities derived from the limited slug and pumping tests in the area are consistent with estimates of the discharge from Oasis Valley and the observed hydraulic gradient between HANDLEY and PM-3. There is significant uncertainty in the assumptions made in the simple analysis, including (1) the assumed fraction of total Oasis Valley groundwater discharge that is attributed to groundwater flow in the Black Mountain tributary flow system, (2) the assumed width of the Black Mountain tributary flow system, (3) the assumed average hydraulic gradient between HANDLEY and PM-3, (4) the assumed HSUs through which groundwater is flowing, and (5) the assumed thickness of the transmissive HSUs.

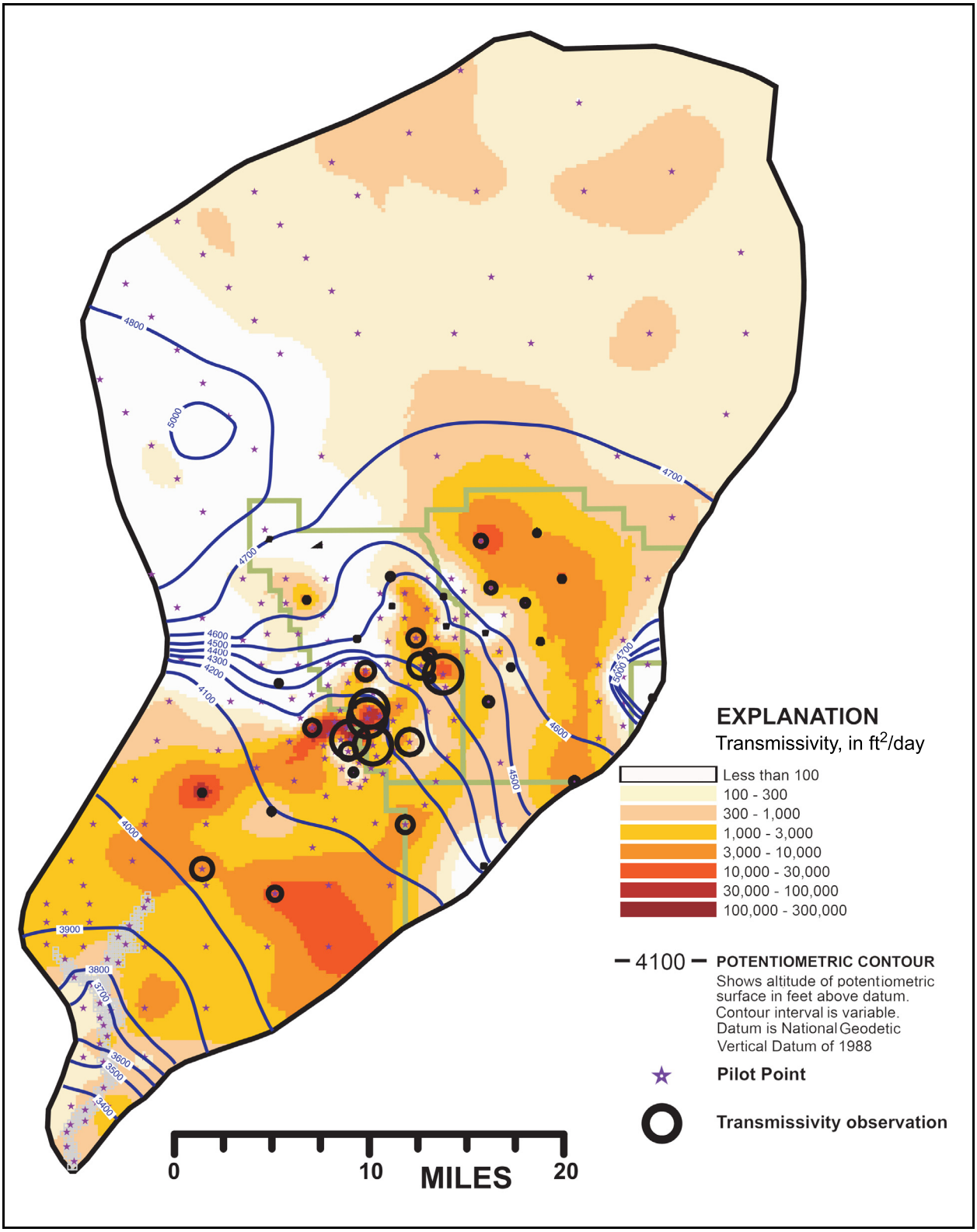

Figure B-6
Estimated Transmissivities in the Vicinity of PM-3
Source: Modified from Jackson et al., 2014a

B.6.0 SUMMARY

The hydraulic properties of the HSUs that intersect PM-3 have been estimated from the limited testing performed at the time the well was drilled and developed along with supplemental analysis based on the low-flow pump jack, which occurred during sampling in 2013. The hydraulic properties of the HSUs that intersect the HANDLEY chimney are more uncertain and are based on limited testing performed in the late 1960s at UE-20j and U-20m before the HANDLEY detonation in 1970. Although the hydraulic continuity of the HSUs between HANDLEY and PM-3 are very uncertain as is the groundwater flow regime in this area, recent estimates of the flow system have used the available transient MWAT and steady-state water-level observations to infer the flow directions and flow rates between HANDLEY and PM-3. These estimates can be used to evaluate the potential for ^3H transport between the potential source at HANDLEY and the observed ^3H values in PM-3-1 (deep) and PM-3-2 (shallow).

B.7.0 REFERENCES

Blankennagel, R.K., and J.E. Weir. 1965. *Water Production and Pumping Test Data for Exploratory Holes, Pahute Mesa, Nevada Test Site*, Technical Letter Special Studies-I-40, Supplement 1. Denver, CO: U.S. Geological Survey.

Blankennagel, R.K., and J.E. Weir, Jr. 1973. *Geohydrology of the Eastern Part of Pahute Mesa, Nevada Test Site, Nye County, Nevada,* Professional Paper 712-B. Denver, CO: U.S. Geological Survey.

Cutillo, P.A., and J.D. Bredehoeft. 2011. "Estimating Aquifer Properties from the Water Level Response to Earth Tides." In *Ground Water*, Volume 49(4): pp. 600–610.

DOE/NV, see U.S. Department of Energy, Nevada Operations Office.

Fenelon, J.M., D.S. Sweetkind, and R.J. Laczniak. 2010. *Groundwater Flow Systems at the Nevada Test Site, Nevada: A Synthesis of Potentiometric Contours, Hydrostratigraphy, and Geologic Structures*, Professional Paper 1771. Reston, VA: U.S. Geological Survey.

Geldon, A.L., A.M.A. Umari, M.F. Fahy, J.D. Earle, J.M. Gemmell, and J. Darnell. 2002. *Results of Hydraulic Tests in Miocene Tuffaceous Rocks at the C-Hole Complex, 1995 to 1997, Yucca Mountain, Nye County, Nevada,* Water-Resources Investigations Report 02-4141. Denver, CO: U.S Geological Survey.

Halford, K., J. Fenelon, and S. Reiner. 2012. *Aquifer-Test Package - Simultaneous Numerical Analysis of Eight Aquifer Tests to Estimate Hydraulic Properties on Pahute Mesa, Nevada National Security Site.* Memorandum to D. Galloway. U.S. Geological Survey, Henderson, NV, available at Nevada Water Science Center Aquifer Tests webpage, accessed 15 July 2014 at http://nevada.usgs.gov/water/aquifertests/index.htm.

Jackson, T., C.A. Garcia, K. Halford, D. Sweetkind, and J. Fenelon. 2014a. *Improving Regional Groundwater Flow Models with Transmissivity Observations.* poster presented at UGTA Technical Information Exchange, 16 July 2014. Las Vegas, NV.

Jackson, T.R., C.A. Garcia, K.J. Halford, N. Darnar, and J.M.Fenelon. 2014b. *Integrated Analysis of 10 Large-Scale Multi-Well Aquifer Tests at Pahute Mesa*. Poster presented at UGTA Technical Information Exchange, 16 July 2014. Las Vegas, NV.

Kilroy, K.C., and C.S. Savard. 1996. *Geohydrology of Pahute Mesa-3 Test Well, Nye County, Nevada*, Water-Resources Investigations Report 95-4239. Carson City, NV: U.S. Geological Survey.

Kwicklis, E.M., T.P. Rose, and F.C. Benedict. 2005. *Evaluation of Groundwater Flow in the Pahute Mesa – Oasis Valley Flow System Using Groundwater Chemical and Isotopic Data*, LA-UR 05-4344. Los Alamos, NM: Los Alamos National Laboratory.

Laczniak, R.J., J.L. Smith, P.E. Elliott, G.A. DeMeo, M.A. Chatigny, and G. Roemer. 2001. *Ground-Water Discharge Determined from Estimates of Evapotranspiration, Death Valley Regional Flow System, Nevada and California*, Water-Resources Investigations Report 01-4195. Denver, CO: U.S. Geological Survey.

N-I, see Navarro-Intera, LLC.

Navarro-Intera, LLC. 2012. *Pahute Mesa Well Development and Testing Analyses for Wells ER-20-8 and ER-20-4, Nevada National Security Site, Nye County, Nevada*, N-I/28091-061. Las Vegas, NV.

Navarro-Intera, LLC. 2014. Written communication. Subject: *Pahute Mesa Well Development and Testing Analyses for Wells ER-EC-12 and ER-EC-13, Nevada National Security Site, Nye County, Nevada.* Las Vegas, NV.

Orkild, P.P. 1969. *Summary Geologic Report on the U20m Emplacement Hole, Pahute Mesa, Nevada Test Site:* U.S. Geologic Survey Open-File Report USGS-474-7, Denver, CO.

Pawloski, G.A. 1999. *Development of Phenomenological Models of Underground Nuclear Tests on Pahute Mesa, Nevada Test Site-Benham and TYBO,* UCRL-ID-136003. Livermore, CA. Lawrence Livermore National Laboratory.

Rose, T.P., F.C. Benedict, Jr., J.M. Thomas, W.S. Sicke, R.L. Hershey, J.B. Paces, I.M. Farnham, and Z.E. Peterman. 2006. *Geochemical Data Analysis and Interpretation of the Pahute Mesa - Oasis Valley Groundwater Flow System, Nye County, Nevada, August 2002*, UCRL-TR-224559. Livermore, CA: Lawrence Livermore National Laboratory; Reno, NV: GeoTrans Inc. and Desert Research Institute; Denver, CO: U.S. Geological Survey; and Las Vegas, NV: Harry Reid Center for Environmental Studies.

U.S. Department of Energy, Nevada Operations Office. 2000. *United States Nuclear Tests, July 1945 through September 1992*, DOE/NV--209-REV 15. Las Vegas, NV.

Wood, D.B. 2007. *Digitally Available Interval-Specific Rock-Sample Data Compiled from Historical Records, Nevada Test Site and Vicinity, Nye County, Nevada*: U.S. Geological Survey Data Series 297, Rev. 2.00, 96 p.

Appendix C

Analysis of Possible Flow Path from HANDLEY to PM-3 Using Numerical Modeling

C.1.0 INTRODUCTION

A simple and numerically efficient modeling approach incorporating 3-D flow aspects defined by the Pahute Mesa Phase II HFM was developed using streamlines to define 2-D streamtube fence models. The models extended from the HANDLEY detonation to PM-3 and to Oasis Valley. The streamtube models were used to simulate ^3H transport from the HANDLEY detonation and evaluate the possibility of ^3H from the HANDLEY being the source of the ^3H observed at PM-3.

The focus of the analyses of the potential UGTA sources for the observed ^3H at PM-3 presented in this appendix is on the HANDLEY detonation. However, other underground detonations could have been the source of the observed ^3H, including DELAMAR, TENABO, EGMONT, DARWIN, and PURSE. DELAMAR, TENABO, EGMONT, and DARWIN are detonations that are closer to PM-3 than HANDLEY; however, the inferred water level in the vicinity of these detonations is less than 4,200 ft (1,280 m) amsl (Figure 1-6), which is below the water level observed at PM-3. Although there is significant uncertainty in the water-level surface in this area, it is unlikely that the hydraulic potential in any feature intersected by the exchange volume or chimney of these detonations would be above the potential at PM-3, thus precluding contamination from these sources being transported to PM-3. The PURSE detonation is about 7.2 km northeast of PM-3, and it is conceivable that ^3H from PURSE could be transported toward the south–southwest along the Purse fault about 400 m west of the PURSE working point. Significant uncertainty exists in the water levels near PURSE; however, water levels inferred by Fenelon et al. (2010) indicate that the water level near PURSE may be about 10 m above the water level observed at PM-3 (Figure 1-6). Although the structural deformation is more in a southerly or south–southwesterly direction instead of the southwesterly direction that would be necessary to provide a groundwater flow path between PURSE and PM-3, the possibility of flow from PURSE to PM-3 cannot be precluded given the lack of subsurface geologic and hydrogeologic information in the area between HANDLEY (U-20m), PURSE (U-20v), and PM-3. Although HANDLEY is considered the most likely UGTA source for the ^3H at PM-3 because it is along the likely groundwater flow path, there remains uncertainty in this interpretation.

C.1.1 Streamtube Modeling Approach

The concept of the streamtube model assumes that the mass flow rate along the streamline is constant in both space and time without exchange of water and solute with other streamtubes. The assumption of constant mass flow along the streamline does not necessarily imply constant velocity, and the spacial variability is introduced through variability of the streamtube model width, which represents the distance between streamlines in non-uniform flow. The streamtube modeling presented herein also assumes that variability in horizontal flow direction with depth is small and that the streamline's horizontal coordinates can be approximated from the water table's potentiometric surface.

C.1.2 Streamtube Model Mathematics

A streamline is defined as the curves at every point being tangent to the velocity vector in a flow field. The mathematical expression for a streamline is defined as the vector product of velocity and streamline being equal to zero at each point. That is

$$\vec{V} \times d\vec{s} = 0 \qquad (C\text{-}1)$$

or in steady incompressible flow

$$\frac{dx}{V_x(x,y,z)} = \frac{dy}{V_y(x,y,z)} = \frac{dz}{V_z(x,y,z)} \qquad (C\text{-}2)$$

In planar flow, Equation (C-2) can be written terms of specific discharge q_x and q_y instead of velocity as

$$\frac{dx}{q_x} = \frac{dy}{q_y} \qquad (C\text{-}3)$$

If the stream function ψ is defined such that

$$q_x = \frac{\partial \psi}{\partial y} \quad and \quad q_y = -\frac{\partial \psi}{\partial x} \qquad (C\text{-}4)$$

then Equation (C-3) is satisfied by direct substitution providing a solution of $\Psi = \Psi(x,y) = constant$, which describes the geometry of the streamline (Bear and Verruijt, 1987; White, 1991; and others).

By definition, lines of constant ψ are lines across which there is no flow; and for a planar flow, a streamline is represented by the functional relationship $\psi(x,y) = C$. The difference ($\Delta\psi$) between the values of ψ on any two streamlines defines the mass flow (Q) between the streamlines.

The streamtube model represents the flow between two streamlines with a flow rate Q, which can be characterized by flow parallel to a central streamline = ψ and cross-section width = w as

$$Q = \int_{\Delta w} q\,dw = \Delta\psi \qquad \text{(C-5)}$$

where

$\Delta\psi$ can be approximated as

$$\Delta\psi = \psi(w + \Delta w/2) - \psi(w - \Delta w/2) \qquad \text{(C-6)}$$

Introducing Darcy's Law provides the equation to calculate a streamtube's width (Δw) at each point along the streamline from the hydraulic conductivity and hydraulic gradient at each point as

$$\Delta w = \frac{Q}{(dh/ds)K_h t} \qquad \text{(C-7)}$$

where

dh/ds = hydraulic gradient along the streamline at distance s (L/L)

K_h = effective horizontal hydraulic conductivity at distance s along the streamline (L/T)

t = flowing aquifer thickness at distance s along the streamline (L)

Significant heterogeneity in rock properties is present along the flow paths originating from the Pahute Mesa detonation locations. The water and radionuclides originating at the detonation working point must path through many rock types with properties ranging from confining units to fractured rock aquifers. As the streamline intersects rocks of lower hydraulic conductivity, the streamtube width must increase to maintain a constant conductance, thereby accommodating the assumption of constant flux. The increase in streamtube width exposes the solute to larger amounts of rock and increased attenuation due to matrix diffusion and/or sorption, as flow must spread and slow as it moves through a larger rock volume.

A streamtube model approximating flow and transport in a 3-D flow field may be constructed as a 2-D fence model by calculating the transmissivity at each cell column and uniformly adjusting the column's width at each cell along the streamline. The vertical heterogeneity of hydraulic conductivity and/or porosity at each column is maintained and constant conductance is maintained by the width adjustment. The streamtube fence models width is calculated by querying the HFM model at discrete horizontal distance intervals along the streamline downgradient of the inlet area, thereby returning the vertical lithology of columns at specified intervals.

The effective horizontal hydraulic conductivity of each discrete column is given by

$$K_h = \sum_{i=1}^{n} \frac{K_i d_i}{d} \qquad \text{(C-8)}$$

where

K_h = effective horizontal hydraulic conductivity (L/T)

K_i = individual layer hydraulic conductivity (L/T)

d_i = individual layer thickness (L)

d = total thickness (L)

The width of the each column located downgradient of the source area is then adjusted by the ratio of the product of source area effective horizontal conductivity and hydraulic gradient, which defines Q in Equation (C-7), to the downgradient product of effective horizontal conductivity and hydraulic gradient. The end result is a streamtube model that preserves the streamline gradient while maintaining constant flow along the streamtube. The streamtube modeling may be implemented in a conventional groundwater simulator and the streamtube models were constructed with the FEHM simulator (Zyvoloski et al., 1997a and b). The streamtube model's column width adjustment is accomplished using the FEHM simulator's option of variable thickness for 2-D problems.

C.2.0 CONSIDERATION OF UNCERTAINTY

The uncertainties associated with the HANDLEY streamtube modeling are evaluated with alternative conceptualizations or datasets. The most significant uncertainties considered in the streamtube modeling presented herein include the following:

- **The Direction of Hydraulic Gradient.** Groundwater beneath Pahute Mesa generally flows in a southwest direction. The water that moves through the underground testing areas on Pahute Mesa is eventually discharged at springs and seeps in Oasis Valley (Fenelon et al., 2010). Although the general direction of flow is understood, there are no wells between the HANDLEY detonation and PM-3, and the exact direction of groundwater flow is uncertain. Two flow paths are considered from the HANDLEY detonation: (1) a streamline from the potentiometric surface interpretation of Fenelon et al. (2010), and (2) a straight line connection between HANDLEY and PM-3. Although the magnitude of the hydraulic gradient along these two possible flow paths is also uncertain, this uncertainty is not directly quantified or evaluated in the streamtube modeling.

- **Hydraulic Conductivity.** The streamtube modeling approach is very sensitive to the hydraulic conductivity at the HANDLEY detonation working point, because the regional gradient and hydraulic conductivity at the model inlet define the flow rate through the streamtube. Alternate hydraulic conductivity datasets are considered in the streamtube modeling, including the Phase I HDD (SNJV, 2004) and more recent USGS modeling (Halford et al., 2012).

- **Fracture Flow and Transport Properties**. The fractured rock aquifers between HANDLEY and PM-3 largely control ^3H transport. Alternate fracture spacing and fracture conceptual models are considered, including conceptualizations that the fractures are arranged as parallel plates or that multiple fracture sets are orthogonal resulting in cubic matrix blocks.

- **^3H Source Term.** Significant uncertainty exists in the initial distribution of ^3H (and other radionuclides in the HANDLEY source term. Of particular uncertainty is the extent and shape of the exchange volume, which is generally considered to be a multiple of the cavity radius (the R_c multiplier). For ^3H, the exchange volume is assumed to range from 1.5 to 3 R_c. The presence of a high-permeability chimney allows buoyancy effects from test-related heat to potentially drive groundwater upward into the chimney. The modeling presented herein assumes that the radionuclides are initially distributed uniformly throughout the largest possible exchange volume (3 R_c) and a 1 R_c saturated chimney to maximize the possibility for transport. The estimated accuracies for NNSS inventories is provided in Bowen et al. (2001), and the residual ^3H inventory is accurate to approximately 300 percent. The governing equation for groundwater transport is linear in terms of initial concentration, and the uncertainty in initial inventory can be assessed by multiplying the simulated concentrations by

a factor of 1/3 and 3 to bound radiologic source term uncertainty. The uncertainty in release rate from the chimney/cavity due to uncertainty in rock properties is captured by the hydraulic conductivity and fracture properties uncertainty.

The alternative conceptualizations and datasets considered by the streamtube modeling are discussed in further detail in Section C.3.0.

C.3.0 PAHUTE MESA HYDROGEOLOGIC DATA

The streamtube model development requires defining a potentiometric surface extending from the HANDLEY detonation to Oasis Valley, and estimating the hydrologic and transport parameters for the lithology present within the streamtube model.

C.3.1 Pahute Mesa Potentiometric Surface

The potentiometric surface used for the streamtube model was derived from the interpretation of the Pahute Mesa groundwater systems performed by the USGS (Fenelon et al., 2010) and additional water-level measurement data from wells in Area 20 of the NNSS.

The hand-drawn contours from Fenelon et al. (2010) were interpolated onto a dense uniform grid and then smoothed to remove any local sinks not associated with the known discharges at Oasis Valley. The Fenelon et al. (2010) interpretation of groundwater flow direction was modified using more recent water-level data from wells in the area (Elliot and Fenelon, 2013). For example, the Fenelon et al. (2010) gradient direction near the BENHAM detonation is southwest. However, plutonium identified by isotopic analysis to be from the BENHAM detonation has been observed in ER-20-5, which is located mostly south of the detonation.

Figure C-1 illustrates the modified potentiometric surface used to generate the HANDLEY streamtube model and streamlines from several other detonations. The red lines on this figure are the inferred geochemistry flow paths from Rose et al. (2006), while the black lines are flow paths from the detonation working points derived from the modified potentiometric surface, assuming the hydraulic properties are homogeneous and isotropic. The gradient at the HANDLEY detonation extracted from the modified potentiometric surface is 0.0088 m/m. The modified Fenelon et al. (2010) potentiometric surface does not place PM-3 directly downgradient of the HANDLEY detonation. The streamline originating from HANDLEY passes several kilometers east of PM-3. To account for this discrepancy, a straight line streamline that directly connects HANDLEY and PM-3 is also considered in the analysis. The straight line streamline departs from the direction of maximum gradient and is thereby termed a “pseudo” streamline in this analysis. The hydraulic gradient used in the pseudo streamline simulations is from the unaltered streamline originating from HANDLEY.

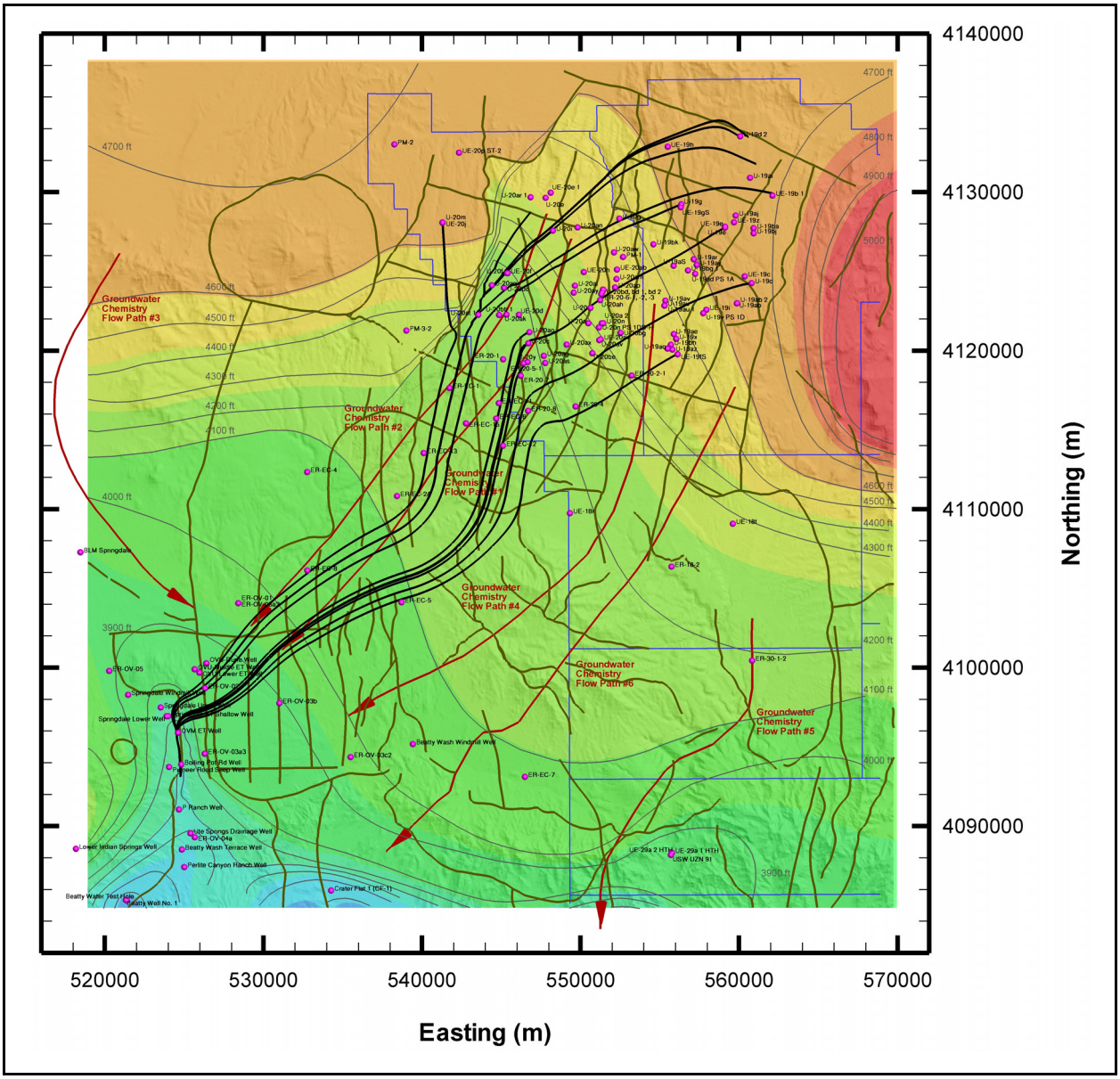

Figure C-1
Potentiometric Surface Used for Generating HANDLEY Streamtube Models

Using the gradient along the pseudo streamline extracted from the potentiometric surface would underestimate the groundwater velocity because the streamline departs from the path of maximum gradient. Figure C-2 illustrates streamlines originating at PM-3, HANDLEY, and the pseudo streamline that directly connects HANDLEY to PM-3. Figure B-4 illustrates the hydrostratigraphy along the pseudo streamline between HANDLEY and PM-3.

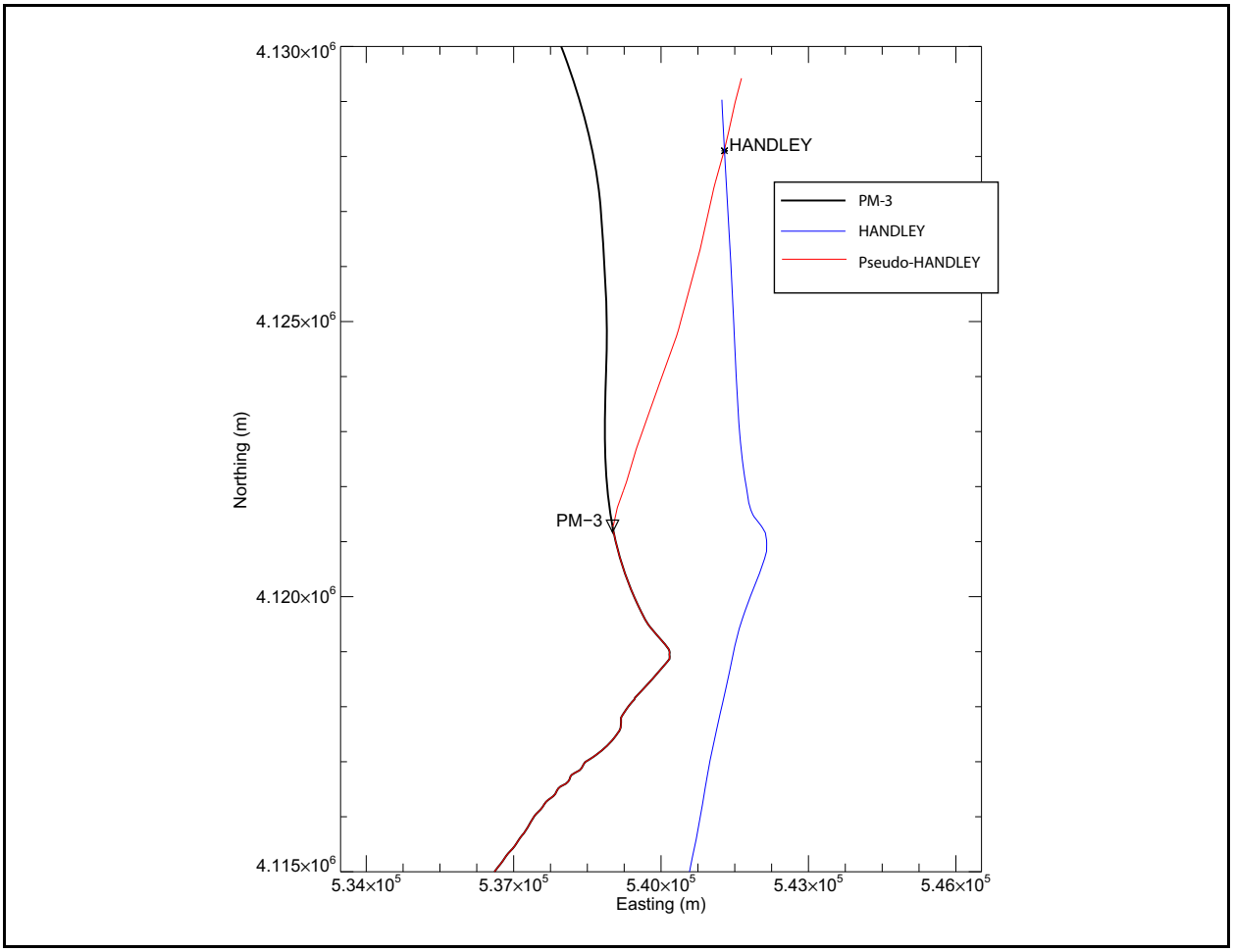

Figure C-2
Streamlines Originating from PM-3, HANDLEY, and Pseudo-HANDLEY

C.3.2 Hydraulic and Transport Parameters

The USGS has performed simultaneous numerical analysis of eight aquifer tests to estimate hydraulic properties on Pahute Mesa (Halford et al., 2012). A total of six models were created to simulate drawdowns in six wells: ER-20-8 #2, ER-EC-11, ER-20-7, ER-20-8, ER-20-4, and ER-EC-12. The six models used 13 material types that represent simplified HSUs. The models were calibrated by adjusting the hydraulic conductivity of pilot points in each HSU and interpolating the pilot point values to model node locations using Kriging. Table C-1 describes the USGS model material types and summarizes the permeability of each material type. The USGS models included an area much larger than the Pahute Mesa to Oasis Valley area of interest, and the volumetric average hydraulic conductivity values summarized in Table C-1 are for a rectangular subset area of the USGS model that only includes a 19-by-18-km refined area centered around the pumping and drawdown wells. The

Table C-1
USGS Model Material Types Description and Permeability

Description	Material Abbreviation	Permeability		
		Volumetric Average	Minimum	Maximum
		(m^2)		
Thirsty Canyon tuffs and intracaldera rocks of the Rainier/Ammonia caldera	TCVA/TMCM	1.35E-12	4.35E-13	1.82E-12
Crater Flat Group interval, including CFCM, CFCU, and BFCU; pre-Crater Flat units (Belted Range and pre-Belted Range), including BRA and PBRCM; LCA (in the area of the Bench)	TMA/PVTA	4.35E-13	1.07E-13	1.46E-12
Benham lava aquifer	BA	7.82E-12	5.05E-13	1.91E-10
upper Paintbrush confining unit	UPCU	9.44E-15	2.96E-15	5.34E-14
Tiva Canyon aquifer, including PLFA	TCA	9.31E-14	7.71E-15	4.74E-13
lower Paintbrush confining unit	LPCU	9.53E-13	1.04E-14	1.81E-11
Topopah Spring aquifer	TSA	9.61E-13	1.03E-14	1.03E-10
Calico Hills units, including CHVCM, CHZCM, CHCU, and IA	CH	1.55E-13	2.18E-14	8.38E-13
Crater Flat Group interval, including CFCM, CFCU, and BFCU; pre-Crater Flat units (Belted Range and pre-Belted Range), including BRA and PBRCM; LCA (in the area of the Bench)	CF/BR/PBR/LCA	1.74E-14	2.25E-18	5.94E-14
LAVA intersecting various units	LAVA1	3.94E-13	2.52E-13	6.13E-13
LAVA intersecting various units	LAVA2	2.01E-11	8.09E-13	3.42E-10
LAVA intersecting various units	LAVA3	4.76E-12	4.31E-14	6.15E-11
LAVA intersecting various units	LAVA4	1.71E-13	7.29E-14	3.27E-13

m^2 = Square meter

average hydraulic conductivity of the USGS model aquifers and confining units are generally within two orders of magnitude of each other, and the variability within each material type is moderate and is about two orders of magnitude with the exception of the Crater Flat Group interval and the TSA.

The USGS model HSUs and Phase II HFM HSUs were reconciled by calculating the total volume of each USGS model material type within each Phase II HSU. The USGS model and Phase II HFM generally have a poor spatial agreement, and a single USGS model HSU may contain several Phase II HSUs.

Due to the uncertainty and importance of the HSU hydraulic conductivity on the streamtube flow and transport calculations, alternate hydraulic conductivity data sources are used to parameterize the

streamtube models, including (1) the Phase I HDD (SNJV, 2004), calculated as the geometric average of the dominant hydrogeologic unit (HGU) hydraulic conductivities within each Phase II HFM HSU; (2) the USGS models, calculated as the volumetric average of all USGS model cells within each Phase II HFM HSU; and (3) the USGS models, calculated as the transmissivity average from vertical profiles at each Pahute Mesa detonation. The Phase I HDD presented hydraulic conductivity data by Phase I HSUs and data representative of the Pahute Mesa HGUs were selected from the HSU data. Table C-2 presents the Pahute Mesa Phase I HSUs selected to represent the streamtube model HGUs. Table C-3 summarizes the permeability values from the three data sources.

Table C-2
Pahute Mesa Phase I HSUs Selected To Represent the Streamtube Model HGUs for the Phase I HDD Parameterization

HGU	Hydraulic Conductivity Log10 (m/day)	Representative HSU	Data Source
TCU	-1.0	FCCU, UPCU, LPCU, CFCU, and BFCU Average	Pahute Mesa HDD Table 5-4 (Shaw, 2003)
WTA	0.1	TMA, TCA, and TSA	Pahute Mesa HDD Table 5-4 (Shaw, 2003)
LFA	0.1	WWA, PLFA, and KA	Pahute Mesa HDD Table 5-4 (Shaw, 2003)
UCCU	-2.2	UCCU	Pahute Mesa HDD Table 5-4 (Shaw, 2003)
ICU	-2.5	BMICU, ATICU, RMICU, CCICU, CHICU, and SCICU	Pahute Mesa HDD Table 5-4 (Shaw, 2003)
CA	-0.3	LCA3 and LCA	Pahute Mesa HDD Table 5-4 (Shaw, 2003)

Simulation of matrix diffusion in fractured rock requires the assumption of a fracture continuum with a specific geometry. The fracture continuum is assumed to consist of parallel plates and consistency between fracture properties is maintained by calculating the fracture porosity from the hydraulic conductivity and fracture spacing using the cubic law.

The cubic law describing the volumetric flow rate between parallel, smooth plates is given by Domenico and Schwartz (1990) as

$$Q = \frac{\rho_w g b^3}{12\mu}(w)\frac{\partial h}{\partial L} \qquad \text{(C-9)}$$

Table C-3
Permeability and Porosity Data Used in the Streamtube Models
(Page 1 of 3)

HSU	Primary HGU Lithology	Phase I HDD Permeability Calculated from Primary HGUs (m^2)	Phase I HDD Permeability Cubic Law Porosity	Permeability Calculated from USGS Model by Volumetric Average	USGS Model Volumetric Average Permeability Cubic Law Porosity	Permeability Calculated from USGS Model by Working Point Thickness Average	USGS Model Working Point Thickness Average Cubic Law Porosity
ATICU	ICU	3.75E-15	Not Fractured	3.75E-15	Not Fractured	9.18E-13	Not Fractured
RMICU	ICU	3.75E-15	Not Fractured	1.27E-14	Not Fractured	4.98E-13	Not Fractured
CCICU	ICU	3.75E-15	Not Fractured	3.75E-15	Not Fractured	1.17E-12	Not Fractured
CHICU	ICU	3.75E-15	Not Fractured	3.75E-15	Not Fractured	3.75E-15	Not Fractured
BMICU	ICU	3.75E-15	Not Fractured	3.75E-15	Not Fractured	3.75E-15	Not Fractured
MGCU	GCU	3.75E-15	Not Fractured	3.75E-15	Not Fractured	4.89E-14	Not Fractured
RVICU	ICU	3.75E-15	Not Fractured	3.75E-15	Not Fractured	1.20E-14	Not Fractured
SCICU	ICU	3.75E-15	Not Fractured	3.75E-15	Not Fractured	3.75E-15	Not Fractured
LCCU	CCU	7.47E-15	0.00002	1.07E-12	0.00008	1.42E-14	0.00002
LCA	CA	5.94E-13	0.00016	2.00E-14	0.00005	1.42E-14	0.00005
UCCU	CCU	7.47E-15	0.00002	1.28E-14	0.00002	1.42E-14	0.00002
LCA3	CA	5.94E-13	0.00016	1.16E-12	0.00020	1.42E-14	0.00005
LCCU1	CCU	7.47E-15	0.00002	1.24E-14	0.00002	1.42E-14	0.00002
SCVCU	TCU	1.18E-13	0.00006	7.69E-13	0.00012	5.37E-13	0.00011
PBRCM	WTA_LFA_TCU	6.41E-13	0.00014	3.85E-14	0.00005	5.10E-14	0.00006
BRA	WTA_LFA	1.49E-12	0.00020	3.28E-14	0.00006	1.82E-14	0.00005
BFCU	TCU	1.18E-13	0.00006	3.11E-14	0.00004	2.49E-14	0.00004
LVTA2	VTA	1.49E-12	Not Fractured	1.49E-12	Not Fractured	1.49E-12	Not Fractured
SWA	WTA	1.49E-12	0.00022	1.49E-12	0.00022	1.49E-12	0.00022
KA	LFA	1.49E-12	0.00018	1.49E-12	0.00018	1.49E-12	0.00018
CFCU	TCU	1.18E-13	0.00006	9.50E-14	0.00006	6.45E-14	0.00005
CFCM	LFA_TCU	4.20E-13	0.00011	8.78E-14	0.00006	1.25E-13	0.00007
IA	LFA	1.49E-12	0.00018	1.38E-13	0.00008	1.69E-13	0.00009
CHLFA5	LFA	1.49E-12	0.00018	1.77E-13	0.00009	1.81E-13	0.00009
CHLFA4	LFA	1.49E-12	0.00018	1.82E-13	0.00009	1.80E-13	0.00009
CHLFA3	LFA	1.49E-12	0.00018	1.79E-13	0.00009	1.82E-13	0.00009
CHLFA2	LFA	1.49E-12	0.00018	1.78E-13	0.00009	2.93E-13	0.00011
CHLFA1	LFA	1.49E-12	0.00018	8.14E-13	0.00015	1.87E-13	0.00009
CHZCM	TCU	1.18E-13	0.00006	3.84E-13	0.00009	1.66E-13	0.00007
CHVTA	VTA	1.49E-12	Not Fractured	1.53E-13	Not Fractured	1.13E-13	Not Fractured
YMCFCM	WTA_LFA_TCU	6.41E-13	0.00014	1.16E-12	0.00017	1.16E-12	0.00017
TSA	WTA	1.49E-12	0.00022	1.49E-12	0.00022	3.31E-13	0.00013
PLFA	LFA	1.49E-12	0.00018	1.56E-12	0.00019	1.59E-12	0.00019
LPCU	TCU	1.18E-13	0.00006	5.20E-13	0.00010	3.13E-13	0.00009

Table C-3
Permeability and Porosity Data Used in the Streamtube Models
(Page 2 of 3)

HSU	Primary HGU Lithology	Phase I HDD Permeability Calculated from Primary HGUs (m^2)	Phase I HDD Permeability Cubic Law Porosity	Permeability Calculated from USGS Model by Volumetric Average	USGS Model Volumetric Average Permeability Cubic Law Porosity	Permeability Calculated from USGS Model by Working Point Thickness Average	USGS Model Working Point Thickness Average Cubic Law Porosity
PVTA	VTA	1.49E-12	Not Fractured	1.75E-13	Not Fractured	1.53E-12	Not Fractured
TCA	WTA	1.49E-12	0.00022	1.99E-12	0.00024	9.67E-13	0.00019
MPCU	TCU	1.18E-13	0.00006	1.20E-11	0.00030	9.56E-12	0.00027
SPA	LFA	1.49E-12	0.00018	1.55E-11	0.00040	1.55E-11	0.00040
UPCU	TCU	1.18E-13	0.00006	3.84E-12	0.00020	2.47E-12	0.00017
BA	LFA	1.49E-12	0.00018	5.36E-12	0.00028	1.32E-11	0.00038
PBPCU	TCU	1.18E-13	0.00006	2.07E-12	0.00016	1.32E-11	0.00031
CPA	LFA	1.49E-12	0.00018	9.52E-13	0.00016	8.99E-13	0.00016
PCM	WTA_LFA_TCU	6.41E-13	0.00014	6.41E-13	0.00014	1.17E-12	0.00017
WWA	LFA	1.49E-12	0.00018	1.49E-12	0.00018	1.49E-12	0.00018
FCCU	TCU	1.18E-13	0.00006	2.63E-12	0.00018	2.81E-12	0.00018
RMWTA	WTA	1.49E-12	0.00022	1.15E-12	0.00020	1.17E-12	0.00020
TMLVTA	VTA	1.49E-12	Not Fractured	8.43E-13	Not Fractured	1.07E-14	Not Fractured
TMWTA	WTA	1.49E-12	0.00022	2.42E-12	0.00025	1.07E-12	0.00019
THCU	TCU	1.18E-13	0.00006	1.41E-12	0.00014	1.13E-12	0.00013
THCM	LFA_TCU	4.20E-13	0.00011	2.13E-12	0.00019	1.77E-12	0.00017
THLFA	LFA	1.49E-12	0.00018	1.33E-12	0.00018	1.17E-12	0.00017
TMUWTA	WTA	1.49E-12	0.00022	1.49E-12	0.00022	1.09E-12	0.00019
ATCCU	TCU	1.18E-13	0.00006	1.42E-12	0.00015	1.21E-12	0.00014
ATWTA	WTA	1.49E-12	0.00022	1.28E-12	0.00020	1.19E-12	0.00020
BWCU	TCU	1.18E-13	0.00006	1.14E-12	0.00014	1.13E-12	0.00013
BWWTA	WTA	1.49E-12	0.00022	1.08E-12	0.00019	1.12E-12	0.00020
ATMLFA	LFA	1.49E-12	0.00018	1.49E-12	0.00018	1.17E-12	0.00017
FCLMLFA	LFA	1.49E-12	0.00018	1.49E-12	0.00018	1.17E-12	0.00017
FCLLFA	LFA	1.49E-12	0.00018	1.49E-12	0.00018	1.16E-12	0.00017
FCWTA	WTA	1.49E-12	0.00022	1.49E-12	0.00022	1.16E-12	0.00020
FCWTA1	WTA	1.49E-12	0.00022	1.24E-12	0.00020	1.22E-12	0.00020
FCULFA7	LFA	1.49E-12	0.00018	1.49E-12	0.00018	1.17E-12	0.00017
FCULFA5	LFA	1.49E-12	0.00018	1.49E-12	0.00018	1.15E-12	0.00017
FCULFA4	LFA	1.49E-12	0.00018	8.80E-13	0.00015	9.03E-13	0.00016
FCULFA3	LFA	1.49E-12	0.00018	1.49E-12	0.00018	1.49E-12	0.00018
FCULFA2	LFA	1.49E-12	0.00018	1.19E-12	0.00017	1.17E-12	0.00017
FCULFA1	LFA	1.49E-12	0.00018	7.60E-13	0.00015	7.74E-13	0.00015
FCUMLFA	LFA	1.49E-12	0.00018	1.49E-12	0.00018	1.17E-12	0.00017

Table C-3
Permeability and Porosity Data Used in the Streamtube Models
(Page 3 of 3)

HSU	Primary HGU Lithology	Phase I HDD Permeability Calculated from Primary HGUs (m^2)	Phase I HDD Permeability Cubic Law Porosity	Permeability Calculated from USGS Model by Volumetric Average	USGS Model Volumetric Average Permeability Cubic Law Porosity	Permeability Calculated from USGS Model by Working Point Thickness Average	USGS Model Working Point Thickness Average Cubic Law Porosity
FCCM	LFA_TCU	4.20E-13	0.00011	1.03E-12	0.00015	1.10E-12	0.00015
FCULFA6	LFA	1.49E-12	0.00018	1.49E-12	0.00018	1.17E-12	0.00017
SMLFA	LFA	1.49E-12	0.00018	1.49E-12	0.00018	1.49E-12	0.00018
DVA	WTA_LFA	1.49E-12	0.00020	1.49E-12	0.00020	1.15E-12	0.00018
DVCM	WTA_LFA_TCU	6.41E-13	0.00014	6.41E-13	0.00014	1.15E-12	0.00017
TCVA	WTA_LFA	1.49E-12	0.00020	2.55E-12	0.00024	4.19E-13	0.00013
YVCM	WTA_LFA_VTA	1.67E-12	0.00021	1.67E-12	0.00021	1.67E-12	0.00021
AA	AA	5.94E-12	Not Fractured	1.15E-12	Not Fractured	1.15E-12	Not Fractured

where

Q = volumetric flow rate (L^3/t)
ρ_w = density of water (M/L^3)
g = gravitational acceleration (L/t^2)
b = fracture aperture (L)
μ = viscosity of water (M/Lt)
w = fracture width perpendicular to the flow direction (L)
$\frac{\partial h}{\partial L}$ = hydraulic gradient (L/L)

Darcy's law, which calculates the water discharge or flow rate through a porous medium, is given by Domenico and Schwartz (1990) as

$$Q = KA\frac{\partial h}{\partial L} \qquad \text{(C-10)}$$

where

K = hydraulic conductivity (L/t)
A = product of w and fracture spacing and is the discharge area perpendicular to the flow direction (L^2)

The fracture porosity is defined as

$$\phi_f = \frac{v_f}{v_t} \qquad \text{(C-11)}$$

where

ϕ_f = fracture porosity (dimensionless)
v_f = fracture volume (L^3)
v_t = total volume (L^3)

With some algebraic manipulation, the product of the fracture spacing (e) and unit fracture width perpendicular to the flow direction ($w = 1$) can be substituted for discharge area (A) in Equation (C-10). After making this substitution, Equations C-9 and C-10 are solved for the volumetric flow rate (Q) and then set equal to solve for the fracture aperture (b)

$$b = \left(\frac{eK12\mu}{\rho g}\right)^{1/3} \qquad (C\text{-}12)$$

The fracture aperture (b) can be substituted for the fracture volume (v_f), and the fracture spacing (e) can be substituted for the total volume (v_t) in Equation (C-11). The solution for the fracture aperture (b) and spacing e is then substituted into Equation (C-12) to yield the fracture porosity.

The water flow rate in a fractured rock is most strongly influenced by the size and number of critical necks of the fractures, but the solute residence times is most strongly influenced by the larger voids within the fractures. Consequently, the effective fracture aperture for transport is larger than that for flow (National Research Council, 1996). Kwicklis et al. (1998) developed a regression equation relating hydraulic aperture (b_h) and physical aperture (b_m) for Yucca Mountain tuff as

$$b_h = 0.5575 \times b_m \qquad (C\text{-}13)$$

The fracture aperture and spacing are from NNSS datasets (Shaw, 2003; SNJV, 2005). Adequate fracture spacing data for parameterization by HSU are not available, and the parameterization is performed by the dominant HGUs within each HSU. If several HGUs are present within the HSUs, the geometric average of the HGU spacing is used. All rock types are assumed to be fractured except alluvium, vitric tuff, and the intrusive confining units. Streamtube simulations were performed using spacings of mean values and the end points for a 95 percent confidence interval. These spacings are the 50, 2.5, and 97.5 percentile values. The spacing values were constrained by the minimum or maximum of the observed spacing values. Table C-4 summarizes the fracture spacing data.

An alternate conceptualization of matrix diffusion is also simulated that assumes three sets of orthogonal fractures that form cubic matrix blocks in combination with the HDD hydraulic

Table C-4
Fracture Spacing Data Summary

HGU	Log Spacing				Spacing Data Source
	Mean	Standard Deviation	2.5/97.5 Percentile	Observed Minimum/Maximum	
	(m)				
TCU	0.75	0.71	-0.64/2.14	-0.631/2.27	Pahute Mesa TDD Appendix E.4.0 (Shaw, 2003)
WTA	0.51	0.51	-0.49/1.50	-0.37/1.49	Pahute Mesa TDD Appendix E.4.0 (Shaw, 2003)
LFA	0.61	0.65	-0.67/1.89	-0.42/1.93	Pahute Mesa TDD Appendix E.4.0 (Shaw, 2003)
CCU	1.07	0.38	0.33/1.81	0.05/1.48	Yucca Flat Fracture Analysis Report Table 8-1 (SNJV, 2005)
LCA	0.49	0.45	-0.40/1.38	-0.18/1.48	Yucca Flat Fracture Analysis Report Table 8-1 (SNJV, 2005)

conductivity parameterization. The cubic law assuming that flow is only in two sets of fractures aligned parallel to the hydraulic gradient is

$$Q = 2\frac{\rho_w g b^3}{12\mu}(w)\frac{\partial h}{\partial L} \qquad (C\text{-}14)$$

and the fracture porosity is

$$\phi_f = \frac{3b_m}{e} \qquad (C\text{-}15)$$

For the alternate conceptualization, the FEHM software assumes that matrix diffusion occurs into idealized spherical blocks.

The effective diffusion coefficient is calculated from the tortuosity and matrix porosity as described by

$$D_{eff} = \frac{1}{\tau}D_{free} \qquad (C\text{-}16)$$

and

$$\frac{1}{\tau} = \phi^n \qquad (C\text{-}17)$$

where

D_{eff} = effective diffusion coefficient

τ = tortuosity

D_{free} = free diffusion coefficient

ϕ = matrix porosity

n = exponent determined to be 1.33 by a least squares regression for all rock types at the NNSS (SNJV, 2007)

The USGS modeling study likely represents the best estimation of hydraulic conductivity available for the Pahute Mesa testing area in southwest Area 20. The streamtube model transmissivity at the 82 Pahute Mesa detonation working points calculated from the three hydraulic conductivity data sources are compared to the USGS model transmissivities in Figures C-3 through C-5. As expected, the parameterization by USGS model hydraulic conductivity at the working points has the best agreement with the USGS models, and transmissivity values are generally within a factor of two of each. The differences seen between the USGS model and the streamtube model transmissivity is due to the poor spatial agreement between the Phase II HFM HSUs and the USGS model HSUs, and the assumption of homogeneous HSU properties in the streamtube models. The working point transmissivities from the USGS model volumetric averages most often overpredict transmissivity values, but most values are within a factor of two of the USGS model values. The HDD hydraulic conductivity parameterization results in the transmissivity values that are generally an order of magnitude greater than that in the USGS models. Although the USGS models likely provide a good estimate of hydraulic conductivity in southwest Area 20, the data are less reliable in the area between the HANDLEY detonation and PM-3.

The transmissivity and potentiometric gradient at the HANDLEY working point is of particular importance to the streamtube modeling because the two parameters define the flow rate through the streamtube. The exploratory well UE-20j was drilled adjacent to the HANDLEY emplacement hole in 1964. The well was drilled to a TD of 5,690 ft bgs, and the bottom 3,950 ft of the well was left uncased to allow for hydraulic testing of the saturated HSUs. A pumping test was conducted by pumping the well at 56 gpm for 23 hours, and the interpreted transmissivity of the pumping test was 7,900 ft^2/day over the 3,950 ft of open borehole (Blankennagel and Weir, 1973).

PM-3 was drilled in 1988 to a TD of 3,019 ft bgs and was also left uncased to allow for hydraulic testing. Before the pumping test, the bottom 500 ft of open interval collapsed during injection testing,

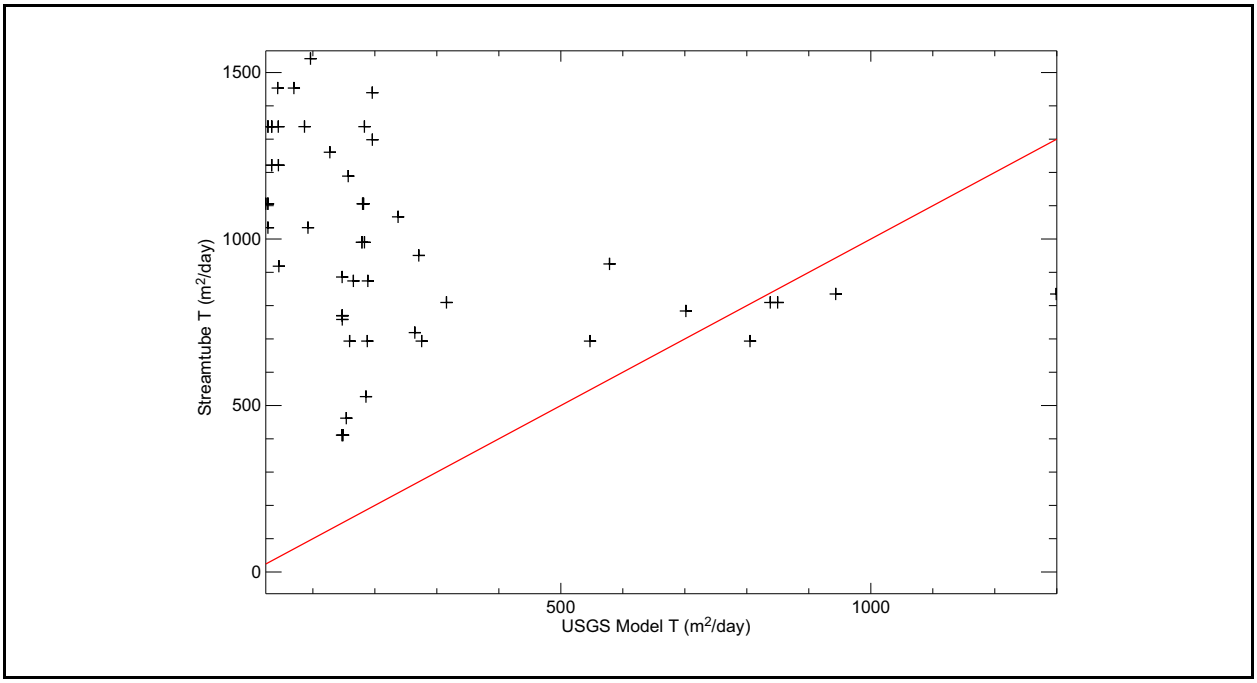

Figure C-3
Comparison of Working Point Transmissivity from the USGS Models and Streamtube Model Parameterized from HDD Data

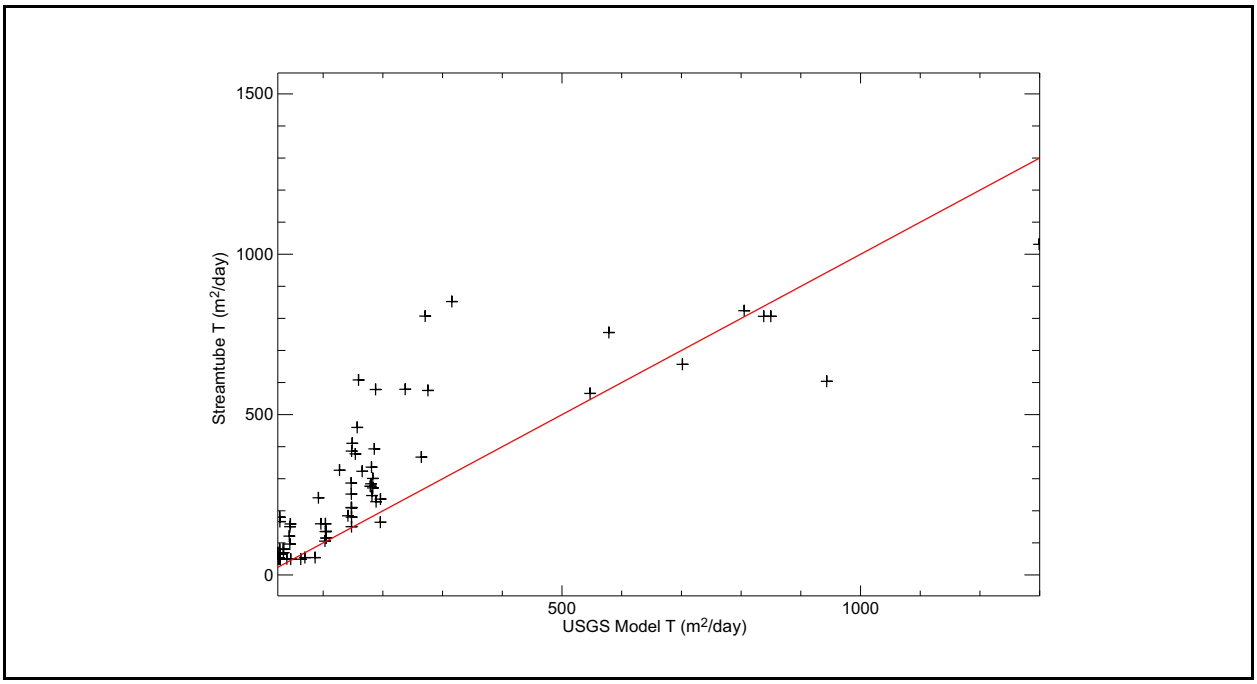

Figure C-4
Comparison of Working Point Transmissivity from the USGS Models and Streamtube Model Parameterized from the USGS Model Calculated as the Volumetric Average within Each HFM HSU

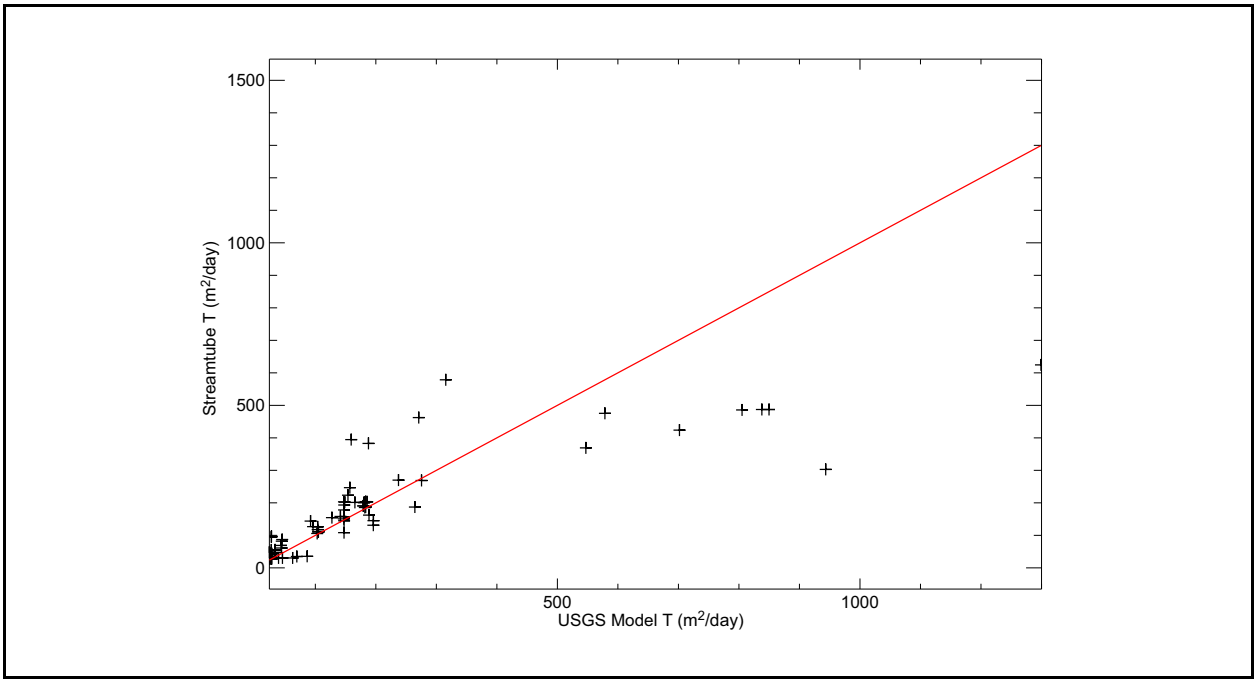

Figure C-5
Comparison of Working Point Transmissivity from the USGS Models and Streamtube Model Parameterized from the USGS Model Hydraulic Conductivity Calculated as Thickness Average at All Pahute Mesa Working Points

and the remaining open hole only extended to a depth of 2,605 ft. It was assumed that there was no communication below the collapse depth because of a low interpreted transmissivity for this portion of the borehole (Kilroy and Savard, 1996). A pumping test on the well was performed in 1988 over the remaining 1,132-ft open interval. The transmissivity was interpreted to be 38 to 70 ft^2/day assuming an unconfined aquifer, or 360 to 840 ft^2/day assuming a confined aquifer (Kilroy and Savard, 1996).

Table C-5 summarizes the pumping test and streamtube model transmissivities at UE-20j and PM-3. The streamtube model transmissivities were calculated from the models' hydraulic conductivity over the wells' open borehole intervals. At UE-20j, the streamtube model derived from the Fenelon et al. (2010) potentiometric surface and the straight line streamline have the same lithology. However, the two streamtube models have different lithologies at PM-3 because the Fenelon et al. (2010) streamline passes east of the PM-3 well location. At UE-20j, the HDD hydraulic conductivity data have a transmissivity that is approximately equal to the pump test value, but the USGS model-derived hydraulic conductivity data have a transmissivity much lower than the pump test value. The USGS modeling included the BRA in a composite unit (Crater Flat/pre-Crater Flat Group) (Halford et al.,

Table C-5
Streamtube Model Transmissivity at UE-20j and PM-3

Hydraulic Conductivity Data Source	UE-20j Transmissivity (ft^2/day)		PM-3 Transmissivity (ft^2/day)	
	Fenelon et al. (2010) Streamline	Pseudo Streamline	Fenelon et al. (2010) Streamline	Pseudo Streamline
Pump Test	7,900		38 to 840	
HDD	8,533	8,533	322	1,568
USGS Model Volume Average	409	409	1,294	2,745
USGS Model Working Point Transmissivity Average	496	496	720	1,448

2012), which generally had a conductivity that is lower that of a very conductive WTA. At PM-3, the streamtube model following a straight line to PM-3 has a much higher transmissivity than the PM-3 pump test value because the TCA hydraulic conductivity is very high in the three hydraulic conductivity data sources. At PM-3, the Fenelon et al. (2010) streamline streamtube models using either the HDD or USGS model-based hydraulic conductivity data sources have a transmissivity near the PM-3 pump test value, primarily because the TCA is above the water table at the assumed PM-3 location, thereby placing the well screen only in the low-permeability CHZCM and LPCU HSUs.

The transmissivity at the HANDLEY detonation is anomalously high compared to the aggregate in northwest Area 20. USGS modeling studies of the Pahute Mesa–Oasis Valley groundwater flow system have estimated transmissivities in northwest Area 20 away from HANDLEY and in the Gold Flat area north of the NNSS to be much lower than that predicted by the UE-20j pump test (Jackson et al., 2014a and b). These studies restrict the very high HANDLEY detonation transmissivity to a small area surrounding the detonation, and transmissivity calculated from a groundwater flow budget for a larger area encompassing the recharge area in northwest Area 20 and Gold Flat will be much smaller than that observed at UE-20j.

C.4.0 HANDLEY SOURCE TERM

The ^{3}H source term for the HANDLEY detonation is calculated from the Bowen et al. (2001) unclassified inventory using the yield-weighted fraction of the Area 20 inventory and correcting the 1992 inventory to the time of the detonation (March 26, 1970). The HANDLEY yield published in DOE/NV (2000) is "greater than 1 Mt" and a value of 1 Mt is used in the yield-weight calculation, which provides an initial ^{3}H inventory on March 26, 1970 of 1.325E+07 Ci. The depth of burial is 1,209 m, and the calculated cavity radius is 98 m using the announced yield and cavity-yield relationship from Pawloski et al. (1999).

The source term is released within a zone consisting of the 1 R_c saturated chimney and a 3 R_c exchange volume. A distance of 3 R_c is thought to be the maximum extent for a ^{3}H exchange volume (N-I, 2013). The simulations use a unit concentration source and scale the simulated concentrations by an initial concentration calculated within the saturated portion of a cylindrical 1 R_c chimney and 3 R_c spherical exchange volume assuming a cavity/chimney porosity of 0.4 and 3 R_c exchange volume fracture porosity of 2E-04. This yields a volume of 6.25E+09 L, most of which is in the chimney and cavity due to their higher porosity. The calculated initial ^{3}H concentration is 2.12E+09 pCi/L or about 100,000 times the MCL. This initial ^{3}H concentration in the source zone would decay to about 1.9E+08 pCi/L by 2013, the time of the most recent sampling of PM-3. Although the analyses performed and summarized in Section C.5.0 focus on ^{3}H transport downgradient from HANDLEY, additional analyses related to the relative transport of ^{14}C, ^{36}Cl, and ^{129}I are also relevant. The HANDLEY source term for these other mobile radionuclides can be determined using the same assumptions as above. Rounding the results to two significant figures, the initial yield-weighted concentration in the HANDLEY source zone are as follows:

- **^{14}C:** 4,800 pCi/L (or 2.4 times the ^{14}C SDWA MCL of 2,000 pCi/L)
- **^{36}Cl:** 1,600 pCi/L (or 2.3 times the ^{36}Cl SDWA MCL of 700 pCi/L)
- **^{129}I:** 5.7 pCi/L (or 5.7 times the ^{129}I SDWA MCL of 1.0 pCi/L)

C.5.0 SIMULATION RESULTS AND DISCUSSION

Figures C-6 through C-9 illustrate the streamtube model and observed ^3H concentrations at PM-3. The streamtube model based on the Fenelon et al. (2010) streamline, HDD hydraulic conductivity, and mean fracture spacing data predicts ^3H will arrive at PM-3 in agreement with the observed concentrations. The streamtube model based on the pseudo streamline also predicted that ^3H will arrive at PM-3 at concentrations near the observations, but the breakthrough lagged behind the observations by approximately 25 years. The streamtube model simulations using the USGS modeling-based hydraulic conductivities only predicted ^3H will arrive at PM-3 coincident with the observations when the upper 95 percent confidence interval of fracture spacings is used (97.5 percentile value).

The alternate fracture conceptual model assuming three sets of orthogonal fractures in combination with the HDD hydraulic conductivity predicted breakthrough coincident with observations only using the 97.5 percentile fracture spacing. The calculated fracture aperture using the cubic law for the alternate fracture conceptual model is smaller than that from a parallel plate fracture model because the additional set of fractures doubles the cross-sectional area available to transmit water. The additional sets of fractures also increase the ratio of fracture area to matrix volume. Both the smaller aperture and increased ratio of fracture area to matrix volume increase the amount of attenuation resulting from matrix diffusion and slow transport velocity.

Within the USGS modeling, the BRA was included in a composite unit (Crater Flat/pre-Crater Flat Group) (Halford et al., 2012), and the average hydraulic conductivity of the composite unit was much lower than the Phase I HDD hydraulic conductivity of the BRA. The permeabilities of the streamtube model BRA HSU from the HDD, USGS model by volumetric average, and the USGS model working point transmissivity average are 1.5E-12, 3.3E-14, and 1.8 E-14 m^2, respectively. The streamtube simulations using the USGS model-based parameterizations had substantially slower transport within the BRA compared to the HDD parameterization. The USGS model was primarily calibrated to pump test data in southwest Area 20 of the NNSS, and the hydraulic conductivity within the USGS model between the HANDLEY detonation and PM-3 may not have been accurately estimated.

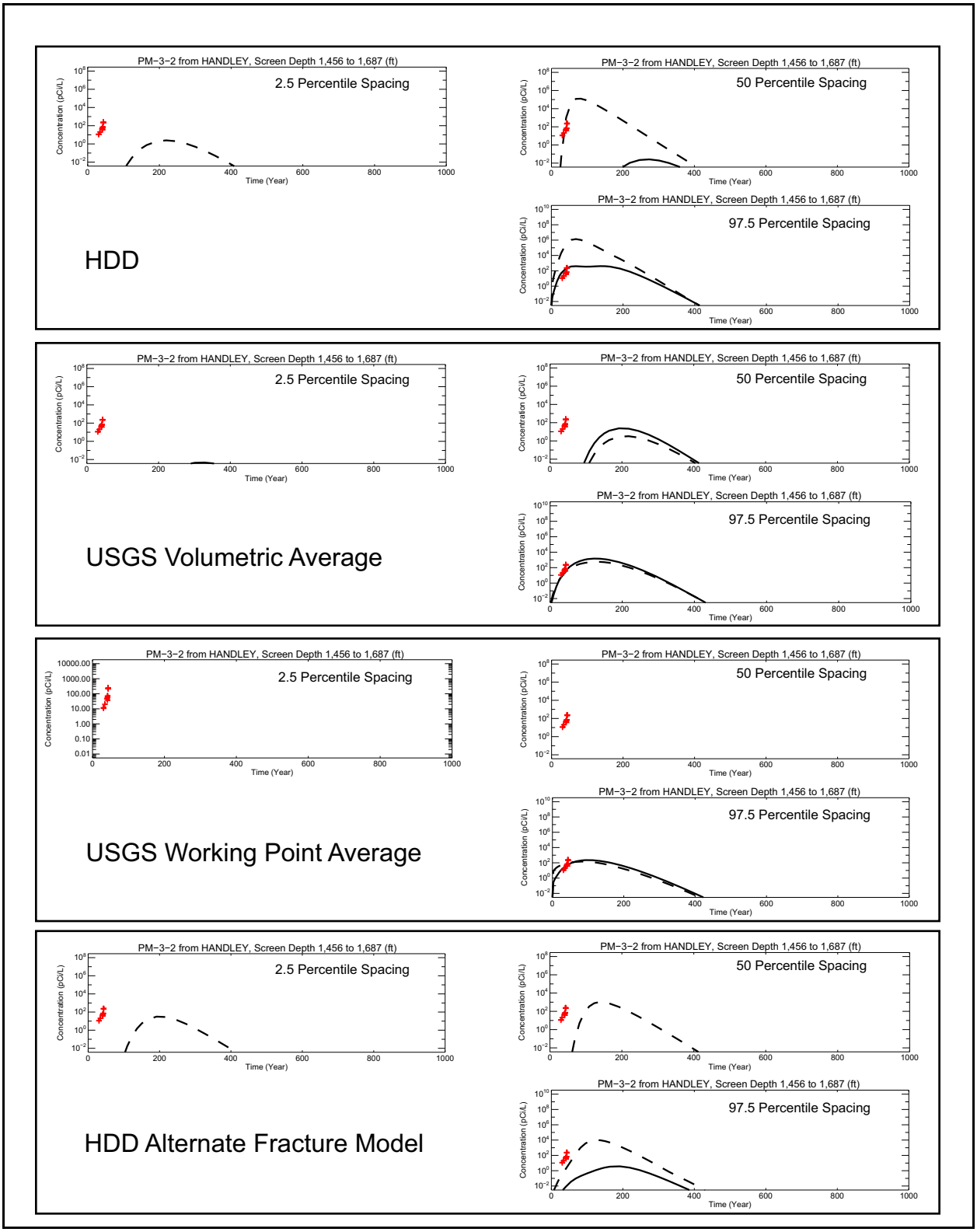

Figure C-6
Modified Fenelon et al. (2010) Streamline Simulated Breakthrough and Observed ^3H Concentrations at PM-3-2 (Shallow)

Note: Dashed line is maximum at any vertical location; solid line is well screen; red crosses are observations.

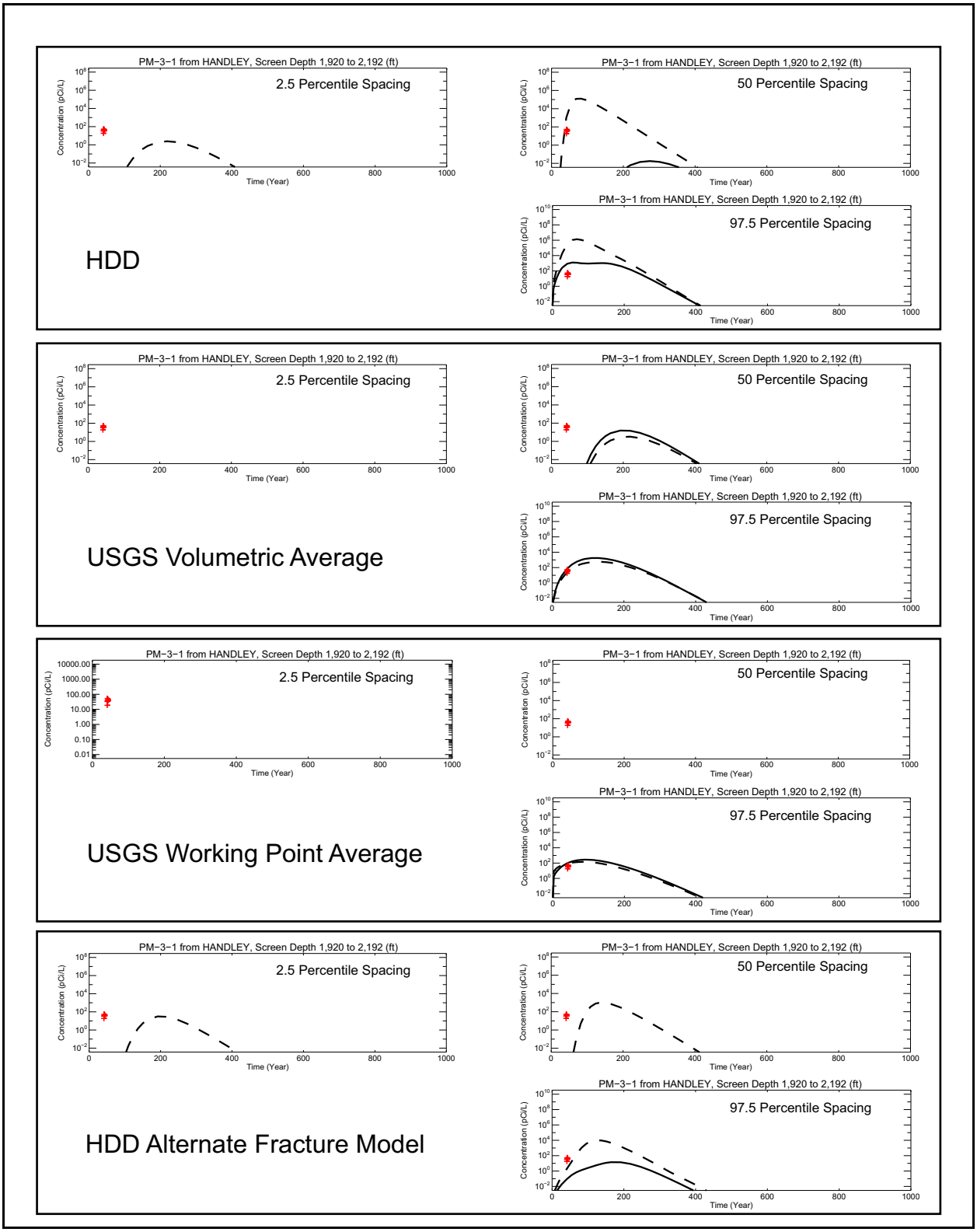

Figure C-7
Modified Fenelon et al. (2010) Streamline Simulated Breakthrough and Observed ^3H Concentrations at PM-3-1 (Deep)

Note: Dashed line is maximum at any vertical location; solid line is well screen; red crosses are observations.

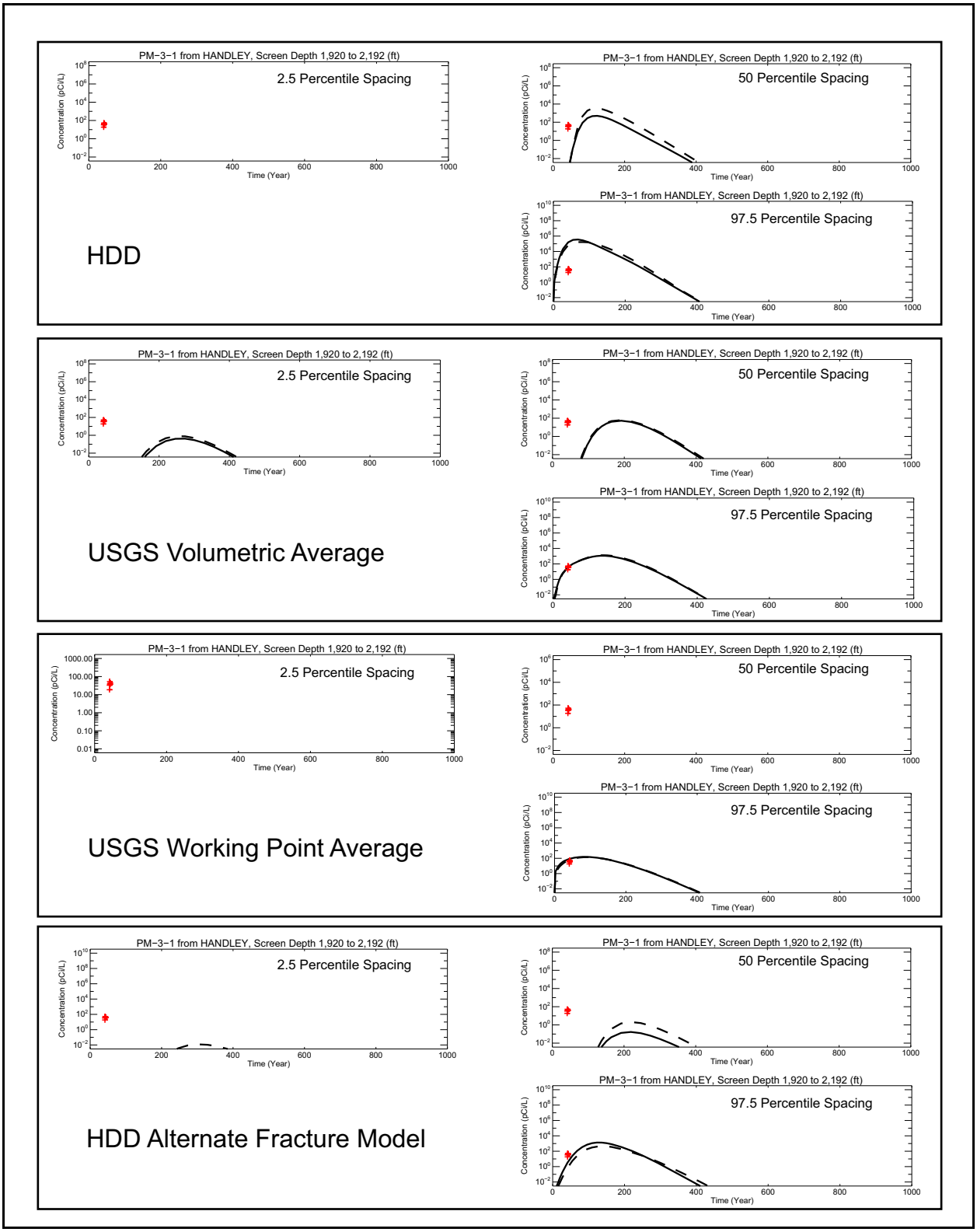

Figure C-8
Straight Line Streamline Simulated Breakthrough and Observed ^3H Concentrations at PM-3-1 (Deep)

Note: Dashed line is maximum at any vertical location; solid line is well screen; red crosses are observations.

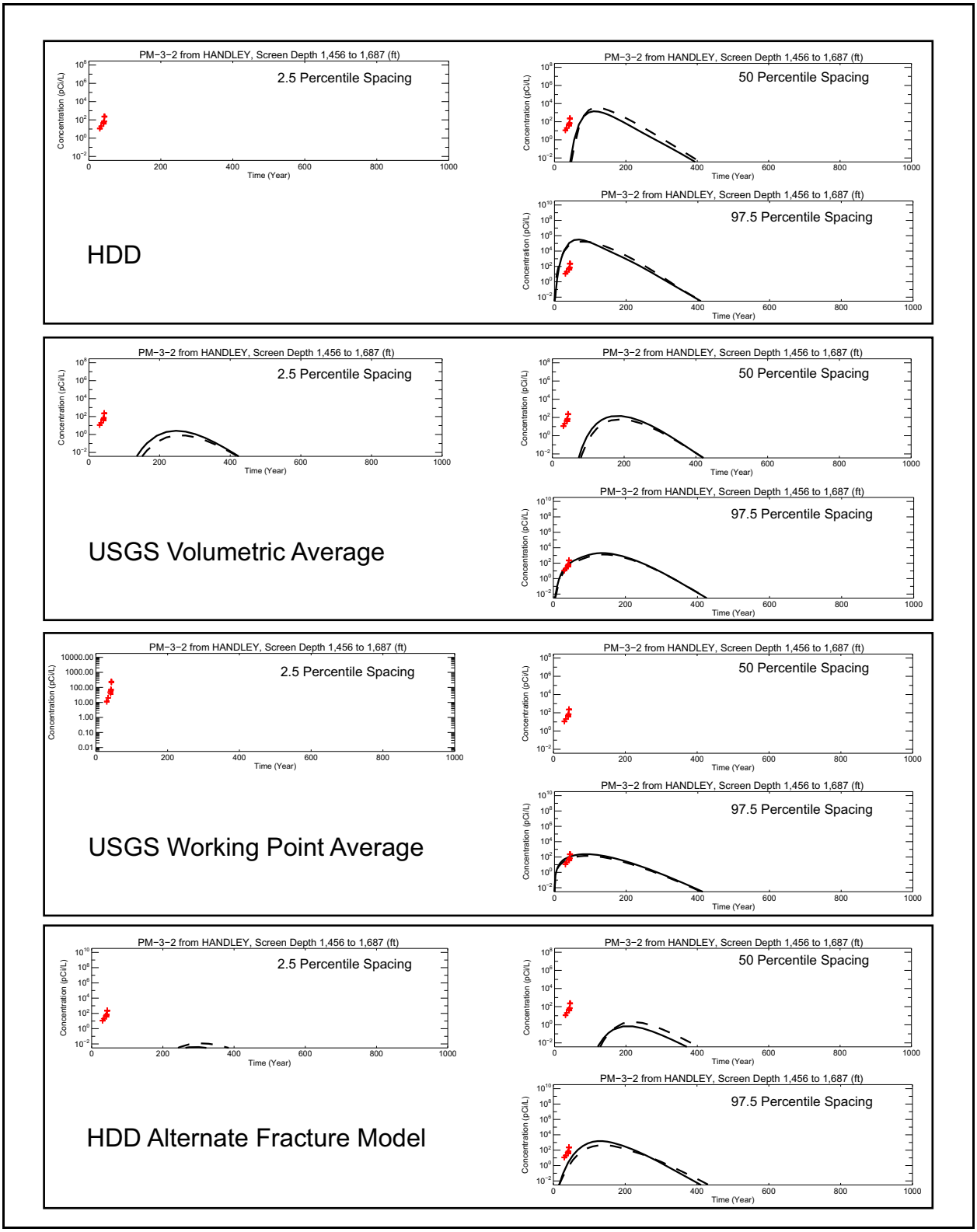

Figure C-9
Straight Line Streamline Simulated Breakthrough and Observed ^3H Concentrations at PM-3-2 (Shallow)

Note: Dashed line is maximum at any vertical location; solid line is well screen; red crosses are observations.

Within the streamtube models, the BRA is parameterized as a dual-porosity fractured rock, and it is the primary conduit for groundwater flow and radionuclide transport away from HANDLEY. The arrival of ^{3}H coincident with observations at PM-3 simulated by the streamtube models using the HDD parameterization and the arrival of ^{3}H lagging behind observations simulated by the USGS modeling-based parameterizations suggest that the hydraulic conductivity of the BRA must be approximately 1 m/day in the presence of matrix diffusion to facilitate ^{3}H breakthrough at the concentrations observed in PM-3. The WTA and LFA HGUs fracture porosity calculated for HDD parameterization using the cubic law is of the same magnitude as the values obtained from inverse modeling of the BULLION forced gradient experiment (Reimus and Haga, 1999), but the USGS model-based parameterization fracture porosity is approximately and order of magnitude lower than the BULLION values. Nonetheless, the conceptualization of fractures as parallel plates is a very crude approximation of flow and transport in fractured rock and attenuation from matrix diffusion may have been over- or underestimated, thereby allowing a range possible hydraulic conductivity values that could produce breakthrough at PM-3 in agreement with observations.

In summary, the streamtube simulations of ^{3}H transport from the HANDLEY detonation to PM-3 are uncalibrated and simply used a range of flow and transport properties thought to bound possible radionuclide transport rates. Simulations using the best point estimate of fracture spacing and HDD hydraulic conductivities indicate that the ^{3}H observed in PM-3 may be from the HANDLEY detonation.

In addition to the ^{3}H transport analyses from the potential HANDLEY source zone and comparison to observed ^{3}H concentrations, it is informative to compare the relative concentrations of other mobile (i.e., non sorbing) radionuclides at PM-3 to their initial source zone concentration. Using the maximum values of the observed concentrations of ^{14}C, ^{36}Cl, and ^{129}I from Table A-1 and ^{3}H from Table A-2, the following ratios (rounded to two significant figures) to the initial source zone concentrations at HANDLEY are calculated (with the source zone concentration of ^{3}H being decayed to 2013):

- **^{3}H:** 355 pCi/L/1.9E+08 pCi/L = 1.9E-06
- **^{14}C:** 0.153 pCi/L/4,800 pCi/L = 3.2E-05
- **^{36}Cl:** 2.07E-03 pCi/L/1,600 pCi/L = 1.3E-06
- **^{129}I:** 8.82E-05 pCi/L/5.7 pCi/L = 1.5E-05

The similarity in these results indicates that it is likely that the source of the observed radionuclide concentrations at PM-3-2 (shallow) (and, by likely extension, to PM-3-1 [deep]) is the HANDLEY detonation. These radionuclides are all considered to be nonsorbing and would have similar transport behavior along their likely transport path from HANDLEY to PM-3. The similarity in the ratios of the observed concentration of these mobile radionuclides to the assumed source zone concentration is generally not observed in other locations on the NNSS in large part because the ^{14}C, ^{36}Cl, and ^{129}I have been lost to the vadose zone portion of the exchange volume. A similar or greater lack of consistency between the concentration of ^{14}C, ^{36}Cl, and ^{129}I and the concentration of ^{3}H would be expected for Plowshare tests where the gaseous precursors of ^{14}C, ^{36}Cl, and ^{129}I are likely lost to the atmosphere, thus significantly reducing their concentrations in the soil water relative to the ^{3}H concentration. In contrast, the HANDLEY detonation was conducted 821.83 m beneath the water table, and it is likely the initial activity of ^{14}C, ^{36}Cl, and ^{129}I remains in the aqueous phase in the cavity and chimney until transported laterally downgradient in the BRA or other transmissive zones.

C.6.0 REFERENCES

Bear J., and A. Verruijt. 1987. *Modeling Groundwater Flow and Pollution (Theory and Applications of Transport in Porous Media)*. Dordrecht, Netherlands: D. Reidel Publishing Company.

Blankennagel, R.K., and J.E. Weir Jr., 1973, *Geohydrology of the Eastern Part of Pahute Mesa, Nevada Test Site, Nye County, Nevada*: U.S. Geological Survey Professional Paper 712-B, 35 p.

Bowen, S.M., D.L. Finnegan, J.L. Thompson, C.M. Miller, P.L. Baca, L.F. Olivas, C.G. Geoffrion, D.K. Smith, W. Goishi, B.K. Esser, J.W. Meadows, N. Namboodiri and J.F. Wild. 2001. *Nevada Test Site Radionuclide Inventory, 1951–1992*. Los Alamos, NM: Los Alamos National Laboratory.

DOE/NV, see U.S. Department of Energy, Nevada Operations Office.

Domenico, P.A., and F.W. Schwartz. 1990. *Physical and Chemical Hydrogeology*, Second Edition. New York, NY: John Wiley & Sons.

Elliot, P.E., and J.M. Fenelon. 2013. *Database of Groundwater Levels and Hydrograph Descriptions for the Nevada Test Site Area, Nye County, Nevada*, Data Series 533 Version 4.0. Reston, VA: U.S. Geological Survey.

Fenelon, J.M., D.S. Sweetkind and R.J. Laczniak. 2010. *Groundwater Flow Systems at the Nevada Test Site, Nevada: A Synthesis of Potentiometric Contours, Hydrostratigraphy, and Geologic Structures*, USGS Professional Paper 1771. Reston, VA: U.S. Geological Survey.

Halford, K., J.F. Fenelon and S. Reiner, U.S. Geological Survey. 2012. Memorandum to D. Galloway (WSFT–West) titled "AQUIFER-TEST PACKAGE—Simultaneous Numerical Analysis of Eight Aquifer Tests To Estimate Hydraulic Properties on Pahute Mesa, Nevada National Security Site," 21 September. Henderson, NV.

Jackson, T.R., C.A. Garcia, K.J. Halford, D. Sweetkind, and J.M. Fenelon. 2014a. *Improving Regional Groundwater Models with Transmissivity Observations*, U.S. Geologic Survey Poster, Underground Testing Area Technical Information Exchange Conference, 16 July. Las Vegas, NV.

Jackson, T.R., C.A. Garcia, K.J. Halford, N. Damar, and J.M. Fenelon. 2014b. *Integrated Analysis of 10 Large-Scale Multi-Well Aquifer Tests at Pahute Mesa*, U.S. Geologic Survey Poster, Underground Testing Area Technical Information Exchange Conference, 16 July. Las Vegas, NV.

Kilroy, K.C., and C.S. Savard. 1996. *Geohydrology of Pahute Mesa-3 Test Well, Nye County, Nevada*, Water-Resources Investigations Report 95-4239. Carson City, NV: U.S. Geological Survey.

Kwicklis, E.M., F. Thamir, R.W. Healy, and D. Hampson. 1998. *Numerical Simulation of Air- and Water-Flow Experiments in a Block of Variably Saturated, Fractured Tuff from Yucca Mountain, Nevada*, Water-Resources Investigations Report 97-4274. Denver CO: U.S. Geological Survey.

N-I, see Navarro-Intera, LLC.

National Research Council. 1996. *Rock Fractures and Fluid Flow, Contemporary Understanding and Applications.* Washington, DC: National Academy Press.

Navarro-Intera, LLC. 2013. *Yucca Flat/Climax Mine CAU Flow and Transport Model, Nevada National Security Site, Nye County, Nevada,* Rev. 0, N-I/28091--065. Las Vegas, NV.

Pawloski, G.A. 1999. *Development of Phenomenological Models of Underground Nuclear Tests on Pahute Mesa, Nevada Test Site—BENHAM and TYBO*, UCRL-ID-136003. Livermore, CA: Lawrence Livermore National Laboratory.

Reimus, P. W., and M.J. Haga. 1999. *Analysis of Tracer Responses in the BULLION Forced-Gradient Experiment at Pahute Mesa, Nevada,* LA-13615. Los Alamos, NM: Los Alamos National Laboratory.

Rose, T.P., F.C. Benedict, Jr., J.M. Thomas, W.S. Sicke, R.L. Hershey, J.B. Paces, I.M. Farnham, and Z.E. Peterman. 2006. *Geochemical Data Analysis and Interpretation of the Pahute Mesa - Oasis Valley Groundwater Flow System, Nye County, Nevada, August 2002*, UCRL-TR-224559. Livermore, CA: Lawrence Livermore National Laboratory; Reno, NV: GeoTrans Inc. and Desert Research Institute; Denver, CO: U.S. Geological Survey; and Las Vegas, NV: Harry Reid Center for Environmental Studies.

Shaw, see Shaw Environmental, Inc.

SNJV, see Stoller-Navarro Joint Venture.

Shaw Environmental, Inc. 2003. *Contaminant Transport Parameters for the Groundwater Flow and Contaminant Transport Model of Corrective Action Units 101 and 102: Central and Western Pahute Mesa, Nye County, Nevada*, Rev. 0, Shaw/13052-201-CD. Las Vegas, NV.

Stoller-Navarro Joint Venture. 2004. *Hydrologic Data for the Groundwater Flow and Contaminant Transport Model of Corrective Action Units 101 and 102: Central and Western Pahute Mesa, Nye County, Nevada,* Rev. 0, S-N/99205-002; Shaw/13052-204. Las Vegas, NV.

Stoller-Navarro Joint Venture. 2005. *Underground Test Area Fracture Analysis Report for Yucca Flat Wells ER-2-1, ER-6-1#2, ER-7-1, and ER-12-2 Nevada Test Site, Nevad*a, Rev. 0, S-N/99205--040. Las Vegas, NV.

Stoller-Navarro Joint Venture. 2007. *Phase I Contaminant Transport Parameters for the Groundwater Flow and Contaminant Transport Model of Corrective Action Unit 97: Yucca Flat/Climax Mine, Nevada Test Site, Nye County, Nevada*, Rev. 0, S-N/99205--096. Las Vegas, NV.

U.S. Department of Energy, Nevada Operations Office. 2000. *United States Nuclear Tests, July 1945 through September 1992*, DOE/NV--209-REV 15. Las Vegas, NV.

White, F.M. 1991. *Viscous Fluid Flow*, New York, NY: McGraw-Hill, Inc.

Zyvoloski, G.A., B.A. Robinson, Z.V. Dash, and L.L. Trease. 1997a. S*ummary of the Models and Methods for the FEHM Application—A Finite-Element Heat- and Mass-Transfer Code,* LA-13307-MS. Los Alamos, NM: Los Alamos National Laboratory.

Zyvoloski, G.A., B.A. Robinson, Z.V. Dash, and L.L. Trease. 1997b. *User's Manual for the FEHM Application—A Finite-Element Heat- and Mass-Transfer Code,* LA-13306-M. Los Alamos, NM: Los Alamos National Laboratory.

DISTRIBUTION

	Copies
W.R. Wilborn Environmental Management Operations U.S. Department of Energy National Nuclear Security Administration Nevada Field Office P.O. Box 98518, M/S 505 Las Vegas, NV 89193-8518	1 hard copy
U.S. Department of Energy Office of Scientific and Technical Information P.O. Box 62 Oak Ridge, TN 37831-0062	1 electronic media
Robert Andrews Navarro-Intera, LLC P.O. Box 98952, NSF 167 Las Vegas, NV 89193-8518	UGTA website
Irene Farnham Navarro-Intera, LLC P.O. Box 98952, NSF 167 Las Vegas, NV 89193-8518	UGTA website
Mavrik Zavarin Lawrence Livermore National Laboratory 7000 E. Avenue, L-103 Livermore, CA 94550-9909	UGTA website
Ron Hershey Desert Research Institute 2215 Raggio Pkwy Reno, NV 89512	UGTA website
Kay Birdsell Los Alamos National Laboratory Bikini Atoll Rd., SM30, MS T003 Los Alamos, NM 87545	UGTA website

	Copies
Ken Rehfeldt Navarro P.O. Box 98952, NSF 167 Las Vegas, NV 89193-8518	UGTA website
Sam Marutzky Navarro-Intera, LLC P.O. Box 98952, NSF 167 Las Vegas, NV 89193-8518	UGTA website
Barry Lester Navarro P.O. Box 98952, NSF 167 Las Vegas, NV 89193-8518	UGTA website
Andrew Tompson Lawrence Livermore National Laboratory 7000 E. Avenue, L-103 Livermore, CA 94550-9909	UGTA website
Wayne R. Belcher U.S. Geological Survey Water Resources Division 160 N. Stephanie Street Henderson, NV 89074	UGTA website
Jeff Sanders U.S. Geological Survey Water Resources Division 160 North Stephanie Street Henderson, NV 89074	UGTA website
Robert Graves U.S. Geological Survey Water Resources Division 160 N. Stephanie Street Henderson, NV 89074	UGTA website
Sig R. Drellack National Security Technologies, LLC P.O. Box 98521, M/S NLV 082 Las Vegas, NV 89193-8521	UGTA website

	Copies
Ken Ortego National Security Technologies, LLC P.O. Box 98521, M/S NLV 082 Las Vegas, NV 89193-8521	UGTA website
Chuck E. Russell Desert Research Institute 755 E. Flamingo Las Vegas, NV 89119	UGTA website
Karl Pohlmann Desert Research Institute 755 E. Flamingo Las Vegas, NV 89119	UGTA website
Ed Kwicklis Los Alamos National Laboratory SM-30 Bikini Atoll Rd., MS T003 Los Alamos, NM 87545	UGTA website
Nicole DeNovio Senior Project Hydrogeochemist Golder Associates Inc. 18300 NE Union Hill Road, Suite 200 Redmond, WA 98052	UGTA website
Greg Ruskauff Navarro-Intera, LLC P.O. Box 98952, NSF 167 Las Vegas, NV 89193-8518	UGTA website
Jeffrey Wurtz Navarro-Intera, LLC P.O. Box 98952, NSF 167 Las Vegas, NV 89193-8518	UGTA website
Southern Nevada Public Reading Facility c/o Nuclear Testing Archive P.O. Box 98521, M/S NLV 400 Las Vegas, NV 89193-8521	2 electronic media

	Copies
Northern Nevada Public Reading Facility c/o Nevada State Library & Archives 100 N Stewart Street Carson City, NV 89701-4285	1 electronic media
Environmental Management Records U.S. Department of Energy National Nuclear Security Administration Nevada Field Office P.O. Box 98518, M/S 505 Las Vegas, NV 89193-8518	1 hard copy
Navarro-Intera, LLC Central Files P.O. Box 98952, NSF 156 Las Vegas, NV 89193-8518	1 hard copy